BRNO UNIVERSITY OF TECHNOLOGY
VYSOKÉ UČENÍ TECHNICKÉ V BRNĚ

FACULTY OF CHEMISTRY
FAKULTA CHEMICKÁ

INSTITUTE OF MATERIALS SCIENCE
ÚSTAV CHEMIE MATERIÁLŮ

MORPHOGENESIS AND VISCOELASTIC PROPERTIES OF DIMETHACRYLATE NETWORKS
MORFOGENEZE A VISKOELASTICKÉ VLASTNOSTI DIMETHAKRYLÁTOVÝCH SÍTÍ

DOCTORAL THESIS
DIZERTAČNÍ PRÁCE

AUTHOR — **Ing. Zdeněk Bystřický**
AUTOR PRÁCE

SUPERVISOR — **prof. RNDr. Josef Jančář, CSc.**
ŠKOLITEL

BRNO 2019

BRNO UNIVERSITY OF TECHNOLOGY
FACULTY OF CHEMISTRY

Specification Doctoral Thesis

Department:	Institute of Materials Science	Academic year:	2019/20
Student:	**Ing. Zdeněk Bystřický**		
Study programme:	Macromolecular Chemistry		
Study branch:	Chemistry of Macromolecular Materials		
Head of thesis:	**prof. RNDr. Josef Jančář, CSc.**		

Title of Doctoral Thesis:

Morphogenesis and Viscoelastic Properties of Dimethacrylate Networks

Doctoral Thesis:

The main aim of this thesis is the investigation of kinetics and mechanisms of dimethacrylate copolymer network morphogenesis with the ultimate goal to achieve defined network structures with maximum reproducibility. Then, the relationship between supra–molecular structure, viscoelastic behavior and thermal stability of dimethacrylate networks will be investigated. Time and temperature dependence of the viscoelastic moduli will be determined.The difference in thermal stability will be interpreted in terms of degradation mechanisms, which are highly dependent on the structural characteristics of the corresponding resin system.

Deadline for Doctoral Thesis delivery: 20.11.2019:

Ing. Zdeněk Bystřický Student	prof. RNDr. Josef Jančář, CSc. Head of thesis	doc. Ing. František Šoukal, Ph.D. Head of department

In Brno dated 4.11.2019

prof. Ing. Martin Weiter, Ph.D.
Dean

ABSTRAKT

Tato dizertační práce se zabývá studiem morfogeneze dimethakrylátových sítí. V práci byly využity zjednodušené systémy založené na monomerech, které bývají typicky využívány jako složky matric pryskyřičných kompozitních materiálů využívaných v oblasti záchovné stomatologie. Kinetika a mechanismy formování polymerních sítí byly studovány především s ohledem na strukturu jednotlivých monomerů, jejich vzájemný molární poměr a koncentraci iniciačního systému využitého pro radikálovou polymeraci. Vypočtené profily konverze funkčních skupin a reakčních rychlostí byly využity jako základ pro pochopení a interpretaci mechanismů morfogeneze sítí a porovnání se známými modely. Dále byla studována kinetika termické degradace, která je s morfologií vytvrzených sítí přímo spjata. V rámci takto charakterizovaných systémů byla stanovena teplotní závislost dynamického modulu a byl popsán vztah mezi supra-molekulární strukturou dimethakrylátových sítí a jejich viskoelastickou odezvou v daném teplotním rozmezí.

Kinetika polymerace byla studována pomocí diferenční kompenzační foto-kalorimetrie (DPC) a infračervené spektroskopie (FTIR). Proces termické degradace byl analyzován pomocí termo-gravimetrické analýzy (TGA). Viskoelastické parametry byly charakterizovány pomocí dynamicko-mechanické analýzy (DMA).

Reaktivita jednotlivých systémů je přímo odvozena od molekulární struktury monomerů, která ovlivňuje mobilitu reagujících složek v průběhu polymerace. Kinetika polymerace je řízena především difúzí, přičemž její rychlost je dána tuhostí monomerní páteře, koncentrací funkčních skupin a vlivem fyzikálních interakcí. Omezená mobilita rostoucích řetězců, postranních funkčních skupin i samotných monomerů vede k monomolekulární terminaci makro-radikálů a omezení stupně konverze funkčních skupin. Vzhledem k tomu, že k zásadnímu omezení mobility dochází již v počáteční fázi polymerace, tj. v bodu gelace, je případná termodynamická nestabilita vedoucí k fázové separaci polymerujícího systému potlačena a proces kopolymerace je ve své podstatě náhodný. To bylo prokázáno i prostřednictvím identifikace jedné teploty skelného přechodu u charakterizovaných kopolymerů. Heterogenní charakter morfogeneze je spjat s rozdílnou reaktivitou postranních funkčních skupin. V počátečních fázích polymerace dochází k propagaci reakcí postranní funkční skupiny s radikálem na stejném rostoucím řetězci, což vede ke vzniku tzv. primárního cyklu. Pravděpodobnost cyklizace souvisí především s flexibilitou monomerní páteře. Heterogenita polymerace je charakterizována vznikem vnitřně zesítěných struktur, tzv. mikrogelů, a jejich následným spojováním. Tuhost monomeru naopak přispívá k vyšší efektivitě zesítění a více homogenní morfologii vytvrzené sítě. Heterogenita dimethakrylátových sítí se odráží v mechanismu termické degradace, přičemž přítomnost strukturně odlišných domén vede k rozkladu ve dvou krocích. Průběh soufázového modulu a teplota skelného přechodu korelují s tuhostí polymerních sítí, efektivitou zesítění a přítomností fyzikálních interakcí, které vyztužují strukturu sítě nad rámec kovalentního zesítění. Heterogenní morfologie sítí se projevuje rozšiřováním spektra relaxačních časů. Experimentální data jsou v kvalitativní shodě s existujícími numerickými modely popisujícími kinetiku radikálové polymerace multifunkčních monomerů.

KLÍČOVÁ SLOVA

Dimethakrylátové monomery, radikálová polymerace, kopolymerace, polymerační kinetika, multifunkční polymerní sítě, morfogeneze, viskoelasticita, termická degradace

ABSTRACT

The thesis deals with the investigation of dimethacrylate networks morphogenesis. Simple model resin mixtures used in this work were based on the monomers, which are typically employed as the components of matrix systems of dental resin composites. Kinetics and mechanisms of polymer networks formation were studied with respect to a structure of monomers, molar ratio of comonomers, and a concentration of the radical polymerization initiation system. Calculated profiles of functional groups conversion and polymerization rate were used as a basis for understanding and interpretation of mechanisms of networks morphogenesis and comparison with known models. Furthermore, kinetics of thermal degradation process was studied because it is closely related to the morphology of the networks. Then, temperature dependence of viscoelastic modulus was determined and the relationship between supramolecular structure of dimethacrylate networks and their viscoelastic response within the given temperature range was quantified.

Polymerization kinetics was studied by differential photo-calorimetry (DPC) and infrared spectroscopy (FTIR). Process of thermal degradation was analyzed using thermo-gravimetric analysis (TGA). Viscoelastic parameters were measured using dynamic-mechanical analysis (DMA).

Reactivity of dimethacrylate systems is derived from the molecular structure of monomers, because it affects mobility of reacting species during polymerization. Kinetics of polymerization is controlled by diffusion. Rate of diffusion is given by the monomer rigidity, concentration of functional groups, and an impact of physical interactions. The mobility restrictions, affecting growing chains, pendant side chains and free monomers, lead to monomolecular termination of macroradicals and limited degree of conversion. Since the mobility is restricted severely from the early phases of the reaction, i.e. from the gel point, phase separation is suppressed despite any potential thermodynamic instability, and the copolymerization process is random. This was confirmed by identification of single glass transition temperature in DMA experiments of copolymers. Heterogeneous character of morphogenesis is related to a varying reactivity of pendant functional groups. In the early phases of the polymerization, propagation proceeds via intramolecular attack of the radical site to the pendant, leading to the primary cycle formation. Probability of the cyclization is increased by flexibility of the monomer backbone. Heterogeneity of the curing reaction is characterized by formation of internally crosslinked structures, i.e. microgels, followed by their interconnections. On contrary, rigidity of the monomer leads to a higher effectivity of crosslinking and more homogeneous morphology of the corresponding networks. Presence of the inhomogeneities, characterized by coexistence of structurally distinct regions, is related to a two-step mechanism of thermal decomposition. Progress of the storage modulus and the glass transition temperature correlate with the network stiffness, effectivity of crosslinking, and the presence of physical interactions that reinforce the structure beyond the scope of covalent crosslinking. Structural heterogeneity is manifested by broad transition region indicating wide variations in relaxation times. Experimental data are in qualitative correlation with the numerical models that simulates kinetics of free radical network polymerization.

KEYWORDS

Dimethacrylate monomers, radical polymerization, copolymerization, polymerization kinetics, multifunctional polymer networks, morphogenesis, viscoelasticity, thermal degradation

BYSTŘICKÝ, Z. Morphogenesis and viscoelastic properties of dimethacrylate networks. Brno University of Technology, Faculty of Chemistry, 2019. 104 p., supervisor prof. RNDr. Josef Jančář, CSc.

Declaration

I declare that this thesis has been worked out independently and that all references have been cited correctly and fully. The content of the thesis is the property of the Faculty of Chemistry, Brno University of Technology, and all the commercial uses are allowed only if approved by both the supervisor and the dean of the Faculty of Chemistry, BUT.

…….

Student's signature

Acknowledgement

I would like to sincerely thank to my supervisor, prof. RNDr. Josef Jančář, CSc. for his valuable advices and creation of the good work conditions. My special thanks also belong to Ing. Petr Poláček, PhD. for the willingness to help with the experimental techniques. Thank you both for your support and guidance. Also, I would like to thank my dear Marta for her endless love and patience, my parents for providing me support and convenient conditions and finally, to all my colleagues, at Faculty of Chemistry BUT and ADM, a. s., for always being close to help.

TABLE OF CONTENTS

1 INTRODUCTION

Polymerization of multifunctional monomers leads to the formation of rigid, highly crosslinked networks that have found their use in a variety of applications including dental restoratives, microelectronics, optical lenses, UV-VIS curable adhesives and others. The application area of dimethacrylate monomers is related primarily to the field of restorative dentistry. This began in the mid 1960's with the introduction of suitable monomer species thanks to the pioneer research of Rafael L. Bowen [1,2]. Since then, dimethacrylate monomers-based restoratives have undergone significant development considering filler technology and mechanisms of initiation, whereas the monomer formulations have remained essentially unchanged [3,4].

The systematic studies, including evaluation of conversion, crosslinking, and network structure along with associated physical properties, are required for the optimization of desirable properties for development of durable materials. In order to attain desirable clinical outcomes of dimethacrylate based restoratives, most of the current research affords are associated with the polymerization shrinkage phenomenon and incomplete curing reaction. First of these drawbacks is primarily related to the stress transmission to the adhesive bond and the remaining tooth structure resulting in the marginal crack formation, post-operative sensitivity, and the origination of secondary caries. The relatively moderate degree of double bonds conversion (typically ranging from 50 to 80 %) may be of concern for both the mechanical performance and the possible toxic effects or tissue irritation by untreated, leaching out low-molecular components [4–9]. Due to the complexity associated with the self-limitation of the process of multifunctional network formation, it is a challenging task to shed light on the mechanisms of the polymerization, determine the morphology of cured systems, and localize remaining unreacted double bonds. In the beginning, it is necessary to employ simple model resin mixtures before more complex formulations are taken into consideration. Commercial dental composites include complicated monomer systems with various additives influencing kinetics of polymer network formation. Moreover, presence of solid filler particles of large specific surface area can alter resin cure significantly by radical immobilization and de-activation [9,10].

This dissertation deals with the investigation of the copolymerization kinetics along with the dimethacrylate networks morphogenesis beginning from the structurally distinct simple monomer formulations, continuing with more comprehensive mixtures. The relationship between the morphology, kinetics of thermal degradation and viscoelastic properties will be investigated as well. Through a better understanding of the polymer network formation and property development with respect to the resulting morphology, the ultimate goal of achieving polymers with enhanced clinical outcomes is facilitated.

2 CURRENT STATE OF RESEARCH TOPIC

2.1 Multifunctional monomers, aspects and applications

Free radical polymerization of multifunctional monomers is a way of preparation of high strength, rigid polymer networks, that found applications in many commercial areas including coating industry, UV/VIS curable adhesives, microelectronics, lithography, optics, industrial composite materials, biomaterials in dentistry etc. Polymerizations can be carried out under a wide range of conditions including variations in comonomers structure, number and type of reactive functional groups, alternative ways of initiation, and varying external conditions [11,12]. The initial liquid state is based on the monomers and chemicals promoting the reaction selected specifically to fulfill a variety of material properties demands prior to polymerization as well as in the cured polymer. Monomers are typically selected to yield densely crosslinked glassy polymer networks, that provide properties tailored specifically to a respective application. The choice of monomers includes consideration of viscosity, refractive index, hydrophilic/hydrophobic character, reactivity, and potential contribution to the crosslink density of the polymeric network. Also, polymerization reaction rate can be enhanced by appropriate combination of monomer species [4,13,14]. Nowadays, the preferred curing mode is in particular polymerization induced by absorption of light energy by suitable molecular species (i.e. photopolymerization). This is thanks to the distinct advantages of photopolymerizable materials that can be cured on demand with the reaction rate readily manipulated through the combination of photo-initiator choice and concentration as well as the irradiance and wavelength range introduced by the light source [4].

During polymerization process, there are several distinct stages as the reaction progresses from a liquid pre-gel regime to a rubbery-gelled phase, and finally to a glassy state [4]. However, the morphogenesis of multifunctional networks exhibits a number of interesting features that may result in a formation of polymers with a certain degree of structural heterogeneity [9]. Due to the crosslinking nature, bulk polymerizations of difunctional monomer systems exhibit complex reaction kinetics including auto-acceleration, auto-deceleration, diffusion-controlled termination, limiting functional group conversion, and anomalous pendant functional groups reactivity. The development of respective polymer properties as the function of conversion is critically linked to the structure of developing network and localization of the remaining unreacted functional groups throughout the polymerization process. Moreover, due to the various size and flexibility, there is no equivalent reactivity of the monomers involved in the different resin systems formulations [15–17]. The features mentioned above suggest that the network formation by multifunctional monomers is extremely complex process that exhibits complicated reaction kinetics when compared with formation of linear polymer chains.

The following text is focused on description of the aspects of using dimethacrylate monomers, that are widely used in the field of prosthetic and restorative dentistry. This includes the introduction of respective monomer species and their specific structural features, that affect polymerization kinetics, polymer network morphogenesis, resulting supra-

molecular structure, and mechanical performance of the cured systems. The process of network formation is described beginning from the characterization of the basic reaction steps, including various initiation mechanisms. The aspects of the photo-activation process are highlighted. Then, the special features accompanying the process of multifunctional network formation are overviewed, while considering mainly the structural parameters of individual monomer species affecting their mobility and reactivity during (co)polymerization of dimethacrylate resin systems.

2.2 Dimethacrylate monomers in prosthetic dentistry

The most important acrylate monomer in the field of restorative dentistry was poly(methyl methacrylate) since late 1930's. The discovery of the benzoyl peroxide-tertiary amine redox initiating system allowed methyl methacrylate (MMA) to polymerize at ambient temperature, laid the basis for direct filling resins. This type of material has a number of desirable properties such as ease manipulation and fabrication, esthetics, low solubility, smooth surface texture and a tough, ductile nature [3]. However, conventional acrylic monomers and polymers have several critical deficiencies that limit their clinical performance. Important shortcomings include excessive polymerization shrinkage, incomplete polymerization, insufficient stability in the oral environment associated with the tendency to absorb water due to the high internal energy, inadequate wear resistance, and poor adhesion to hard dental tissues (i.e. enamel and dentin). These and other deficiencies have led to the continuous development of dental polymeric materials threw the wide range of monomers, oligomers and polymers [18,19].

As already mentioned above, modern era of dental acrylic materials is associated with the research of American dentist R. L. Bowen, who synthetized a new monomer, designed specifically for the purposes of restorative dentistry [1,2]. The monomer, 2,2-bis[4-(2-hydroxy-3-methacryloxyprop-1-oxy)-phenyl]-propane (Bis-GMA, Figure 1), was prepared from bisphenol A and glycidyl methacrylate and later also from diglycidylether of bisphenol A and methacrylic acid. This monomer is superior to methyl methacrylate because of its large molecular size and bulky chemical structure, providing lower volatility, lower polymerization shrinkage, more rapid hardening, and production of stronger and stiffer resins [3]. Current changes of polymeric matrix are focused mainly to develop systems with reduced polymerization shrinkage stress, higher double bonds conversion, and lower tendency of dental plaque accumulation [19]. Several articles described future developments, such are self-repairing, re-mineralizing, stimuli-responsive and antimicrobial materials [19–22]. Most of these affords are based on the modifications of different dimethacrylate monomer species. Thus, the nature of the resin composite matrixes has remained fundamentally unchanged since the invention of Bis-GMA in 1960's.

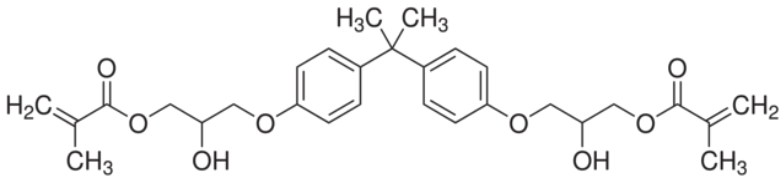

Figure 1: Bis-GMA (Bowen monomer).

Dental composites can be distinguished by differences in formulation tailored to their particular requirements as restoratives, sealants, cements, provisional material, etc. These materials are similar in that they are all based on the polymeric matrix, surface treated reinforcing fillers or fibers (typically made from radiopaque glass and colloidal silica),

pigments, opaquers, and chemicals that promote or modulate the curing reaction. Resin composites are nowadays used for a variety of applications in dentistry, including restorative materials, cavity liners, pit and fissure sealants, core build-ups, inlays, onlays, crowns, provisional restorations, cements for multiple or single tooth prostheses, orthodontic devices, endodontic sealers, root canal posts etc. [19].

2.2.1 Comonomer formulations

Predominantly used monomer in polymeric matrix formulations, often referred to as a base monomer, is already introduced monomer, Bis-GMA. Due to the enormous room temperature viscosity of this base monomer (Table 1), dilution by other compatible monomer species, decreasing overall viscosity of the resin system, is required. These are flexible and low-viscous monomers such are poly(ethylene glycol) dimethacrylates (PEGDMA) with various number of ethylene glycol units in the monomer backbone. The most extensively employed diluent for dental resins is triethylene glycol dimethacrylate (TEGDMA, Figure 2). Besides that, dimethacrylate monomers based on alkyl chain diols can also be used as the reactive diluents (e. g. 1,6-hexanediol dimethacrylate, HDDMA, Figure 2).

A.

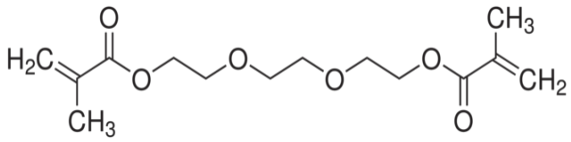

B.

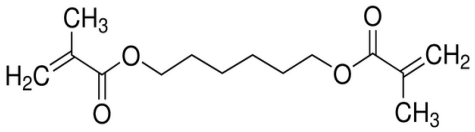

Figure 2: Examples of low viscosity diluent monomers used in the formulations of matrixes of dental composites; A. TEGDMA, B. HDDMA.

The most extensively used alternatives for Bis-GMA as a base monomer are various urethane dimethacrylate monomers (UDMA), such as 1,6-bis(methacryloxy-2-ethoxycarbonylamino)-2,4,4-trimethylhexane (Figure 3), and also non-hydroxylated alternative of Bis-GMA, 2,2-bis[4-(methacryloxypolyethoxy)-phenyl]-propane (Bis-EMA, Figure 3) with various number of ethylene glycol units (typically m + n = 3). Potential of the usage of these monomer species is further discussed below.

A.

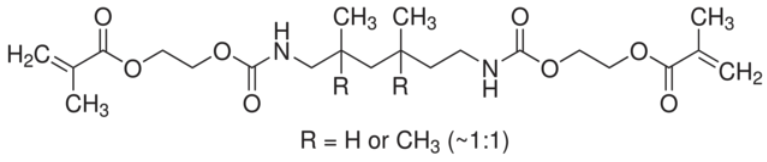

B.

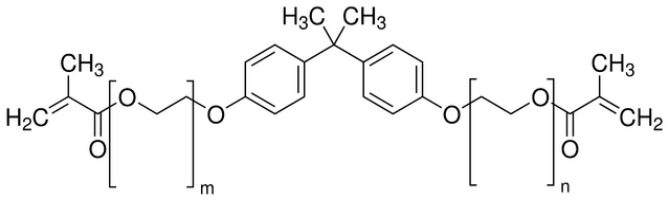

Figure 3: Examples of alternative base monomers used in the formulations of of matrixes of dental composites; A. UDMA, B. Bis-EMA.

Presence of the base monomer in the resin formulation serves to minimize polymerization shrinkage by virtue of its relatively large molecular volume and low double bond concentration. Moreover, the rigidity of the monomer backbone enhances the elastic modulus of the cured polymer. The low viscosity diluent monomer is added to provide good handling properties to the material, and also to afford improved copolymer conversion due to its greater flexibility, mobility, and smaller molecular volume when compared with the high-viscous base monomers [3,17,23]. The lower the viscosity of monomer mixture, the more filler may be incorporated into the resin mixture. Increased filler content significantly improves mechanical performance of the cured material, e.g. strength, stiffness, coefficient of thermal expansion etc. [3,19]. However, the dilution may cause increased water uptake, deterioration of toughness, polymerization shrinkage and as a consequence, deterioration of marginal integrity of a composite [15,24]. Thus, the structural characteristics of different comonomers must be taken into consideration to optimize the clinical performance of resin composites.

2.2.2 Monomer structure and associated properties

As briefly suggested above, structure and included functionality (other than the reactive methacrylate groups) of the monomers determine the properties related to the polymerization kinetics, network morphogenesis and the mechanical performance of the cured systems. As it was stated by Stansbury [4], these properties are largely but not exclusively additive in nature when comonomer mixtures are formulated. The most important structural characteristics of the respective monomer species will be further described in this chapter.

2.2.2.1 Viscosity

Initial resin viscosity is an important parameter from the perspective of the reaction kinetics, since it affects mobility of the reactive species in the polymerizing system [23]. Molecular weight and shape of monomer molecules in the liquid state as well as its potential for intermolecular interactions determines bulk viscous flow behavior of uncured resins. Individual molecules are mutually attracted through van der Waal's forces that range from weak to relatively strong interactions. Dipole-dipole interactions (e.g. hydrogen bonding) represent the strongest interactions between neutral molecules. The strength of intermolecular interactions is important since these effectively make small molecules behave as larger structures [4].

Very low viscosities of the monomers such are TEGDMA or HDDMA are caused by their low molecular weight, and lacking hydrogen bond donor functionalities. On the other hand, Bis-GMA monomer exhibits dramatically high viscosities. The range of its viscosity is based on the small differences in the degree of oligomerization that occurs during the synthetic procedure. The extreme room temperature viscosity of Bis-GMA is derived from the strong hydrogen bonding between hydroxyl groups, which is exclusively intermolecular due to the rigid aromatic core structure [4,7,25]. A weaker, but still significant contribution of π-π aromatic ring interactions in Bis-GMA is demonstrated by the comparison of its viscosity with those of ethoxylated bisphenol A dimethacrylate (Bis-EMA) and TEGDMA [14]. Hydrogen bonding interactions associated with the urethane functional groups of UDMA are significantly weaker than those based on hydroxyl groups of Bis-GMA, as it was shown by Khatri *et al.*, when the series of urethane group containing dimethacrylates were compared with unaffected Bis-GMA [26]. Mentioned study also highlighted another interesting feature of Bis-GMA monomer. In spite of the much lower degree of conversion achieved during the homopolymerization of Bis-GMA, when compared with low viscous urethane derivative monomers, the mechanical strength was greatest for Bis-GMA homopolymer. This is the result of strong hydrogen bonding interactions, serving as the non-covalent physical crosslinks, that effectively reinforce the structure of the cured polymer [4,26]. The hydroxyl groups of Bis-GMA can serve effectively as both the hydrogen bond donors and acceptors. The urethane nitrogen is not strongly electronegative due to the electron donation to the adjacent carbonyl. Hence, it is an ineffective hydrogen bond acceptor. This implies that UDMA hydrogen bonding interactions are weaker, and display greater intramolecular character due to the flexibility of the monomer backbone. Polymerization of UDMA also appears to modestly disrupt its hydrogen bonding interactions. Therefore, hydrogen bonding cannot serve a significant role in the reinforcement of polymer network structure as it is in the case of Bis-GMA based resins [25]. The actual values of the molecular weights, concentration of double bonds, viscosities, and glass transition temperatures of the monomers mentioned above are summarized in the Table 1.

Viscosity effects can dramatically alter polymerization reactivity. However, it is difficult to generalize the effects of various noncovalent interactions in different comonomer formulations, since structural differences and the presence of specific functionalities may have an ultimate impact on the properties of uncured monomer system as well as on the cured polymer.

2.2.2.2 Reactivity

The reactivity of dental dimethacrylates goes hand in hand with the initial viscosity of the resin formulation, and structural features of monomers allowing for molecular mobility. The range of resin viscosities where optimum reactivity is observed is likely that which allows significant monomer diffusion but inhibits macroradicals translation and termination. Thus, initial resin viscosity is a major factor in controlling polymerization kinetics and the final conversion, but not the only one that controls reactivity of monomer formulations [14].

Studies on the formation of homopolymers from oligoethylene glycol dimethacrylates have shown that the reactivity of the monomers increases with increasing distance between the methacrylate groups. Due to the favorable stereochemistry, long chain and flexible dimethacrylates have also been found to exhibit relatively high degrees of double bonds conversion [27]. As both Bis-GMA and Bis-EMA contain rigid aromatic core structure, the limiting double bond conversion and overall reactivity are reduced when compared with diluent monomers (e.g. TEGDMA, HDDMA) or UDMA. However, the lacking hydrogen bonding functionalities, and more flexible ethoxylated linkages in Bis-EMA allow for a greater degree of mobility. This would account for a higher overall conversion when compared with Bis-GMA based formulations. Similar reactivity of the bisphenol A containing monomers at a given viscosity range is contrasted by the considerably higher reactivity of UDMA based resins. Despite the similarities in the initial viscosities of UDMA and Bis-EMA, the greater flexibility of UDMA molecular structure ensures much higher reactivity. Thus, optimal reactivity of the UDMA resin systems is obtained with the addition of relatively small amounts of diluent monomer, whereas systems based on stiff aromatic core monomers require dilution by greater portion of low-viscous flexible monomer to reach optimal reactivity. Generally, any incremental addition of diluent monomer leads to the increase of the reactivity, polymerization rate and limiting double bond conversion in the case of all systems based on combination of base and diluent monomers [14,23,28].

Table 1: Correlation between the molecular weight, concentration of double bonds, viscosity and glass transition temperature of dental monomers [29,30].

Monomer	M_w [g/mol]	C=C [mol/kg]	Viscosity [mPa·s]	Monomer T_g [ºC]
Bis-GMA	512.60	3.90	500 000–800 000	- 10
Bis-EMA	496.58	4.70	3 000–5 000	- 42
UDMA	470.56	4.25	5 000–10 000	- 38
TEGDMA	286.32	6.99	100	- 80

2.3 Radical polymerization of multifunctional monomers

The polymerization process of dimethacrylate monomers is a reaction triggered by free radicals, which are generated by a suitable initiation system. The double bonds of monomeric methacrylate groups are then opened, generating a chain reaction the process is described by three basic steps: initiation, propagation and termination. Schematic and idealized representation (Figure 4) of the basic steps of light induced polymerization of di-functional monomers is illustrated below [6,31].

A. Initiation (k_i)

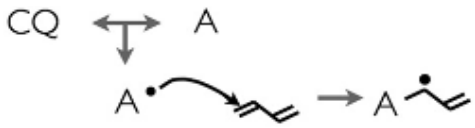

B. Propagation (k_p)

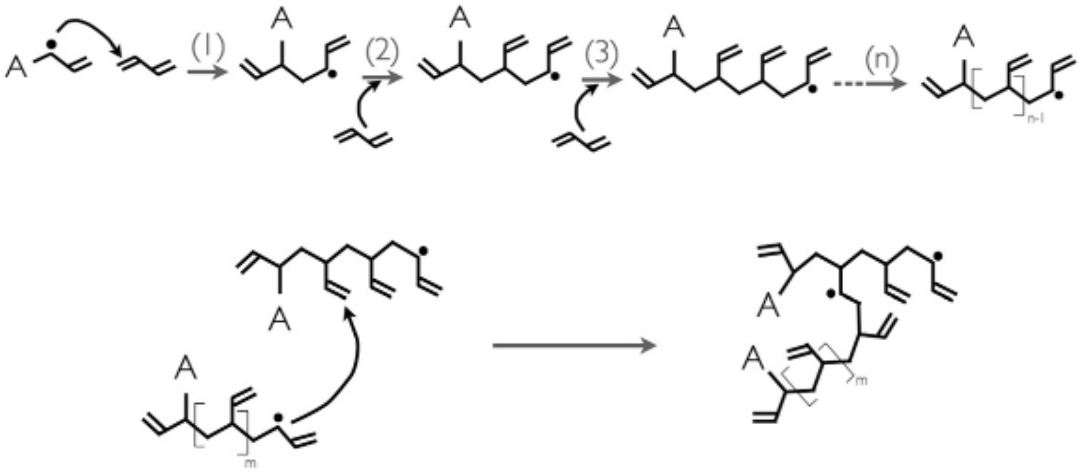

C. Termination (k_t)

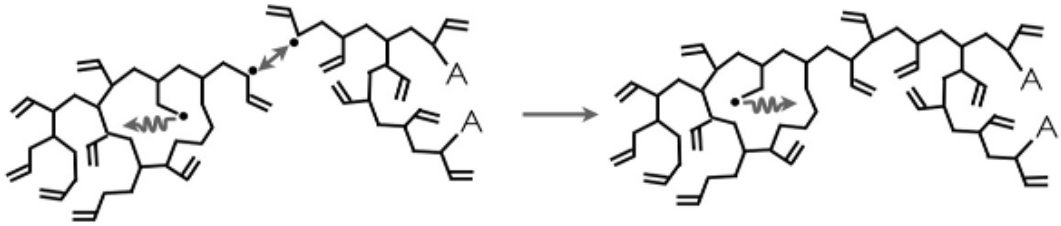

Figure 4: Schematic illustration of three basic steps of light induced polymerization reaction; CQ represents camphorquinone, A tertiary amine, numbers represent the theoretical steps of linear monomer addition. A trapped radical and segmental mobility are illustrated in section C. Associated rate constants ($k_{...}$) are referred in brackets [6].

An active center is created when the free radical attacks the π-bond of a monomer molecule (A). Propagation involves growth of the polymer chain by rapid sequential addition of a monomer to the active center. The polymer can either grow linearly by reaction with monomers, leaving unreacted pendant double bonds, or grow three-dimensionally by reacting with other chains, creating crosslinks [31].

In this chapter, the fundamental steps of multifunctional networks formation are further described. In the first place, this requires the assessment of the kinetic aspects of the polymerization process. Then, the initiation mechanisms are introduced while special attention is paid to the photo-activation process using the most widely employed system for the purposes of dental restoratives containing α-diketone and tertiary amine reductant. At the end of this chapter, the kinetic analysis of the basic steps of photo-polymerization (Figure 4) is stated.

2.3.1 Aspects of the polymerization of multifunctional monomers

The process of multifunctional network formation exhibits anomalous bulk behavior, especially with respect to reaction kinetics. This behavior includes auto-acceleration and auto-deceleration, limiting double bond conversion, unequal functional groups reactivity, trapping of free radicals, and reaction-diffusion-controlled termination and propagation mechanisms [32]. The complexity is caused by the fact that the mobility of the reacting medium varies as the polymerization proceeds. At very low double bonds conversions, propagation and termination reactions are chemically controlled. However, as the network forms, segmental movements of the macroradicals are restricted. At the gel point, mobility restriction mostly affects the radicals located on the growing chains, whereas smaller molecules can still diffuse easily through the polymerizing system. As a consequence, the rate of bimolecular termination decreases dramatically while new growth centers are still created by initiation. Concentration of free radical in the system rapidly increases, which results in a rapid increase of the polymerization rate, R_p (fraction of double bonds converted per second). This elevation of the propagation rate has been termed auto-acceleration. As the reaction progresses, the environment becomes even more restricted along with the diminishing concentrations of residual reactive groups as the reaction proceeds. Thus, propagation reaction also becomes diffusion-controlled, resulting in the significant decrease of R_p. The decline in rate has been called auto-deceleration (Figure 5). The diffusion-controlled kinetics of these polymerizations leads to double bond conversion less than unity [11,23,33].

Another consequence of diffusion-controlled kinetics is the entrapment of free radicals in the polymer network, sometimes termed as the monomolecular termination. However, if the mobility of the system increases again (e. g. by swelling or temperature increase above glass transition temperature), trapped radicals become capable of reacting with remaining double bonds and thus, conversion of double bonds may increase [34].

Considering multifunctional methacrylate monomers, diffusion-controlled termination dominates throughout most of the polymerization (beginning mostly as early as 2 % of double bonds conversion). In the restricted environment, radicals are unable to segmentally move toward each other. Instead, as it was stated by Lovell *et. al.* [23], the radicals propagate through unreacted monomer and pendant double bonds in order to diffuse toward each other and terminate. This termination mode is called diffusion-controlled termination, and within this regime, propagation (k_p) and termination (k_t) kinetic constants are unchanging and related

to each other through a reaction-diffusion proportionality constant, R, and the concentration of double bonds:

$$k_{\mathrm{t}} = Rk_{\mathrm{p}}[\mathrm{M}] \quad (1)$$

In the equation 1, [M] is the concentration of double bonds [23,35]. Value of the proportionality constant typically ranges between 2 and 3 for a wide variety of poly(ethylene glycol) dimethacrylate homopolymerizations.

Special features accompanying the process of dimethacrylate network morphogenesis associated with the mentioned reaction aspects are further described in the chapter 2.4.

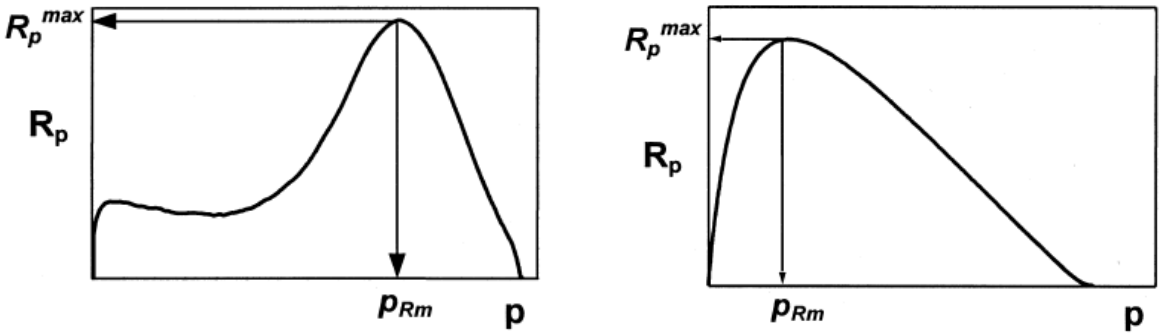

A. B.

Figure 5: Typical shape of kinetic curves of polymerization rate as a function of double bond conversion for the polymerization of A. monomethacrylate monomers, B. dimethacrylate monomers. It is apparent that the polymerization rate curve in crosslinking systems shows auto-acceleration followed by auto-deceleration [11].

2.3.2 Initiation mechanisms

Based on the way of origination of the free radicals, it is possible to distinguish between several ways of the initiation mechanisms. These include so called "*cold curing chemical systems*" that initiate polymerization upon admixing two or more components (i.e. self-activated polymerization), heat initiator systems and light initiator systems. Especially, the light-activated polymerization is a rapidly expanding technology that has found excessive use in many applications including the field of prosthetic dentistry.

2.3.2.1 Self-activated polymerization

The discovery of the benzoyl peroxide-tertiary aromatic amine redox initiator-accelerator system allowing methyl methacrylate to polymerize at ambient temperature, laid the bases for direct filling resins and dental composites in 1940s [3,18].

The initiators are admixed with the monomers shortly before application. The mechanism consists of a nucleophilic attack on the peroxide bond of the organic peroxide mediated by the

nitrogen atom of a tertiary amine (e. g. ethyl-4-dimethylamino benzoate, EDMAB). The positively charged complex is than decomposed forming the free radical elements. As the amine radicals are relatively stable, initiation preferably takes place from the benzoyl-oxide radical. These systems are nowadays mostly used in dual curable adhesive cements and sealants (combination with the systems for light induced polymerization), denture-base materials and for other non-medical purposes [36].

2.3.2.2 Heat-activated polymerization

The free radical initiator (mostly organic peroxide, e.g. dibenzoyl peroxide, dicumyl peroxide) undergoes homolytic cleavage when exposed to elevated temperature. In contrast with the self-induced polymerization, high activation energy of the homolytic cleavage of the peroxide linkage prevents the reaction to take place under the ambient conditions [36]. Obviously, interval of cure temperatures (ranging from ambient temperature up to 250 °C) may seems irrelevant for direct dental restorative applications from the clinical point of view. However, it may be instrumental for an understanding of the processes involved in dimethacrylate network morphogenesis [9,37].

The dependence of the rate constant on the temperature is described by the Arrhenius equation (2), where k is the rate constant of a reaction (number of collisions that results in reaction per second), A is the pre-exponential factor (total number of collisions), T is the absolute temperature, E_a is the activation energy, and R is the universal gas constant. The exponential member expresses the probability that the collision will result in a reaction.

$$k(T) = A \cdot e^{\frac{-E_a}{RT}} \tag{2}$$

The equation implies that along with the increased temperature, the rate constant and the concentration of free radical species in the system increases [36].

2.3.2.3 Photo-polymerization

Light-activated polymerization is nowadays a widely accepted mode for the curing processes required with a wide range of applications including dental restoratives. The photo-polymerization technology is based on the use of photo-reactive systems suited to absorb a light irradiation of the appropriate wavelength and to produce primary radical species able to convert a pool of multifunctional monomers into a crosslinked network. UV induced polymerization is one of the most efficient methods for the generation of highly crosslinked polymers in many industrial areas (e. g. coatings, adhesives). Considering the irritation of oral tissues by UV irradiation, visible-light induced radical polymerization has been accepted as the photo-polymerization technology in the field of prosthetic dentistry.

Understanding to photo-polymerization begins with an understanding of light itself. The most important characteristics of photons are energy (frequency, wavelength), and distribution (number/area/second, irradiance). Impact of these characteristics on polymerization behavior and properties of cured polymer networks has been extensively described by many

researchers [38–47]. Nowadays, most of the commercial dental composite formulations utilize reaction triggered by visible light in the blue region. Light curing units (LCU) are based on the different physical principles. These include quartz-tungsten-halogen (QTH), plasma arc (PAC), laser and light-emitting diode (LED).

Effects of light intensity

Effects of the light intensity (i.e. power transferred per unit area) on the conversion of double bonds, development of crucial mechanical properties, and shrinkage strain of during polymerization of dimethacrylate monomers have been broadly studied by many researchers. As expected, with increasing light intensity, exposure time needed for polymerization decreases. In general, polymers irradiated by the light sources with higher intensity exhibited higher degrees of conversion. However, this may be partially due to the increase of the maximum temperature reached during polymerization when the high intensity light sources were used (e.g. PAC source, 1800 mW/cm^2 over QTH source set to 200 mW/cm^2) [38]. Regardless of the light intensity, linear relationship exists between conversion and final elastic modulus. Hence, specimens cured by equivalent energy densities using short times and high-power density or long times and lower power density produced materials with equivalent mechanical properties [39–41].

However, slowing down the reaction leads to a decrease in the polymerization shrinkage stress. Shrinkage is associated with the polymerization reaction in a complex way. The reduction in shrinkage stress could be attributed to reduced network connectivity, or to an increased propensity for the viscous flow. Reduced light intensity may result in a development of storage modulus slow enough to allow for flow and dissipation of the stress. Hence, optimization of rheological behavior may enhance marginal adaptation of resin composites [42,43]. This may be achieved by applying short pulses of light energy, pre-polymerization at low light intensity followed by final exposure at high intensity (soft start) or a combination of both [31,47].

With regard to find optimal light curing intensity for clinical purposes, it is necessary to consider many variables related to the differences in the material composition and overall curing conditions.

Light sources

A quartz-tungsten-halogen (QTH) light source consists of a halogen bulb with a filament. As current passes through the filament, the wire heats up and as a result, electromagnetic radiation is emitted. Standard irradiance of the QTH sources is ranging around 500 mW/cm^2. The spectrum of QTH radiation is continuous over the visible range, with radiation intensity increasing considerably towards the red end of the spectrum. Most of the spectrum of QTH radiation does not contribute to the polymerization, and it is dissipated by heat. Thus, the QTH sources require infrared blocking filters, selecting the blue-light wavelengths between approximately 400 and 500 nm [31,48]. QTH light sources had dominated over other light curing sources for decades. Nowadays, they are almost entirely replaced by modern sources, particularly by light emitting diodes (LED).

Plasma arc curing (PAC) sources contain xenon plasma lamps. The light is emitted from glowing plasma, which is composed of a gaseous mixture of ionized molecules and electrons. The lamp filled with xenon emits high-intensity light by an electron discharge, characterized by a very high output in a narrow range of wavelengths around 470 nm. Higher light intensity leads to a higher penetration depth is achieved in a short time [49]. However, the question is whether the high irradiance delivered in a short time would lead to an adequate polymerization. Particularly, the issue of concern is associated with the high polymerization rate. Curing by PAC sources occurs very fast and thus, there is the risk of high polymerization shrinkage [31].

Laser sources emit light at a few distinct frequencies within the desired wavelength region and thus, completely eliminating the need for filtering undesired wavelengths. In order to fit the output spectrum of the lasers with the absorption spectrum of the photo-initiators, special lasers for the dental purposes were commercially developed (e.g. AccuCure-3000 for the absorption spectrum of CQ) [31].

Light-emitting-diode (LED) light sources are currently the standard devices in most modern dental practices since the beginning of the 21st century. LED is a semiconductor photonic device of an n-p type, constructed from two layers connected by a junction (n-p junction). One doped with electrons (n, cathode), and the other doped with holes (or defect electrons, p, anode) [31]. The former leads to electron donor states in the band gap just below the conduction band, whereas the latter leads to acceptor states in the band gap just above the valence band. Under a forward biased condition, an electric current is flowing from the p-doped side to the n-doped side, and no current is observed under a reverse biased condition. When a small voltage is applied, electrons and holes are pushed toward the junction, and the distance between them decreases. When the potential barrier is low enough, electrons and holes recombine near the p-n junction and emit photons: an electron in the conduction band can spontaneously return to an empty state in the valence band, during which a photon is produced as well as heat. For the realization of LED curing unit usage in the restorative dentistry, at least two prerequisites had to be fulfilled. Namely, availability of the proper emission wavelength controlled by the width of the band gap and thus, by the composition of both the p- and n- doped materials, and the sufficient emitted power to cure dental materials within a reasonable time [50]. These prerequisites were fulfilled in 1994 when Nakamura *et al*. developed high brightness Ga-N LED's [51]. The crucial advantage that makes LED's ideally suited for the photo-polymerization of dental resin composites is extremely narrow spectral line of emitted light. If the wavelength of the LED is chosen in the range of the maximum absorption spectra of the used photo-initiator, effective and rapid photo-polymerization is the result [50].

Photo-initiators, mechanisms

Success factors of photo-initiators are linked to high absorptivity in the spectral region corresponding to the irradiating lamp emission, high efficacy in terms of the quantum yield for radical formation and high reactivity of the monomer formulation, good solubility in the curable medium, low odor and toxicity and good storage stability. These factors along with

choice of photo-initiator concentration permit a high degree of external control over the photo-polymerization process. A photo-initiator is a molecule that can absorb light and as a result, either directly or indirectly generates a reactive species that can initiate polymerization. Considering the adverse health effects of UV light for oral soft tissues, visible light induced radical polymerization had fast acceptance as the curing method in the field of prosthetic dentistry. Dart and Nemecek invented the system for visible-light photo-activation that contains α-diketone and tertiary amine in 1971 (Imperial Chemical Industries Co. Ltd., UK). This invention opened new possibilities in the field of visible light-curing composites [52,53].

A. B.

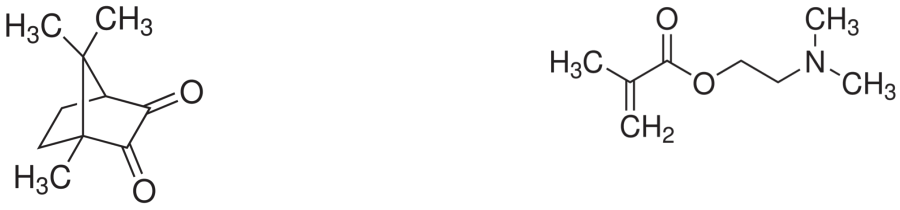

Figure 6: Structure of the most commonly used photo-initiator system, combination of: A. photosensitizer, 2,3-bornanedione (camphorquinone, CQ); B. photo-reducing agent, dimethylaminoethyl methacrylate (DMAEMA).

Photosensitizers commonly possess a carbonyl group, the non-bonding electrons of which can be promoted into a π* anti-bonding orbital by absorption of light of the appropriate wavelength. This leads to a production of a pair of free radicals. With initiators like benzoin methyl ether or acylphosphine oxide, the result of exposure to light is intramolecular α-cleavage (i.e. Norrish type I reaction) to yield two radicals, both of which have the potential to initiate polymerization reaction. The proton abstraction type of initiation occurs with 2,3-bornanedione (camphorquinone, CQ, Figure 6 A.) from a labile source (i.e. Norrish type II reaction). A co-initiator is a separate compound that does not absorb light, but interacts with an activated photo-initiator molecule to produce reactive radical species. In the case of dental restoratives containing CQ, a tertiary amine photo-reductant (e.g. DMAEMA, Figure 6 B.) is used as the co-initiator to provide the reactive radicals that initiate polymerization [53,54].

Here, the activation mechanism of the most commonly used photo-initiating system consisting of camphorquinone and tertiary amine is further described (Figure 7). CQ has the relatively broad absorption spectrum in the visible region (400–550 nm, λ_{max} = 468 nm, responsible for its yellow color). Radiation in this range is absorbed thanks to the the n→π* transition of the α-dicarbonyl chromophore groups [53]. The nonbonding electrons are promoted to a short-lived, excited energy states. This includes singlet CQ state (S, not involve reversal of electron spin) which is subjected to the intersystem crossing to form the triplet CQ (T) state, containing singly occupied orbitals [53]. The half-life of CQ (T) is approximately 0.05 ms. If, prior to its decay or deactivation, the excited CQ (T) molecule encounters an amine molecule through diffusion or pre-existing association, α-hydrogen of tertiary amine is abstracted by CQ (T) through the formation of a charge transfer encounter complex. Within

the exciplex, CQ accepts an electron to form the radical ion pair and then a proton to generate the free-radical species [53]. The CQH· radical does not effectively initiate polymerization because of steric hindrance effects, and it is mainly active in the recombination reactions between radicals. The aminoalkyl radical, A·, is the effective radical that initiates polymerization through an addition reaction onto the monomer double bond. Polymerization may also arise simultaneously from the different reactions, such as hydrogen abstraction from the monomer, or some other proton donor by triplet state of CQ in the absence of the tertiary amine. However, these reactions are not efficient [52–54].

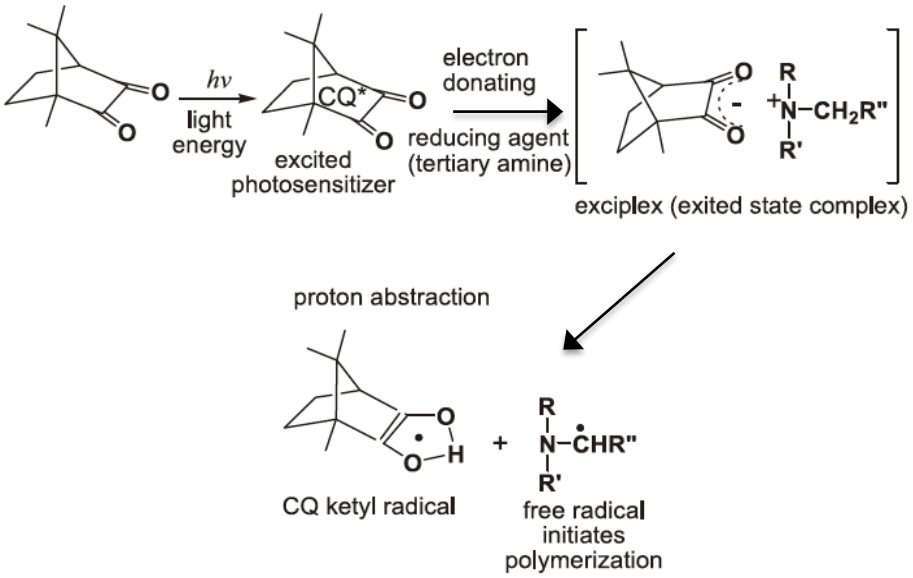

Figure 7: Schematic illustration of hydrogen abstraction photo-initiating mechanism [52].

Overall efficiency of the photo-initiation process depends not only on the quenching of CQ excited states by amines, but also on the processes that lead to the formation of radicals being able to initiate polymerization (e.g. reorientation movements of reactants to reach a favorable geometry), and the processes that lead to the physical quenching preventing radical formation, such are following [54,55]:

- non-radiative physical deactivation of excited state of CQ (S and/or T), followed by the dissipation of heat;
- quenching of the CQ excited states by psychical processes followed by emission of fluorescence and/or phosphorescence;
- physical quenching of the CQ (T) by monomer;
- quenching of the CQ (T) by oxygen;
- back electron transfer from the encounter exciplex;
- deactivation of the free radicals (M· and A·) by oxygen, formation of ineffective peroxy-radicals.

The CQ/tertiary amine photo-initiating system is the most widely used system for the visible light curing composites and thus, most of the current light-curing units are suited for the absorption spectra of CQ. However, CQ is inherently yellow crystalline powder, which may cause problems with aesthetic requirements. Although the yellowing might be reduced during the photo-activation process by photo-bleaching, some portion of the photo-initiator remains unreacted due to insufficient irradiation or physical shielding effects. Also, photo-bleaching is the effect that causes problems in the color matching to natural teeth, since the shade of the material may be slightly changed during polymerization. This places practical limits on the concentration of CQ and consequently, limits the degree of conversion. Low polymerization efficiency results in a reduction of mechanical performance as well as in possible toxic effects from releasing of residual, unpolymerized monomers and oligomers. Efforts to enhance the quality of the polymer matrix have led to the investigation of alternative photosensitizers suitable for dental resins [56].

Commonly investigated alternatives involve other diketones, such are 1-phenyl-1,2-propanedione (PPD) or 2,3-butanedione (BD) [56]. A prominent initiator is the former (PPD, Figure 8). Promising results of using PPD as the base for alternative systems for the light activation have already been shown. It was demonstrated that PPD would be an efficient visible light photo-sensitizer considering efficiency of polymerization, and reducing the yellowing effect provided by CQ [56–58]. PPD also promotes a lower rate of polymerization when compared with CQ containing formulations [58,59]. It was already suggested that the rate of polymerization affects polymerization stress development. Low rate of the reaction may be related to a lower light absorption by PPD in the given wavelength, less efficient interaction with a photo-reductant, differences in the mechanism of free radical species origination (direct cleavage of the C-C bond between the carbonyls of PPD along with the hydrogen abstraction mechanism of both CQ and PPD) and others [58–61]. Furthermore, PPD can act synergistically with CQ to increase the conversion, reduce a photosensitizer concentration, and contribute to a reduction in the color from deep to pale yellow [60–62]. However, the most of the light curing units are optimized for curing CQ containing formulations, while alternative initiators absorb light at shorter wavelengths (the absorption maximum, λ_{max} of PPD is about 410 nm). Thus, the actual results may be distorted and further research is required in order to promote the extensive use of the alternative photo-initiators.

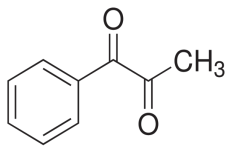

Figure 8: Structure of 1-phenyl-1,2-propanedione (PPD).

2.3.3 Photo-polymerization kinetics

Simplifying assumptions are commonly made in the development of equations in chemical kinetics. This concerns either an assumed or a demonstrable balance in rate processes between the production and extinction of intermediate molecular species (i.e. steady state assumptions).

2.3.3.1 Initiation

Regarding the Lambert-Beer law, light is attenuated with increasing cross-sectional distance from the irradiated surface as a result of light absorption and scattering caused by fillers or other additives, leading to a limited depth of cure. The following equation is considering the thin film approximation in the Lambert-Beer law, relating the absorbed light intensity to the incident light intensity. The absorbed light intensity is then expressed as:

$$I_{\mathrm{a}} = \varepsilon I_0 [C_s] \tag{3}$$

In the equation, ε expresses the extinction coefficient of the photo-initiator (molar absorptivity), $[C_{\mathrm{s}}]$ is the initiator concentration and I_0 is the incident light intensity per unit area. Then, the rate of production of primary free radicals from the photosensitizer (R_{r}) can be formally expressed by following formula:

$$R_{\mathrm{r}} = 2\phi \cdot I_{\mathrm{a}}, \tag{4}$$

Where I_{a} is the light intensity absorbed by the photosensitizer across a thickness element δd and ϕ is the quantum yield for initiation (number of propagating chains produced per number of photons absorbed by the system). The factor 2 is strictly optional and it is used when two radicals are generated for each photosensitizer molecule [31,65].

Detailed kinetic analysis of the individual activation steps, using camphorquinone/tertiary amine photopolymerization system, was made by Cook [66] and later re-interpreted by Watts [67]. Following expression for R_{r} includes mechanistic quantities of the reaction components involved in the efficient photo-activation process:

$$R_{\mathrm{r}} = \beta k_{\mathrm{a}} [\mathrm{A}] \cdot [\mathrm{CQ}_{\mathrm{T}}^{*}] \tag{5}$$

In the equation, β expresses the fraction of excited state complex forming free radicals, and k_{a} is the rate constant for the exciplex formation from reaction of amine and triplet CQ*.

If the additional steady-state assumption is made that the rates of production and consumption of initiator radicals rapidly becomes equal, then the rate of production of primary free radicals from the photosensitizer, R_{r}, is equal to the rate of initiation, R_{i}. This assumption presumes a concentration of photo-reductant to be present at the concentration that matches that of the photo-initiator. For dimethacrylate based resin systems, this assumption is suitable due to the viscous nature and the gelation that occurs at low degree of double bond conversion. Thus, it

can be assumed that the photosensitizer and resultant free radicals do not diffuse rapidly [31,66,67].

2.3.3.2 Propagation

The rate of polymer disappearance (synonymous with the polymerization rate) is given by the sum of rates of initiation and propagation (R_i, R_p), since both of the steps consume monomer. However, the rate of initiation is relatively insignificant compared with the rate of propagation and can be neglected (i.e. when the initiator concentration is very low; the reaction is monitored in the dark phase after the short irradiation), so:

$$-\frac{\mathrm{d[M]}}{\mathrm{d}t} = R_\mathrm{p} = k_\mathrm{p}[\mathrm{M}^*] \cdot [\mathrm{M}] \tag{6}$$

In the equation, [M] is the monomer concentration and [M*] is the total concentration of all chain radicals [31,67]. The equation assumes the equal reactivity of the monomeric and pendant functional groups. The determination of actual polymerization rate coefficients (k_p, k_t) is very difficult due to the complicated behavior of the reaction with respect to the kinetics, especially the early onset of the auto-acceleration. Values of the rate coefficients are often thought as a sum for the different coexisting radical populations contributing to propagation and termination [11,65]. The conversion dependences of polymerization rate coefficients are obtained under special assumptions, including exclusively bimolecular termination mechanism.

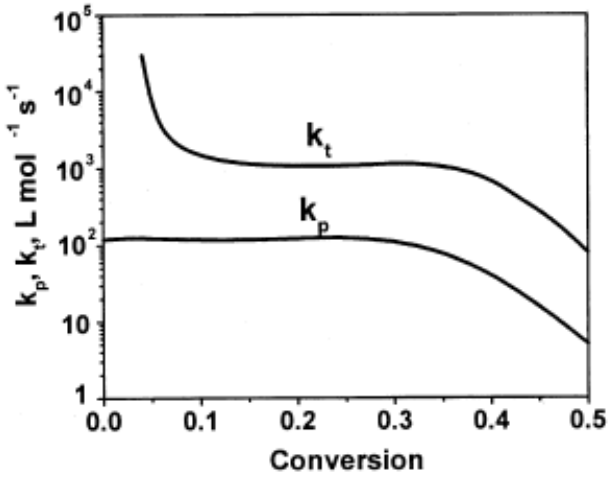

Figure 9: The dependence of the propagation and termination rate coefficients on double bond conversion for DEGDMA monomer [35].

The plot (Figure 9) of k_t vs. conversion shows a rapid decrease at the beginning of the reaction due to an immediate onset of gelation. As the system approaches to the maximum in the polymerization rate, the termination becomes reaction-diffusion controlled and a plateau is observed. The propagation rate coefficient remains relatively constant until a limiting degree

of conversion is reached and the mobility of the monomer is significantly decreased. Finally, as propagation also becomes diffusion-controlled and k_p decreases, k_t correspondingly decreases. The changes of the constants occurring with the increasing conversion are dependent on the type and concentration of the functional groups, resin formulation and polymerization conditions [11,32–35].

2.3.3.3 Termination

Due to the mentioned reaction trends, polymer radicals can be broadly classified into three populations: free radicals that are not attached to the network, radicals attached to the loosely crosslinked portion of the network so that they are spatially restricted but still mobile, and trapped radicals that are surrounded by dead polymer chains without any possibility for further propagation or termination [65–68]. Within very densely crosslinked networks, the trapped radicals are eliminated from the further propagation, and radical trapping may be considered as an additional means of the radical deactivation. Thus, one may consider two types of termination reactions: the usual bimolecular interaction of polymer radicals forming one or two dead polymer chains (bimolecular termination), and the process involving only one polymer radical (monomolecular termination). The way by which the termination in the polymerizing crosslinking system occurs depends mainly on the degree of double bond conversion, and the reaction conditions including monomer structure (crosslink density), temperature, etc. It should be noted, however, that whereas bimolecular termination is irreversible, the radicals eliminated by the monomolecular process could be reactivated by an increase in network mobility, e.g. changing of physical state by the temperature rise or swelling [11].

The simplified bimolecular termination model has been extensively used for the estimation of the polymerization rate coefficients. If a steady-state assumption is again made that the concentration of polymer radicals rapidly attains a constant value, it is equivalent to say that rates of initiation and normal bimolecular termination are equal, and hence:

$$R_t = -2k_t[M^*]^2 \tag{7}$$

For classical bimolecular termination behavior, one would expect R_p to scale with R_i to the ½ power ($\alpha = 0.5$). Rearrangement and substitution in the equation 6 yields:

$$R_p = \frac{k_p}{k_t^{1/2}}[M] \cdot \left(\frac{R_i}{2}\right)^{\alpha} \tag{8}$$

The expression for R_r in the equation 4 may be substituted for R_i in the equation 7 to obtain:

$$R_p = -\frac{d[M]}{dt} = k_p[M] \cdot \left(\frac{\phi \cdot I_a}{k_t}\right)^{0.5} \tag{9}$$

The equation shows that the rate of polymerization is proportional to the square root of the absorbed light irradiance and hence, proportional to the square root of the photo-initiator concentration [31,65–67].

An alternative path of termination, when bimolecular termination is strongly suppressed, involves chain transfer. Increased viscosity suppresses the bimolecular termination at the benefit of termination by transfer. This reaction provides additional mobility to the radical sites by influencing the kinetic chain length, reducing the lifetime of the radicals and hence, reducing the polymerization rate [11]. However, inherent chain transfer termination mode is negligible considering dimethacrylate monomers and thus, the methacrylate systems do not conform to the classical square root dependence (Equation 8). The less than ½ dependence is attributed to the chain length dependent termination effects (long, entangled and highly crosslinked chains exhibit slow termination rate). Since the most facile termination occurs between two relatively short chains, the addition of a chain transfer agent that controls the kinetic chain length distribution is required to considerably affect the termination kinetics (termination becomes more facile for shorter radicals in the system) [69]. Recently, the systems including effective chain transfer agents (e.g. the transfer from thiols to methacrylates) has been proposed in order to delay gelation, reduce the polymerization rate, and reduce the stress development thanks to the enhanced propensity for the viscous flow during polymerization [70–72]. Special features and the ways of alteration of multifunctional networks morphogenesis are further discussed in the next chapter.

2.4 Special features of multifunctional network formation

Understanding the mechanisms of network formation by various multifunctional monomers requires comprehensive approach, especially because the process exhibits abnormalities related to increasing viscosity, decreasing mobility and the heterogeneous distribution of reacting species along with reaction progress. Once more, this includes auto-acceleration, auto-deceleration, limiting functional group conversion (reaction-diffusion-controlled termination), and varying pendant double bonds reactivity.

In general, polymerization kinetics shows changes in the concentrations of the reactive species throughout the polymerization process. Concentration of monomers decreases as the polymer is formed. Consumption of functional groups is greatest during the auto-acceleration period and slows down during the auto-deceleration period. Furthermore, it is necessary to take account the structural parameters of the individual monomer species with respect to the anomalous pendant double bond reactivity (i.e. formation of effective crosslinks vs. inefficient cyclization reactions), and mobility of structurally distinct monomer species throughout the polymerizing system. This may lead to the compositional drift and phase separation of initially homogeneous, multi-component monomer formulation. Since compositional drift occurs coincidentally with network formation, the extent of structural heterogeneity depends on the rate of polymerization, onset of gelation and the degree of crosslinking at any given point during the reaction as well as any attractive or repulsive interactions between components in the resin formulation. The dynamic interplay between the kinetics of network formation and thermodynamics of the polymerizing system, or more simply stated, the competition between polymerization and phase separation, is another important feature that need to be understood while describing the process of multifunctional network formation [16,17,73,74].

All these features, accompanying the polymerization of dimethacrylate (co)monomers, promote the difficulty of modelling the process of network morphogenesis.

2.4.1 Pendant double bond reactivity

Chain polymerization of the multifunctional monomers leads to the formation of pendant double bonds on the growing macroradicals. Further propagation may proceed via three different ways. This involves addition of the next monomer molecule, extending the length of macroradical chain (path a, Figure 10) and intramolecular (path b) or intermolecular (path c) attack of the radical site to the pendant. Path b is the cyclization reaction (intramolecular crosslinking), whereas path c (intermolecular crosslinking), leads to the network formation (i.e. effective crosslinking) [11–16].

The Flory-Stockmayer theory has been used to predict gel point conversions in the systems, having a relatively low density of crosslinks (systems are assumed to be homogeneous and functional groups are assumed to possess equal reactivity). However, as it was experimentally proven by Dušek [74], if the fraction of crosslinking monomers increases, the conversion at the gel point is significantly greater than predicted by the Flory-Stockmayer theory. The

explanation of this behavior lies in the unequal reactivity of the functional groups (i.e. competition between cyclization and effective crosslinking). The pendant double bond cyclization reactions play a significant role in the process of multifunctional networks morphogenesis. As it was already mentioned, the effect of cyclization on the process of network formation has been observed experimentally, including the shift of the gel to the higher conversion than predicted theoretical value. Higher local conversion is promoted because the mobility of the system is not restricted when ineffective crosslinks are formed and thus, the gel point conversion is significantly delayed on the conversion scale. Cyclization is associated with the spatial heterogeneity of the polymer networks where loosely crosslinked regions and more densely crosslinked regions coexist. Since the cycles do not generally contribute to the network structure, the effective crosslink density is considerably reduced. As a consequence, the changes concerning some crucial properties of a cured polymer arise, including deterioration of mechanical properties. This is associated with the crack propagation through the routes of the lowest crosslink density and the highest stress intensity [75], impaired solvent resistance, lowering the glass transition temperature due to the plasticizing contribution of the intramolecular cycles etc. [76–78]. Potential for primary cyclization reaction is related to the stiffness of the monomer backbone and thus, this phenomenon is thought to be almost entirely suppressed when the monomers with a very stiff backbone connecting the functional groups are employed (cycles with more repeating monomer units may be still present) [74].

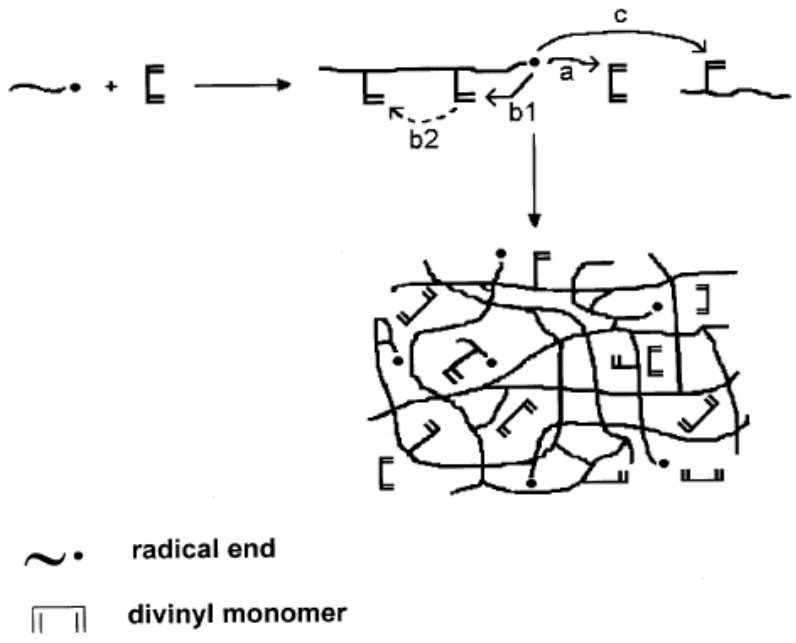

Figure 10: Schema of the network formation by difunctional monomeric units [11].

2.4.2 Origination of structural heterogeneity

As it was suggested above, the origin of structural heterogeneity is associated with a varying pendant double bonds reactivity during the polymerization process [74–77]. Initially, propagation through intramolecular cyclization (path b, Figure 10) is promoted due to an enhanced apparent reactivity of the pendant double bond on the same chain when compared with monomeric functional groups. This is related to a larger concentration of pendants in the vicinity of the radical site. Initial extensive cyclization leads to the formation of the compact structures, so called mono-chain microgel domains [74]. These compact, internally crosslinked structures are formed at the beginning of the polymerization process [11]. After that, the apparent reactivity of the pendant double bonds is decreased due to the various kinds of steric hindrance effects, preventing either inter or intramolecular crosslinking (i.e. excluded-volume effects). This causes a strong diffusion control of the reaction since the groups located in the interior of a branched polymer has certainly less opportunity to react than those located on the periphery [74–79]. Thus, a concentration of the accessible pendant functional groups is considerably decreased when a higher degree of conversion is reached, and the overall reactivity of pendant functional groups decreases, as determined on the bases of kinetic gelation model [76].

A. B.

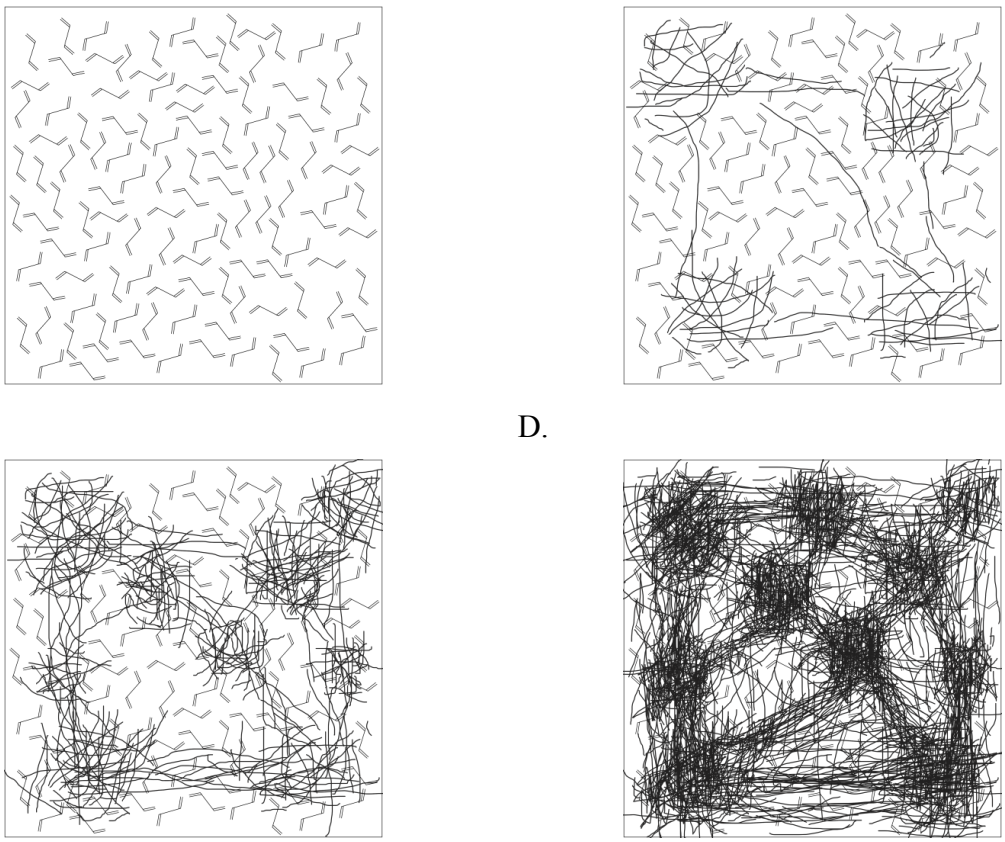

C. D.

Figure 11: Schematic representation of the network formation when extensive cyclization takes place; A. uncured monomer, B. creation of softly interconnected microgel domains, C. densification of micrgel domains and the progress of interconnections, D. further evolution of the network, monomer molecules are gathered in the sparsely cross-linked areas.

Evolution of the structure according to the conclusions of Dušek [74] and others [75–81] is schematically shown in Figure 11. Just at the beginning of the polymerization process, internally crosslinked structures are formed. These structures (i.e. microgel domains) contain in its interior pendant double bonds, which cannot take part in further reactions. Only the pendants located in the peripheral layer are accessible enough to enter further reactions leading to the molecular weight increase. The microgel domain does not have to always correspond in size to one primary chain. It is rather larger, because if the chain transfer reaction occurs, the new primary chains are not separated from the parent ones due to crosslinking. Further reaction (macro-gelation) occurs by the chemical joining of initially formed microgel particles. Thus, polymerization proceeds by the mechanisms completely different from those leading to branching trees (the postulate of the classic Flory-Stockmayer theory). It may rather resemble some kind of chemical aggregation of colloidal particles. Thus, the structure near the gel point is quite heterogeneous. At higher conversions, the "void" space containing monomer molecules is filled in by polymerization, so that the structures with higher conversion appears to be more homogeneous [74].

2.4.3 Phase separation behavior

Heterogeneity of polymer networks based on homogeneous combinations of marginally compatible monomers may be also associated with the thermodynamic instability of the mixture of monomers and polymerizing species during copolymerization. The initial degree of compatibility for given monomers depends mostly on the intermolecular interactions. As the polymerization progresses, in addition to constantly negative entropic changes associated with consumption of monomers, the Flory-Huggins interaction parameter increases, both of which may contribute to increasing free energy of mixing and if diffusion is allowed in the polymerizing system, potentially leading to phase separation [82,83].

The thermodynamically-driven phase separation process is strongly related to the kinetics of network development [66,67,84]. From this perspective, the critical aspect of network morphogenesis is the gel point (see chapter 2.4.5). It is related directly to the kinetics of the reaction, so the point in conversion at which gelation occurs can shift if there is change in the rate of reaction. There is a large reduction of fluidity of the material past the gel point and thus, if it occurs early on the conversion scale (e.g. in the case of dimethacrylate polymerizations), diffusion of incompatible phases may be prohibited. In this case, phase separation is suppressed despite any potential thermodynamic instability [85,86]. Processing conditions of active polymerizations, such as temperature, irradiance (for photo-polymerizing systems) or initiator concentration are also of key importance in the determination of phase separation behavior from the point of view of reaction kinetics. Considering free radical polymerizations, rate of polymerization (R_p, see formula 9) is proportional to the half power of irradiance and to the square root of the initiator concentration. Higher irradiances and higher concentration of photo-initiator lead to a faster development of long-range diffusion restrictions that can interrupt domain formation and rearrangement despite the increase in the free energy of mixing. In other words, the structure of network-forming systems is more quickly locked in place (whether homogeneous or heterogeneous), and if the heterogeneity is

present, conversion progresses locally within each phase, with no opportunity for further compositional rearrangement. However, it is still unclear how the phase separation process potentially alters reaction kinetics, whether localized within each phase or on the global scale [83–87].

2.4.4 Development of storage modulus

When a resin system is cured, the viscosity, elastic modulus and glass transition temperature all increase as the proportion of free monomer is steadily reduced with respect to the growing polymer phase. The growing phase is composed of polymer backbone chains, crosslinks, and pendant reactive groups in ratios that also vary dependent upon the degree of conversion. As it was stated by Stansbury [4], while the glass transition temperature as a critical parameter of the final polymer network is ultimately formed as a consequence of the crosslinking reactions, it can be informative to look at how the T_g and modulus develop during the polymerization process.

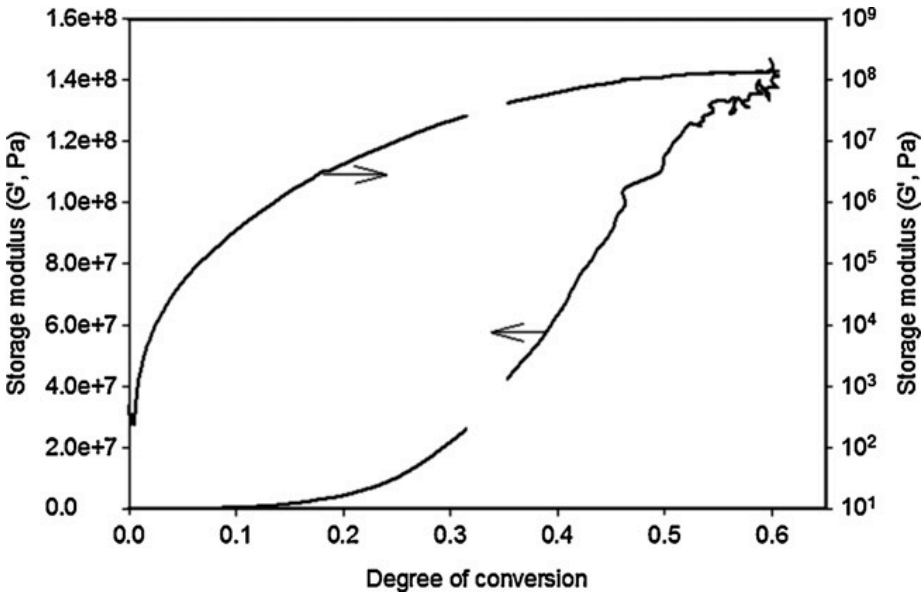

Figure 12: Photo-rheometer analysis of storage modulus development during polymerization of dimethacrylate monomers. Identical data plotted on linear (left) and logarithmical (right) scales [4].

From the dynamic rheological data, the full range of the viscoelastic properties development that occurs during polymerization can be determined. This particularly includes gelation and glass transition. The initial rise in the storage modulus, representing the elastic portion of the dynamic modulus, is related to the progress of gelation. Modulus development is attributed to the formation of polymer chains, as the joints to the infinite gel through both endings of functional groups provide elastic response to load. The unreacted pendants are thought to contribute to the energy dissipation (loss modulus rise, representing the viscous portion). Thus, both the storage and loss modulus initial rise are associated with the formation of a portion of elastically active chains along with unreacted pendant functionalities during the

auto-acceleration period [88]. This is evident on the logarithmic axes while the equivalent linear data clearly demonstrates the very dramatic rise in the storage modulus that corresponds with vitrification (Figure 12). The rubbery modulus regime, located between these two features, is associated with the bulk of the polymerization process [4,89]. Since the rubbery modulus is directly dependent on the effective crosslink density, it is obvious that the gel fraction develops rapidly in the low to moderate conversion range but much more slowly towards the end of the network formation process. This development indicates that crosslink density develops slowly at a low conversion, with a gradual increase in the area of the rubbery plateau. The majority of a late stage conversion is directed toward formation of crosslinks through the reactions of pendant double bonds [17]. A good agreement was found when the dynamic rheological data of modulus development were compared with the static modulus data reflecting the range of conversions reached with partial or full cure polymerizations [90].

2.4.5 Gelation

Just for the basic understanding of the gelation, gel point can be examined from the both chemical and physical points of view. From the chemical point of view, gelation is related to the appearance of an insoluble polymer fraction involving the polymer network extension throughout the bulk of the cured system. Physically, gelation occurs when the bulk transforms from the liquid to the rubbery state. Thus, gelation leads to the transformation of the system accompanied by the divergence of the viscosity to infinity.

The choice of monomer system composition and curing conditions both have the potential to affect the gel point to a large extent. It takes only seconds for an individual chain to fully grow from initiation to termination. Primary chains having large molecular weight and containing numerous pendant double bonds are instantaneously formed at the beginning of the polymerization. As it was stated in the chapter 2.4.2, due to a high dilution of chains at the beginning of the reaction and relatively slow diffusion compared with fast propagation, rapid intramolecular reactions between propagating radical and pendant double bonds at a vicinity are favored. Since the cyclization reactions of flexible monomer species produce ineffective crosslinks, their occurrence delays a gel point conversion when compared with monomers that form primarily effective crosslinks. The number and concentration of reactive functional groups of a monomer also influence the appearance of the gel point. Inclusion of a higher functionality monomer would tend to promote an earlier gel point conversion due to a greater statistical likelihood of the effective crosslinking. Also, higher initiation rate leads to a formation of shorter chains. Therefore, a higher conversion at the gel point is reached since shorter chains with fewer pendants present statistically reduced likelihood for earlier onset of gelation when compared with longer chains [4,16,79]. Some publications described successful attempts to control the polymerization by addition of chain transfer agents into the polymerizing systems. By using these methods (e.g. atomic transfer radical polymerization, ATRP; reversible addition-fragmentation chain transfer RAFT), the supramolecular structure of the resulting networks may be severely altered, because of fast initiation and subsequent slow chain growth [91–93].

Beyond the gel point, the transition from chain-length dependent termination to reaction-diffusion-controlled termination occurs. Consequently, propagating chain radicals rely on spatial extension based on the propagation reaction to encounter other radical and terminate. Resin systems that present higher initial viscosities before polymerization tend to enter this transition to reaction-diffusion-controlled kinetics at an earlier stage of conversion and thus, reach a lower limiting conversion [13,33,94,95].

2.4.6 Vitrification

The glass transition temperature of a polymer network is often times of singular importance in determining the performance and potential usage of polymer networks [96]. For a polymer based direct restorative material to be clinically successful, its operational T_g must exceed not only the imposed cure temperature, but also the temperature fluctuations encountered in a moisture oral environment that includes periodic high stress conditions [4].

Unlike the gel point, which is a well-defined point on the conversion scale, vitrification is strongly dependent on the reaction conditions since it is determined by mobility restrictions that are affected by factors such as temperature and free volume. The decrease in free volume, associated with mobility restrictions of a polymer chain segments typically reduce the reaction rate by orders of magnitude, making it difficult to achieve higher values of the glass transition temperature without increasing the polymerization temperature. The heat released by the exothermic reaction, as well as radiant heat produced by the curing light units, provides the energy to maintain greater mobility within the forming network. Monomer systems with a higher functional groups concentration also partially contribute to the exothermic potential of the reaction [4,97,98].

Dimethacrylate networks are thought to be formed with a certain degree of heterogeneity, which implies a very wide variations in segmental chain mobility and relaxation times. Thus, the transition from the rubbery to the glassy state occurs over a range of functional groups conversions. Due to the process of microgel formation and aggregation, bulk vitrification does not occur until the crosslink density of the regions between the microgel domains reaches the threshold of significant mobility restriction. Therefore, the glass transition temperature should be considered as an average value, but not as a point at which the whole polymer changes from the rubbery to the glassy state [96–100]. With the transition to the bulk glassy state, the rate of polymerization slows by several orders of magnitude (i.e. auto-deceleration). However, network density and associated polymer properties, such as modulus and shrinkage stress, continue to develop. Driving the polymerization to a higher conversion elevates the T_g and creates polymers with more glassy regions. As it was stated by Abu-Elenain *et al.* [90], toward the latter stages of polymerization, crosslink density, related directly to the modulus in the rubbery state, increases rapidly with respect to conversion. The portion of a free monomer relative to pendant reactive groups decreases, with the relatively slow continued late-stage conversion leading mainly to crosslink formation. Even when a free monomer molecule is reacted during the final stage of polymerization, which adds to network mass without appreciably affecting network density, it diminishes a local plasticizing

contribution that effectively raises T_g and modulus [90]. However, some portions of the network may still remain in the rubbery state after curing. The more flexible portions of the restoration may promote monomer leaching, wear, fracture origination, and earlier failure of the restoration [101].

In conclusion, a resulting conversion of double bonds in a given resin system has generally served as the material property indicative for the prospective performance of these materials in use. However, other properties (e.g. modulus, volumetric shrinkage) need to be considered and are of similar importance for the development of durable materials.

3 AIM OF THE THESES

The main aim of this thesis is the investigation of kinetics and mechanisms of dimethacrylate copolymer networks morphogenesis with the ultimate goal to achieve defined network structures with maximum reproducibility. The base for understanding the controlled structure formation is provided by examination of the network-formation kinetic profiles. The kinetics of the polymerization is studied using resin systems containing structurally distinct monomer species, different comonomer molar ratios and varying concentration of photo-initiation system.

Furthermore, the relationship between supra-molecular structure, viscoelastic behavior and thermal stability of dimethacrylate networks is investigated. The relationship between the supra-molecular structure of the networks, storage modulus and damping behavior within a given temperature range is quantified. The differences in thermal stability are interpreted in terms of degradation mechanisms, which are highly dependent on the structural characteristics of a corresponding resin system.

4 EXPERIMENTAL PART

This chapter provides detailed description of materials and methods of characterization used to fulfill the aims of this thesis. The choice of materials includes the most commonly employed monomers and photo-initiation reagents in the formulations of current resin-based composites and dental adhesives. For the purpose of dynamic-mechanical analysis, experimental bodies pre-polymerized by heat-induced polymerization were employed to avoid thermally induced post curing during testing. Simple model resins mixtures are taken into consideration to fully understand the complex process of multifunctional networks formation.

4.1 Materials

Table 2: Materials used for the preparation of studied resin systems.

Full name	Abbreviation	Molecular weight Specific gravity	Supplier
Bisphenol A-glycidyl methacrylate	Bis-GMA	512.60 g/mol 1.16 g/ml	Esschem Europe Ltd
Ethoxylated Bisphenol A dimethacrylate (3 units of ethoxylation)	Bis-EMA	496.58 g/mol 1.12 g/ml	Esschem Europe Ltd
Urethane dimethacrylate	UDMA	470.56 g/mol 1.13 g/ml	Esschem Europe Ltd
Triethylene glycol dimethacrylate	TEGDMA (PEGDMA 3)	286.32 g/mol 1.09 g/ml	Esschem Europe Ltd
Diethylene glycol dimethacrylate	PEGDMA 2	242.27 g/mol 1.07 g/ml	Esschem Europe Ltd
Tetraethylene glycol dimethacrylate	PEGDMA 4	330.38 g/mol 1.08 g/ml	Esschem Europe Ltd
Camphorquinone	CQ	166.22 g/mol /	Sigma Aldrich / Merck
(Dimethylamino)ethyl methacrylate	DMAEMA	157.21 g/mol 0,93 g/ml	Sigma Aldrich / Merck
Dicumyl peroxide	DCP	270.37 g/mol /	Sigma Aldrich / Merck

4.2 Characterization methods

In order to determine important characteristics of polymer networks, experimental methods from the categories of structural analysis and thermo-mechanical testing had been employed. With respect to importance of the parameters obtained, the characterization methods used to fulfill the aims of this thesis are briefly described in this chapter.

4.2.1 Photo-calorimetry

DSC (differential scanning calorimetry) is the thermal analysis technique that measures the heat flow (dH/dt) to and from the sample as the function of time and/or temperature. It is the most widely used method for monitoring the process of polymerization in real time. DPC (differential photo-calorimetry) is the equivalent of DSC used for the characterization of light-curable materials. The measurements are particularly useful for clarification of the reaction kinetics and thermodynamic properties of the sample. Since the heat generated by the consumption of vinyl groups is very large when compared with other possible reactions such as activation and deactivation, it is assumed that other reactions would not have a significant effect on the heat release. Therefore, the rate of polymerization (R_p [mol·l^{-1}·s^{-1}]) in a unit of fractional vinyl conversion per second can be calculated (equation 10) by measuring the heat flow (h, [W/g], using the appropriate resin density, ρ) at a given temperature and dividing the value by the specific heat of the reaction, ΔH_0^{theor} (54,82 kJ/mol for methacrylate double bond, considering the limiting conversion of functional groups in the polymerizing system) [102].

$$R_p = -\frac{d[M]}{dt} = \frac{dH/dt}{\Delta H_0^{theor}} = \frac{h \cdot \rho}{\Delta H_0^{theor}} \tag{10}$$

Based on the assumption that the heat generated during the polymerization process is proportional to the percentage or concentration of the reacted functional groups, the extent of polymerization can be calculated. Integrating the heat flow curve versus time provide the vinyl double bond conversion, $P_{C=C}$ [%], [103]:

$$P_{C=C} = \frac{\int_0^t dH/dt}{\Delta H_0^{theor}} = \frac{\Delta H_t}{\Delta H_0^{theor}} \times 100 \tag{11}$$

4.2.2 Thermo-gravimetric analysis

Thermo-gravimetric analysis (TGA) is a common experimental method used to study the thermal stability, kinetics of degradation processes and degradation mechanisms of polymeric materials. The determination of the parameters of the thermal decomposition provides specific information regarding internal structures of polymers. Thermal degradation is affected by many factors, including molecular weight distribution, branching chains, crosslink density,

chemical structure of monomers, degree of conversion and others. Copolymers exhibit more intricate thermal behavior affected by the ratio of monomers used [104–106].

4.2.3 Infrared spectroscopy

Fourier-transform mid-infrared spectroscopy (FT mid-IR) and the obtained absorption spectra were used for the purposes of the monomer conversion measurements. The method is based on the measurement of intensity decrease of the methacrylate stretching mode absorption at 1637 cm^{-1} after polymerization reaction (Figure 13). These procedures rely on the presence of a stable absorption band that does not change as a consequence of polymerization. For example, in case of Bis-GMA based resins, the aromatic absorption band at 1608 cm^{-1} may serve as an internal standard [107–109].

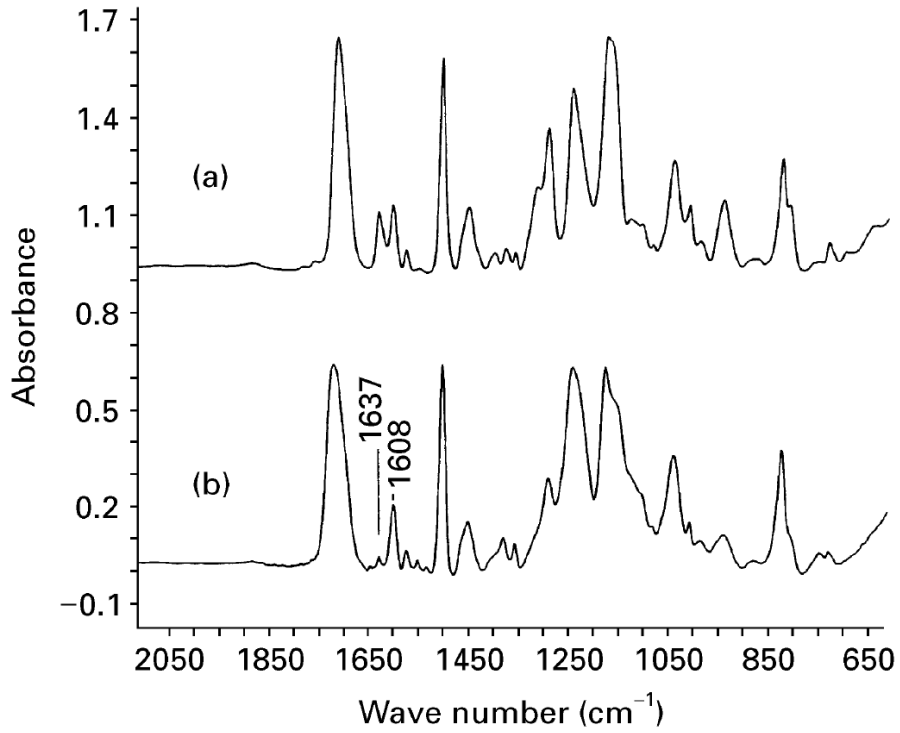

Figure 13: Infrared spectrum of neat Bis-GMA monomer, before and after curing [37].

4.2.4 Dynamic-mechanical analysis

Dynamic-mechanical analysis (DMA) was employed as a very useful technique to measure the relaxation characteristics of crosslinked networks and their bulk mechanical properties. The technique measures the complex modulus and the viscosity as a function of time or temperature based on the number of conditions adjusted by the operator. This is accomplished by the application of an oscillatory load on the specimen in tensile, compression, shear, torsion or bending modes of operation [110]. By varying the frequency, one can differentiate between the relaxation of a polymer backbone and the unreacted or pendant side chains and obtain valuable information about the structural characteristics of a polymer sample.

The negative logarithmic frequency dependence of the mechanical behavior takes the same form as temperature.

In brief, viscoelastic parameters include primarily the components of the dynamic modulus. This includes the storage modulus (E'), the measure of the material elasticity (the ability of a material to store energy), and the loss modulus (E'') expressing the ability of material to dissipate the energy (the difference in applied and returned energy). The complex modulus (E^*) is approximately equal to the value of storage modulus and is sometimes loosely referred to as elastic modulus, E. The loss tangent ($\tan\delta = E''/E'$) is a useful dimensionless parameter that determines the macroscopic physical properties such as the damping for free vibrations. Tangent delta ($\tan\delta$) is defined as the ratio of the loss modulus to the storage modulus and is the indicator of how well a material can dissipate the energy. It has a complex relationship to the distribution of the relaxation times. A breadth of the transition region is related both to the crosslink density and a degree of structural heterogeneity.

The course of the storage modulus captured over a range of temperatures or frequencies shows clearly the different regions of the viscoelastic behavior. Considering crosslinked polymers in general, the modulus decreases from the glassy region, passes through the glass transition region characterized by a sharp decrease in modulus, and then reaches the rubbery plateau region. Viscoelastic liquid region cannot be reached because of the chemically cross-linked character of the cured material. A value of the storage modulus in the rubbery plateau region indicates a level of the crosslink density of the polymer network. However, the rubber elasticity theory cannot be used to estimate the crosslink density on the quantitative bases because of non-Gaussian chain statistics in these highly crosslinked network systems (see Chapter 2.4). Therefore, the rubbery modulus can be used as a measure of the crosslink density on the qualitative basis, and the actual values cannot be calculated [91,111–114].

4.3 Experiments overview

This chapter summarizes the way of preparation of different resin formulations and curing procedures of experimental bodies characterized by the aforementioned experimental methods. From the manufacturer, the monomers with a high purity grade were obtained (maximum content of 100 ppm of MeHQ as an inhibitor), and were used as received without further purification. Composition and designation of all of the studied resin formulations are summarized in Table 3 (light cured samples for DPC, FTIR and TGA analysis) and Table 4 (heat cured samples for DMA and FTIR analysis).

4.3.1 Photo-polymerization kinetics (DPC)

Prior to mixing, the monomers (see Chapter 4.1) were heated up and kept at 60 ºC for one hour to reduce its viscosity. Then, the monomers were dosed in appropriate molar ratios into the light-impermeable vials and mixed by means of magnetic-stirring for one hour. After that, the components of photo-initiation system were added in the appropriate molar concentrations and dissolved by mixing the system for another hour. The same molar concentrations of camphorquinone (CQ) and (Dimethylamino)ethyl methacrylate (DMAEMA) were added into the resin mixtures in order to keep the equimolar ratio of photo-sensitizer and photo-reductant to obtain comparative results according to equation 5. Composition and designation of all of the studied resin formulations are summarized in the Table 3. Prior to measurement, the resin systems were stored in the fridge at 5 ºC. Before the weighing of the samples into the aluminum pans, the resins were kept in thermostat at 37 ºC for 60 minutes. The measurement was carried out immediately after the placement into the aluminum pans.

Monitoring of the polymerization process was carried out using DSC 2920 calorimeter (TA Instruments, USA) equipped with the extension for photo-calorimetry. Two aluminum pans were placed in the sample holder of DSC furnace. Resin samples weighing approximately 10 mg (N = 5 for each resin formulation) were placed in one pan, while the other pan was left empty as a reference. Resin formulations were tempered at 37 ºC in the DSC furnace for 1 minute, and then irradiated by light emitted from the mercury-xenon gas discharge lamp (Oriel, Newport) for 10 minutes, using FSQ-BG 40 filter (Newport) with the maximum transmission wavelength of 470 nm. Measurements were carried out at constant temperature of 37 ºC under nitrogen atmosphere (70 ml/min flow) to avoid the formation of oxygen inhibition layer. Heat flow [mW] vs. time [s] was continuously recorded (N = 5 for each resin formulation). Conversion of double bonds and polymerization rate were calculated based on the measured heat flow profiles according to equations 10 and 11.

4.3.2 Determination of degree of double bonds conversion (FTIR)

A sample (droplet) of unpolymerized resin was placed over the diamond crystal and the absorbance peaks before curing were obtained in the attenuated total reflection (ATR) mode. The cured resin droplets removed from the aluminum pans after DPC analysis were used as the cured specimens to determine the decrease of intensity of aliphatic C=C peak at 1637 cm^{-1}

after curing. The measurement was performed immediately after the DPC analysis. The cured resin droplets were laid over the crystal and fixed by the sample holder. In the same way, the degree of double bonds conversion was determined for the heat-cured samples. The absorbance peaks were obtained for un-polymerized resins and the polymerized droplets, that had been cured simultaneously with the experimental bodies intended for the DMA analysis in the silicone rubber mold. After curing, the resin droplets were treated the same way as the experimental bodies (see chapter 4.3.4), and the measurement was performed prior to DMA analysis.

FTIR spectra of cured and uncured resin samples (N = 5 for each resin formulation) were obtained using Tensor 27 spectrometer (Bruker, USA) in ATR mode with diamond crystal, set up to 64 scans and 4 cm^{-1} resolution. The percentage of unreacted double bonds was determined from the ratio of absorbance intensities of aliphatic C=C peak at 1637 cm^{-1} against internal standards before and after curing of the specimens. As internal standards, aromatic peak at 1608 cm^{-1} for Bis-GMA and Bis-EMA based systems, carbonyl peak at 1720 cm^{-1} for neat TEGDMA (PEGDMA) systems, and secondary amine group at 1527 cm^{-1} for UDMA system were used. The same resin systems were analyzed by FTIR and DPC to compare the degree of double bonds conversion obtained by both methods.

4.3.3 Kinetics of thermal degradation (TGA)

The resin formulations for the purpose of TGA analysis were mixed by the same manner as for the colorimetric analysis. Afterwards, the resin systems were cured in the form of discs (5 mm diameter, 1 mm height). The samples were prepared by pouring the resin into the silicon rubber mold, tempered at 37 ºC for 15 minutes, covered with mylar strips and put into the light-curing chamber Targis Power (Ivoclar Vivadent, Schaan, Liechtenstein). The source consists of 75 W halogen lamp emitting radiation between 400 and 580 nm and has maximum peak at 470 nm. The samples were irradiated for 4 minutes on each side. The measurement was carried out immediately after the curing.

Kinetics of degradation process was monitored using thermo-gravimetric analyzer Q 500 (TA Instruments, USA). Cured resin samples about 20 mg each were used (N = 3 for each resin formulation). First, the specimens were held at 50 ºC for 2 minutes for the temperature stabilization throughout the sample bulk and then heated up to 600 ºC. The measurements were performed at 10 ºC/min heating rate under a constant nitrogen flow of 60 ml/min. Sample mass vs. temperature were continuously recorded. The same resin systems were analyzed as in the case of DPC. TGA analysis was performed in order to characterize the systems cured under the same conditions while using structurally different monomer species. The measurements were partially affected by the thermally-induced post-curing, especially in the cases when the effect of molar concentration of photo-initiation system was studied. However, in agreement with the conclusions reported in the literature [104–106], the data obtained by the characterization of kinetics of thermal degradation process provide valuable insight into the structural parameters of photo-cured dimethacrylate networks.

Table 3: Summary of the light-cured resin systems characterized by DPC, FTIR and TGA.

Designation	Monomer formulation	Concentration of photo-initiators
Bis-GMA	Neat monomer	1.4 mol. %
Bis-EMA	Neat monomer	1.4 mol. %
UDMA	Neat monomer	1.4 mol. %
TEGDMA	Neat monomer	1.4 mol. %
PEGDMA 2	Neat monomer	1.4 mol. %
PEGDMA 3 (TEGDMA)	Neat monomer	1.4 mol. %
PEGDMA 4	Neat monomer	1.4 mol. %
Bis-EMA 0.2	Neat monomer	0.2 mol. %
Bis-EMA 0.6	Neat monomer	0.6 mol. %
Bis-EMA 1.0	Neat monomer	1.0 mol. %
Bis-EMA 1.4 (Bis-EMA)	Neat monomer	1.4 mol. %
Bis-EMA 1.8	Neat monomer	1.8 mol. %
TEGDMA 0.2	Neat monomer	0.2 mol. %
TEGDMA 0.6	Neat monomer	0.6 mol. %
TEGDMA 1.0	Neat monomer	1.0 mol. %
TEGDMA 1.4 (TEGDMA)	Neat monomer	1.4 mol. %
TEGDMA 1.8	Neat monomer	1.8 mol. %
Bis-GMA:TEGDMA 2:1	Molar ratio 2:1	1.4 mol. %
Bis-GMA:TEGDMA 1:1	Molar ratio 1:1	1.4 mol. %
Bis-GMA:TEGDMA 1:2	Molar ratio 1:2	1.4 mol. %
Bis-EMA:TEGDMA 2:1	Molar ratio 2:1	1.4 mol. %
Bis-EMA:TEGDMA 1:1	Molar ratio 1:1	1.4 mol. %
Bis-EMA:TEGDMA 1:2	Molar ratio 1:2	1.4 mol. %

4.3.4 Viscoelasticity of the networks (DMA)

The experimental bodies were cured in the silicon rubber molds providing the rectangular shape of 40 x 4 x 2 mm. The resins intended for heat curing were activated by addition of dicumyl peroxide in the concentration of 1.4 mol. % into the monomer mixture. The resins were poured into the silicon rubber mold and then cured in the vacuum oven at 120 ºC for

90 minutes and post-cured at 220 ºC for another 90 minutes. The cured samples were allowed to cool to the room temperature for 60 minutes, rinsed with acetone in order to remove oxygen inhibition layer and the overflows were trimmed. The samples were stored in the thermostat at 37 ºC for 24 hours prior to the analysis. Only heat-cured samples were used for the purposes of DMA to avoid thermally-induced post-curing during the analysis. The method of curing is irrelevant from the clinical point of view, but is instrumental for an understanding of the viscoelastic behavior of dimethacrylate networks.

The analysis was performed using DMA RSA G2 solid analyzer (TA Instruments, USA). Simply supported mode was preferred for dimethacrylate glassy networks in order to avoid buckling effects. Bending load was applied at 1 Hz frequency in a three-point bending 25 mm mode at a dynamic scan rate of 5 °C/min and 0.01 % deformation. Rectangular samples ($N = 5$ for each resin formulation) were placed into the analyzer geometry and the aforementioned viscoelastic parameters were recorded within the temperature range of 40–250 ºC.

Table 4: Summary of heat-cured resin systems characterized by DMA and FTIR.

Designation	Monomer formulation	Concentration of initiator
Bis-GMA	Neat monomer	1.4 mol. %
Bis-EMA	Neat monomer	1.4 mol. %
UDMA	Neat monomer	1.4 mol. %
TEGDMA	Neat monomer	1.4 mol. %
Bis-GMA:TEGDMA 2:1	Molar ratio 2:1	1.4 mol. %
Bis-GMA:TEGDMA 1:1	Molar ratio 1:1	1.4 mol. %
Bis-GMA:TEGDMA 1:2	Molar ratio 1:2	1.4 mol. %
Bis-EMA:TEGDMA 2:1	Molar ratio 2:1	1.4 mol. %
Bis-EMA:TEGDMA 1:1	Molar ratio 1:1	1.4 mol. %
Bis-EMA:TEGDMA 1:2	Molar ratio 1:2	1.4 mol. %

5 RESULTS AND DISCUSSION

5.1 Morphogenesis of dimethacrylate network

As it was discussed in the theoretical part, the process of tetra-functional networks morphogenesis is extremely complex, especially with regards to the reaction kinetics. The number of interesting morphological peculiarities arise from the differences in the structure of the employed monomer species, the ratio of different comonomers in the resin formulations, length of the monomer backbone, concentration of initiator and outer conditions (i.e. temperature and light intensity). The effects directly related to the formulation of resin systems are further studied in this chapter.

The DPC kinetic profiles provide a lot of important parameters, including a maximum rate of polymerization ($R_{p,\,max}$), position of the $R_{p,\,max}$ on the conversion scale (i.e. onset of auto-deceleration), a degree of limiting double bond conversion and a basic idea about mechanisms of network morphogenesis. Vinyl conversion was also measured by FTIR to compare the results of both methods. These findings were further discussed in relation to the data obtained from TGA analysis (i.e. kinetics of thermal decomposition).

5.1.1 Effects of monomer structure

The structural parameters of different monomer species clearly affect polymerization kinetics to a vast extent. The curves (Figure 14 and 15) show considerable differences in curing behavior despite the constant temperature, molar concentration of photo-initiators and light intensity of the curing unit. Table 5 shows the key kinetic parameters for homopolymerization of studied monomers. The results of limiting degree of double bond conversion as determined by DPC and FTIR differ in the range of 2–5 %. These differences are associated with the sensitivity and resolution of both methods, neglection of other possible reactions generating heat during DSC experiments beyond consumption of vinyl groups, weighing errors, and possible post-cure when the sample was moved from DPC measuring cell to FTIR apparatus.

Table 5: Mean and standard deviation values of maximum rate of polymerization ($R_{p,\,max}$), degree of conversion ($P_{C=C}$) at $R_{p,\,max}$ and limiting degree of conversion ($P_{C=C}$) as determined by DPC and FTIR; neat monomers.

Designation	$R_{p,\,max}$ [mol/l·s]	$P_{C=C}$ at $R_{p,\,max}$ [%]	$P_{C=C}$ [%], DPC	$P_{C=C}$ [%], FTIR
Bis-GMA	0.0156 (0.0011)	4.67 (0.32)	29.58 (0.45)	33.16 (0.69)
Bis-EMA	0.0452 (0.0014)	10.19 (0.06)	56.90 (1.45)	52.18 (1.29)
UDMA	0.1047 (0.0050)	13.19 (0.75)	57.80 (1.94)	55.14 (0.75)
TEGDMA	0.0448 (0.0015)	35.15 (1.27)	68.68 (1.17)	63.17 (1.32)

Among others, neat Bis-GMA monomer shows lowest $R_{p,\,max}$ (Figure 15), earliest onset of auto-deceleration period and lowest degree of double bond conversion. Dramatic increase in reaction rate in the early stage of polymerization is attributed to strong diffusion limitations of the termination (i.e. immediate gelation). However, since the initial resin viscosity is very high in case of Bis-GMA, the propagation reaction (i.e. movement of remaining monomers) becomes restricted also very early within the conversion scale ($P_{C=C}$ at $R_{p,\,max}$ = 4.67 %). Strong mobility restrictions associated with the vitrification cause very low limiting degree of conversion (29.58 % DPC, 33.16 % FTIR). The explanation of these findings relies in the potential for very strong and mostly intermolecular hydrogen bonding between monomers, causing a decreased mobility of monomer molecules during the polymerization, and rigid aromatic structure of Bis-GMA backbone with a large radius of gyration, decreasing the mobility of pendant functional groups during polymerization. The accessibility of pendant functional groups is severely limited due to the steric hinderance effects.

On the contrary, Bis-EMA (ethoxylated variant of Bis-GMA) shows different kinetic behavior with respect to the degree of conversion at $R_{p,\,max}$ ($P_{C=C}$ at $R_{p,\,max}$ = 10.19 %) and limiting conversion (56.90 % DPC, 53.18 % FTIR). Lacking hydrogen-bonding donor sites (substitution of 2-hydroxypropyl groups between aromatic core and methacrylate groups in Bis-GMA for flexible ethoxylated linkages in Bis-EMA) results in much lower initial viscosity by orders of magnitude (Table 1), allowing for a greater mobility in the bulk of the reacting system. The ether groups of Bis-EMA cannot participate in hydrogen bonding with each other. Thus, the main factor that limits the reaction progress is the rigid aromatic core structure. Similar conclusions, relating the differences of polymerization behavior of structurally similar monomer species to the potential for physical interactions, were reported in the literature [7,14,21–23].

Different reaction behavior was observed in case of UDMA monomer. The highest reaction rate was observed in case of UDMA homopolymerization, however, the degree of conversion at $R_{p,\,max}$ ($P_{C=C}$ at $R_{p,\,max}$ = 13.19 %) and especially degree of limiting conversion (57.80 % DPC, 55.14 % FTIR) are comparable with the same kinetic parameters of Bis-EMA homopolymerization. Lower initial viscosity and higher reaction rate allowed access to higher conversion levels. As it was shown by Lemon *et al.* [25], Khatri *et al.* [26] and Barszczewska-Rybarek [115], lower viscosity of UDMA based resins is related to the fact, that hydrogen bonding interactions associated with the urethane functionalities are significantly weaker than those associated with hydroxyl functionalities and may poses more intramolecular character. The higher reactivity of UDMA monomer is related to the flexible structure of its monomer backbone, including aliphatic core, urethane functional groups, and ethoxylated linkages between methacrylate functional groups. Also, as it was suggested by Sideridou *et al.* [13,30], the reactivity of UDMA may be related to other factors, including abstraction of labile hydrogen atoms from the carbamate groups. Due to these chain transfer reactions, caused by –NH– groups, the mobility of radicals increases and an alternative path of the propagation reaction is offered. These are the reasons why propagation proceeds further before it becomes diffusion-controlled. Furthermore, the flexibility of the monomer backbone is also associated with better accessibility of pendant functional groups in the vicinity of the radical site. This may, however, increase the reactivity and promote higher methacrylate groups conversion,

but the formation of primary cycles does not contribute to the effective crosslink density. The occurrence of primary cyclization reactions in UDMA homopolymers was reported by Achilias *et al*. [105] and later by Vouvoudi *et al*. [106].

Bimodal profile of reaction rate is evident in case of TEGDMA homopolymerization. This phenomenon was described by several studies [14,16,23] and has been interpreted in terms of low monomeric viscosity and primary cyclization. Bimodal profile is related to a delayed onset of diffusion-controlled termination. This effect goes hand in hand with low initial resin viscosity and extensive reactivity through primary cyclization, creating ineffective crosslinks. This behavior delays gelation and thus, the onset of auto-acceleration is also delayed. Thanks to the aforementioned parameters, especially the degree of conversion at $R_{p,\,max}$, reached by far the highest value when compared with other monomers ($P_{C=C}$ at $R_{p,\,max}$ = 35.15 %) despite the highest concentration of the double bonds per unit mass. The extent of cyclization during polymerization of TEGDMA was predicted on the basis of kinetic gelation models [76,116]. Initially, primary cyclization dominates and the cycles are formed at the expense of unreacted monomers, since pendant double bonds have an increased reactivity in the localized region of the free radical. This behavior is responsible for genesis of structural heterogeneity (i.e. formation of microgel domains). As conversion increases, the probability of crosslinking also increases and the network is formed. This decrease of reactivity through primary cyclization is the result of the inaccessibility of the pendant functional groups to the radical sites as they become sterically hindered. Afterwards, the reactivity of monomeric functional groups exceeds that of the pendant groups and polymerization continues until all functional groups are inaccessible to the radicals. Based on the kinetic models, the fraction of pendant double bonds that undergo primary cyclization approaches 80 % at the beginning of the polymerization, and dominates over secondary cyclization reactions and effective crosslinking over the wide range of functional groups conversion. The probability of primary cyclization severely decreases with increasing molecular weight of the monomers, because pendant functional group is further from the propagating radical. This may be the reason of lower extent of primary cyclization reactions in the case of UDMA homopolymerizations.

Another model enabling the estimation of probability of primary cyclization with regard to the stiffness of the monomer backbone was developed by Elliot *et al.* [16]. TEGDMA pendants undergo cyclization almost three-times more often than Bis-GMA pendants under the same conditions (i.e. pendants are surrounded by the same quantity of radicals, the probability of crosslink formation is the same). This difference is given by the flexibility of the aliphatic monomer backbone when compared with stiff aromatic backbone of Bis-GMA. The probability of cyclization is the highest immediately after the formation of the pendant, when the propagating radical is in the vicinity. However, if this is prevented due to the stiffness of the monomer and a sterically unfavorable ring would be formed, the probability of primary cycle formation is fairly low. Bimodal profile was not seen in case of UDMA homopolymerization, even though the occurrence of primary cyclization reactions is also very likely to occur due to the flexibility of monomer backbone. This difference is related to the lower probability of primary cyclization [76,116] and higher initial viscosity [25], resulting in almost immediate gelation, earlier onset of auto-acceleration and steady rise of the reaction rate.

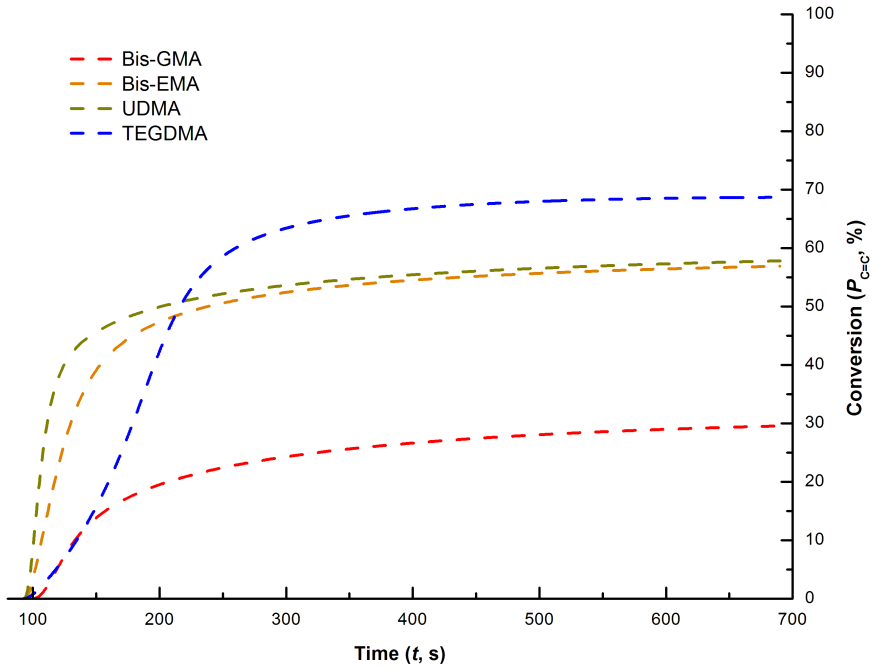

Figure 14: Photo-polymerization kinetic data, degree of double bond conversion as a function of time; neat monomers.

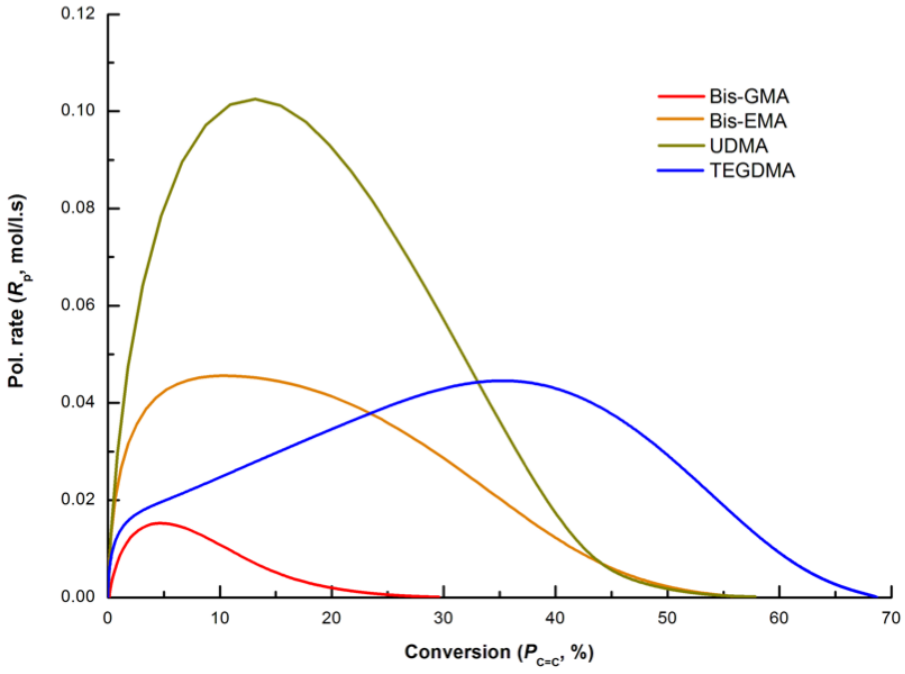

Figure 15: Photo-polymerization kinetic data, reaction rate (R_p) normalized by the initial double bond concentration; neat monomers.

The study of thermal degradation kinetics provides a valuable information regarding the morphology of dimethacrylate networks. This may be helpful for further interpretation of the conclusions formulated on the basis of photo-polymerization kinetics, even though a post-curing is expected to occur resulting in the slight network development. Table 6 shows the threshold parameters of thermal degradation process of dimethacrylate homopolymers Thermal decomposition is a radical depolymerization, where either end chain or random scission of the macromolecular chains occurs. As it was reported by Pielichowski *et al*. [117], in case of PMMA, end chain scission initiated at vinylidene groups is favored at low temperatures and random scission at high temperatures. Figure 16 shows the schematic representation of thermal degradation process of multifunctional networks.

Table 6: Mean and standard deviation values of temperature where thermal degradation start (T_0), and the first (T_1) and second (T_2) maximum of thermal decomposition and residual mass at 600 ºC; neat monomers.

Designation	T_0 [ºC]	T_1 [ºC]	T_2 [ºC]	**Residual mass at 600 ºC [%]**
Bis-GMA	258.26 (0.72)	/	399.71 (1.22)	14.22 (0.52)
Bis-EMA	238.97 (1.23)	/	418.71 (0.34)	0.94 (0.13)
UDMA	228.40 (2.68)	331.33 (0.51)	427.46 (0.80)	0.43 (0.14)
TEGDMA	212.37 (2.89)	300.68 (0.46)	379.12 (0.99)	0.46 (0.45)

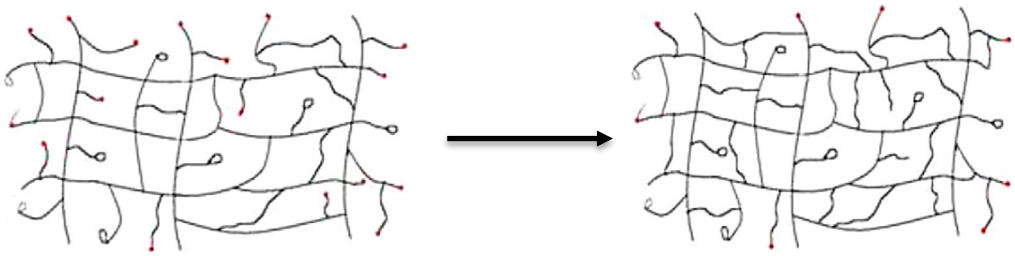

Post-curing, further network development; 40–200 ºC

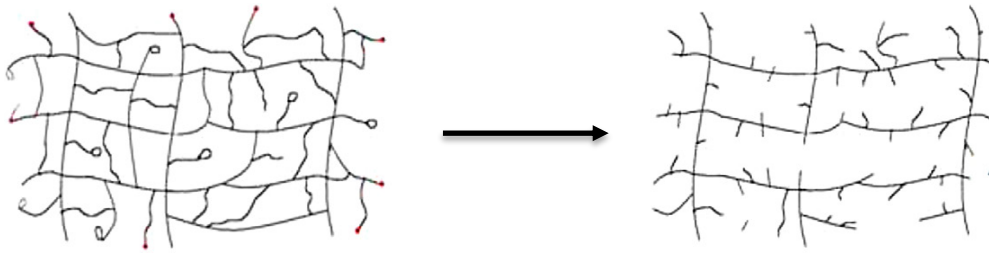

Residual monomers decomposition, pendants scission, defect structures subtraction; 200–350 ºC

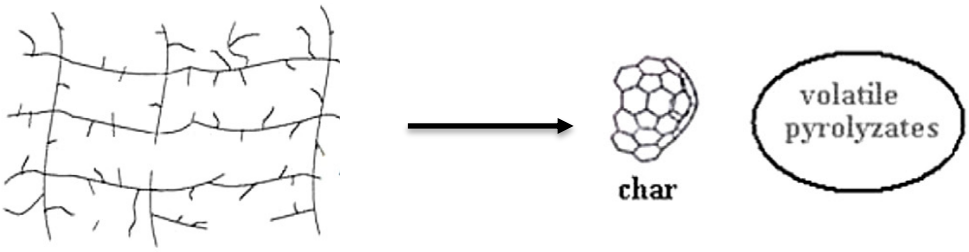

Network decomposition; 350–550 ºC

Figure 16: Schematic representation of mechanism of post-curing and thermal degradation process of dimethacrylate networks [104–106].

As expected for highly crosslinked polymers, thermal decomposition is complex heterogeneous process consisting of several distinct steps. The initial loss may be associated with the degree of effective crosslinking and degree of vinyl conversion. As it was published by Teshima *et al*. [104], who performed a TGA-MS analysis of dimethacrylate copolymers, the initial products of pyrolysis are methacrylic acid (MA) and 2-hydroxyethyl methacrylate (HEMA) in a similar way to the degradation of PMMA. The fact that the amount of these compounds decreases with increasing conversion in the initial and second phase of thermal decomposition suggests, that MA and HEMA were generated from residual unpolymerized monomers and pendant functional groups. In a later stage of decomposition, propionic acid (PA) from the ends of polymer chains and phenol generated from a random chain scission in the final stage of decomposition were clearly identified.

In case of Bis-GMA homopolymer, degradation is completed in only one step, starting at 260 ºC (T_0), and reaching the maximum rate at 400 ºC (T_2). Similar behavior was observed in case of Bis-EMA homopolymer, but with lower residual mass (carbonization yield). As it was discussed above, the probability of primary cyclization is severely limited because of the presence of stiff and rigid aromatic monomer backbone. Due to the steric hinderance effects, these monomers are not able to react intramolecularly with the radical on the same propagating chain until several repeat units had been added and thus, resulting morphology is more homogeneous. The degradation at higher temperatures is attributed to the existence of only small number of inhomogeneities in the structure of the networks based on monomers with stiff backbone. The temperature giving the maximum rate of thermal decomposition (T_2) is higher in case of Bis-EMA due to the higher degree of covalent crosslinking and the fact, that the hydrogen bonding interactions in Bis-GMA are weakened abruptly due to the steady rise of the temperature [25].

In contrast, thermal degradation proceeds in two distinct steps in the case of UDMA and TEGDMA homopolymers (Figures 17, 18). The initial weight loss of TEGDMA begins at 212 ºC, and the decomposition rate maxima occurred at 300 ºC and 382 ºC. These thresholds are slightly higher in case of UDMA, starting the degradation at 228 ºC, and reaching the decomposition rate maxima at 331 ºC and 427 ºC. These results go hand in hand with the assumptions made on the basis of polymerization kinetics. Due to the varying

reactivity of functional groups, in agreement with the computer simulations based on kinetic gelation models, and the interpretation of the published experimental data, microgel domains are created around multiple initiation sites upon exposure to polymerization light, followed by their agglomeration into clusters and their interconnections [74–77,116–119]. As it was already discussed above, at low conversions the reactivity of pendant functional groups far exceeds the reactivity of monomeric functional groups. This leads to the formation of multiple loops and highly crosslinked regions embedded in a less crosslinked matrix. In a later stage, when conversion increases, pendant functional groups become hindered in the inner structure of the microgels and less crosslinked matrix is formed. The appearance of two degradation steps is attributed to the heterogeneous morphology of the networks. The first step reflects the degradation that originates in the loosely crosslinked regions of the network, whereas the second step is associated with the decomposition of the densely crosslinked domains. Higher thermal stability of UDMA is related to the appearance of hydrogen bonding interactions [25] and the fact, that cyclization is more likely when the spacer length between methacrylic groups is smaller [16]. The lower extent of cyclization is evident from the dTGA curves (Figure 18) when the proportions of first and second degradation steps are compared. Corresponding conclusions related to the mechanisms of thermal degradation were reported in the literature, where it had been interpreted based on the determination of activation energies of the distinct phases of degradation processes [105,106,120].

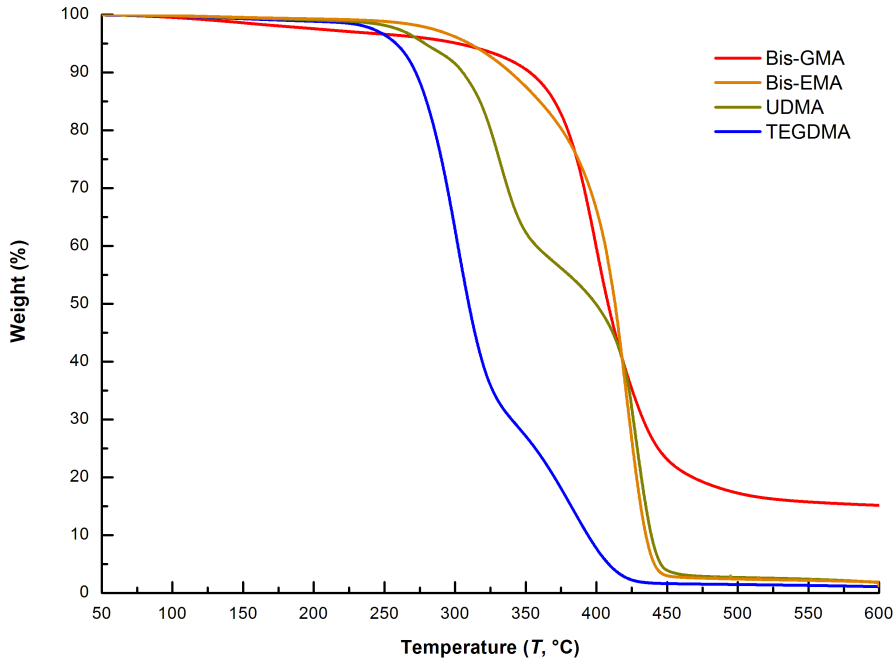

Figure 17: TGA scans, mass loss vs. temperature; neat monomers.

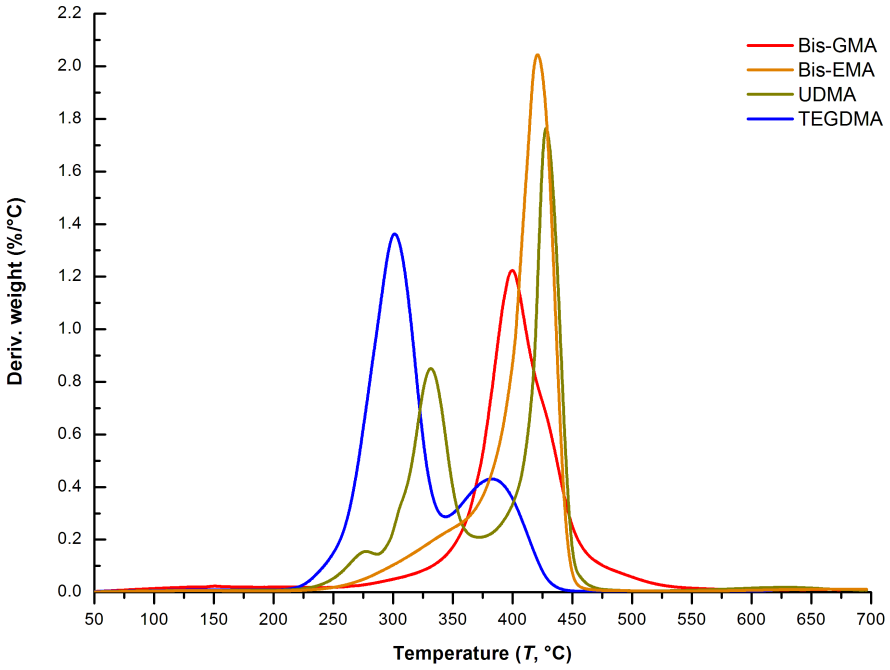

Figure 18: Derivative curves, mass loss vs. temperature; neat monomers

5.1.2 Effects of comonomers ratio

Synergistic effect of base and diluent monomers combination on the polymerization rate, onset of auto-deceleration and the limiting degree of double bond conversion was found in both Bis-GMA and Bis-EMA based comonomer systems with TEGDMA. Copolymerization kinetic profiles obtained at the constant temperature, molar concentration of photo-initiators and light intensity of the curing unit are shown in Figures 19–22. Table 7 summarizes the main kinetic parameters of dimethacrylate copolymerizations.

Table 7: Mean and standard deviation values of maximum rate of polymerization ($R_{p,\,max}$), degree of conversion ($P_{C=C}$) at $R_{p,\,max}$ and limiting degree of conversion ($P_{C=C}$) as determined by DPC and FTIR; Bis-GMA/TEGDMA and Bis-EMA/TEGDMA copolymers.

Designation	$R_{p,\,max}$ [mol/l·s]	$P_{C=C}$ at $R_{p,\,max}$ [%]	$P_{C=C}$ [%], DPC	$P_{C=C}$ [%], FTIR
Bis-GMA	0.0156 (0.0011)	4.67 (0.32)	29.58 (0.45)	33.16 (0.69)
Bis-GMA:TEGDMA, 2:1	0.0489 (0.0016)	9.50 (0.54)	45.78 (1.20)	42.21 (3.75)
Bis-GMA:TEGDMA, 1:1	0.0551 (0.0012)	14.91 (0.22)	55.42 (1.16)	51.42 (2.77)
Bis-GMA:TEGDMA, 1:2	0.0548 (0.0021)	20.34 (1.04)	59.22 (1.56)	57.50 (3.39)
Bis-EMA	0.0452 (0.0014)	10.19 (0.60)	56.90 (1.45)	52.18 (1.29)
Bis-EMA:TEGDMA, 2:1	0.0556 (0.0017)	22.74 (0.70)	63.44 (1.99)	60.05 (0.70)
Bis-EMA:TEGDMA, 1:1	0.0527 (0.0029)	26.86 (0.53)	64.44 (0.85)	61.83 (1.17)
Bis-EMA:TEGDMA, 1:2	0.0490 (0.0025)	30.70 (0.75)	65.44 (0.22)	62.73 (0.47)
TEGDMA	0.0448 (0.0015)	35.15 (1.27)	68.68 (1.17)	63.17 (1.32)

Copolymerization kinetic profiles show intermediate behavior between those of the corresponding monomers. In the case of Bis-GMA based copolymers, dramatic increase of reactivity was observed, because the mobility of monomers in the reacting system increased. This is due to the following factors associated with growing proportion of TEGDMA. First, the viscosity of the resin mixture decreased, allowing for greater mobility of the reacting species, second, the concentration of functional groups in the reacting system increased due to the incorporation of the monomer with lower molecular weight, and third, reactivity of pendant functional groups increased due to the higher flexibility of diluent monomer backbone. Thus, the propagation reaction becomes restricted by diffusion in the later stages of the reaction and the $R_{p,\,max}$ and vitrification of the emerging network is shifted to the higher conversions (Table 7, Figure 20). The limiting degree of conversion was affected by dilution by the same manner, since the more flexible reacting species with lower molecular volume are able to react further by the segmental diffusion, even after the diffusion-controlled mechanism of propagation prevails. In relation to this assumption, the reports concerning the compositional drift occurrence during copolymerization of base and diluent monomers were

identified in the literature [17,122]. The analysis of leachable components proved that the composition of extracts was not proportional to the composition of initial mixture and that the contribution of low-viscous diluent increases with increasing conversion.

It is obvious, that $R_{p,\,max}$ increased in the case of all copolymerized systems when compared with neat monomers (Figure 20). As it was reported by Dickens *et al.* [14], the initial viscosity influences the reactivity up to the rate where auto-acceleration stops. The reactivity is optimal within the range of viscosities when significant monomer diffusion is allowed on one side, and the segmental movements of macroradicals are restricted due to the gelation on the other. The highest polymerization rate was identified in the case of equimolar mixture of base and diluent monomer, suggesting that in this case, the viscosity was optimal to reach the highest reactivity under the given conditions (i.e. temperature, initiator concentration, light intensity). At lower concentration of diluent monomer, diffusivity of monomers becomes restricted earlier on the conversion scale. In Bis-GMA based resin formulations, this effect is amplified due to the strong hydrogen bonding interactions. In this case, two ether linkages and two methacrylate ester carbonyl groups in TEGDMA can act as the hydrogen bond acceptors. Intermolecular hydrogen bonding between Bis-GMA and TEGDMA can cumulatively enhance the viscosity effects, allowing rapid onset of auto-acceleration [25,124]. Another effect of copolymerization may be the suppression of cyclization reactions. In agreement with kinetic gelation models [76,116], the pendant functional groups become sterically hindered earlier on the conversion scale if the network with increased proportion of effective crosslinks is formed. Indeed, bimodal reaction rate profile was identified only when TEGDMA monomer was in molar excess. Regarding this resin formulation, both lower initial resin viscosity and greater tendency towards primary cyclization, delay the mobility limitation threshold associated with diffusion-controlled mode of termination (i.e. gelation), that allows effective auto-acceleration.

Furthermore, corresponding molar mixtures including ethoxylated analogue of Bis-GMA were studied in order to describe the differences in their reactivity associated with lacking hydrogen bonding sites. As it was discussed above, the extremely high viscosity of Bis-GMA requires the addition of substantial amount of diluent monomer in order to optimize the reactivity. The logarithmic scale of viscosity due to the strong intermolecular hydrogen bonding was identified in Bis-GMA based resin mixtures, ranging between 0.1 and 1000 Pa·s, with respect to molar ratio of base and diluent monomer. On the other hand, the viscosity of Bis-EMA based resin mixtures does not increase dramatically with the increasing content of base monomer (0.1–2 Pa·s) [14]. Thus, an aromatic core structure is not the most important aspect contributing to the reaction behavior. However, the 2-hydroxypropyl groups in Bis-GMA compared to ethoxy groups in Bis-EMA are the main factor causing the differences in copolymerization kinetics. This is due to the impact on viscosity of the resin systems and possible interactions between hydrogen bond donor and acceptor sites.

The increase in reactivity in Bis-EMA based systems was accomplished by addition of relatively small amount of TEGDMA. The addition of TEGDMA causes the severe shift of $R_{p,\,max}$ on the conversion scale and increase of limiting degree of conversion (Table 7, Figures 21, 22). These effects are associated with the lacking hydrogen bonding potential. The

segmental diffusion in the polymerizing systems is facilitated and thus, higher degree of conversion is reached at the onset of auto-deceleration. Bimodal reaction rate profile seen in the case of TEGDMA homopolymerization, is also obvious in the copolymerizations with Bis-EMA (Figure 22). As it was discussed above, this is associated with both low initial viscosity and extensive primary cyclization, delaying the effects associated with the mobility restrictions. In TEGDMA rich resin mixtures, the termination occurs initially by translation (chain-length dependent diffusion of macroradicals). In the later stages, auto-acceleration occurs as a result of decreased frequency of bimolecular termination. The ability of the large radicals to diffuse towards each other becomes impaired, and chain radicals become more mobile by reacting through unreacted monomers. This progress of the reaction is related to the bimodality of the reaction rate profile. The evidence that this effect is primarily related to the initial viscosity of the resin system was published by Young and Bowman [97], who studied the effect of polymerization temperature on reaction-diffusion-controlled termination in the case of DEGDMA homopolymerizations. As the temperature and mobility of the reacting species decrease, the termination becomes diffusion-controlled in the earlier stages of the reaction. As demonstrated for the series of TEGDMA containing resin systems (Figure 22), the onset of reaction-diffusion-controlled termination moves closer to Bis-EMA homopolymerization, where this mechanism dominates from the beginning. In other words, while the rate of termination and propagation decrease during the polymerization course, the changes in relative ratios of these rates are the key factors determining the overall reaction rate profile. When the termination becomes diffusion-controlled, a break in the reaction rate profile is identified, indicating the change in the proportionality between propagation and termination reactions. Afterwards, the propagation is still reaction-controlled, until the decrease associated with diffusion-controlled propagation occurs (i.e. auto-deceleration).

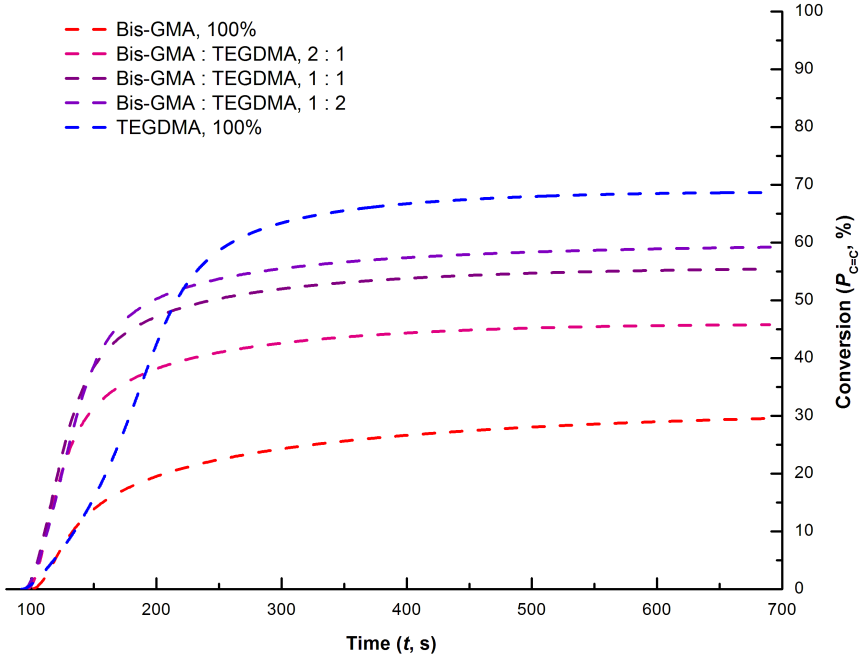

Figure 19: Photo-polymerization kinetic data, degree of double bond conversion as a function of time; Bis-GMA based systems.

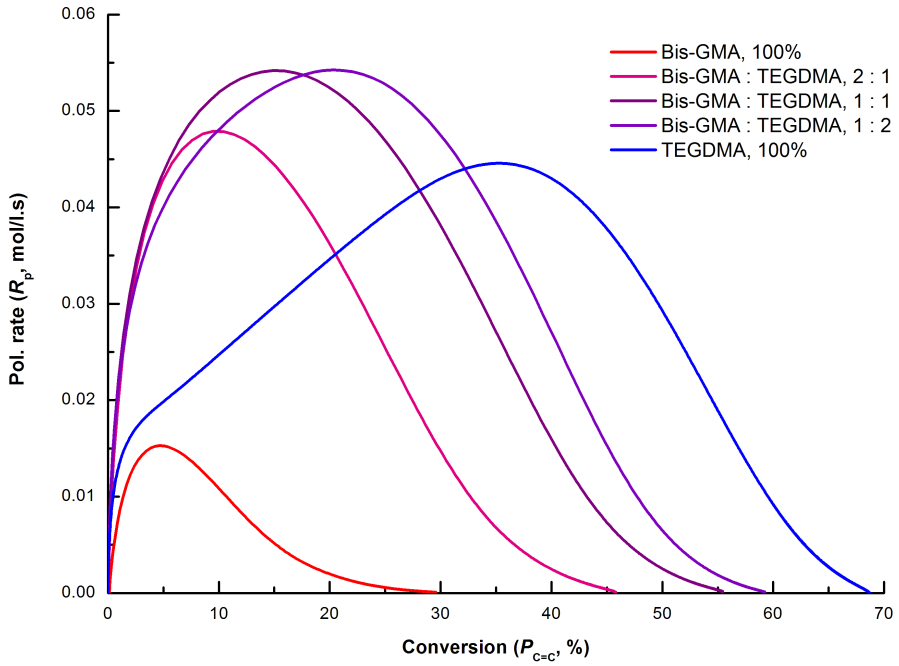

Figure 20: Photo-polymerization kinetic data, reaction rate (R_p) normalized by the initial double bond concentration; Bis-GMA based systems.

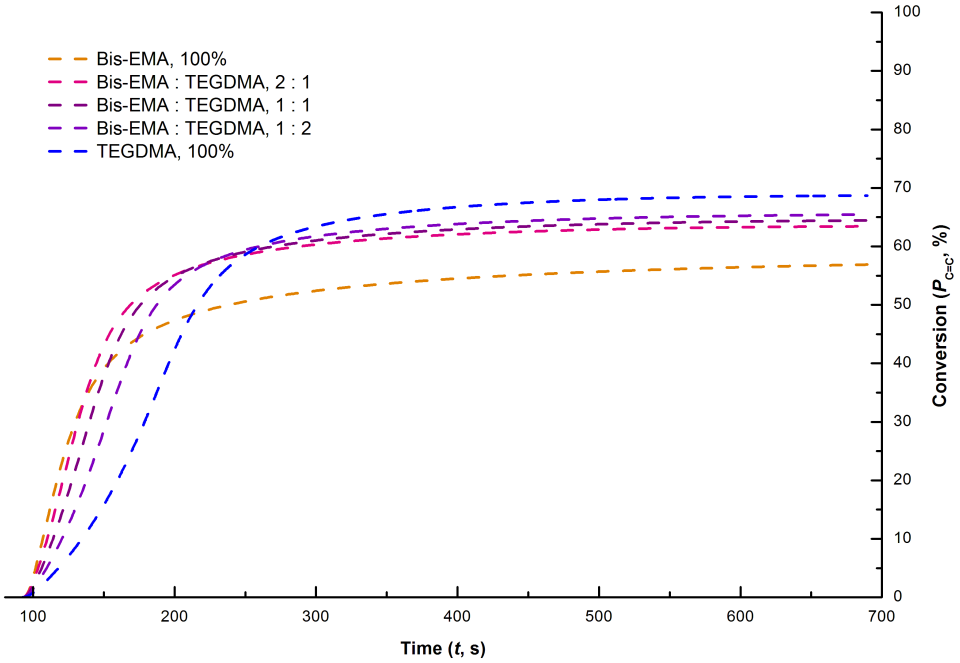

Figure 21: Photo-polymerization kinetic data, degree of double bond conversion as a function of time; Bis-EMA based systems.

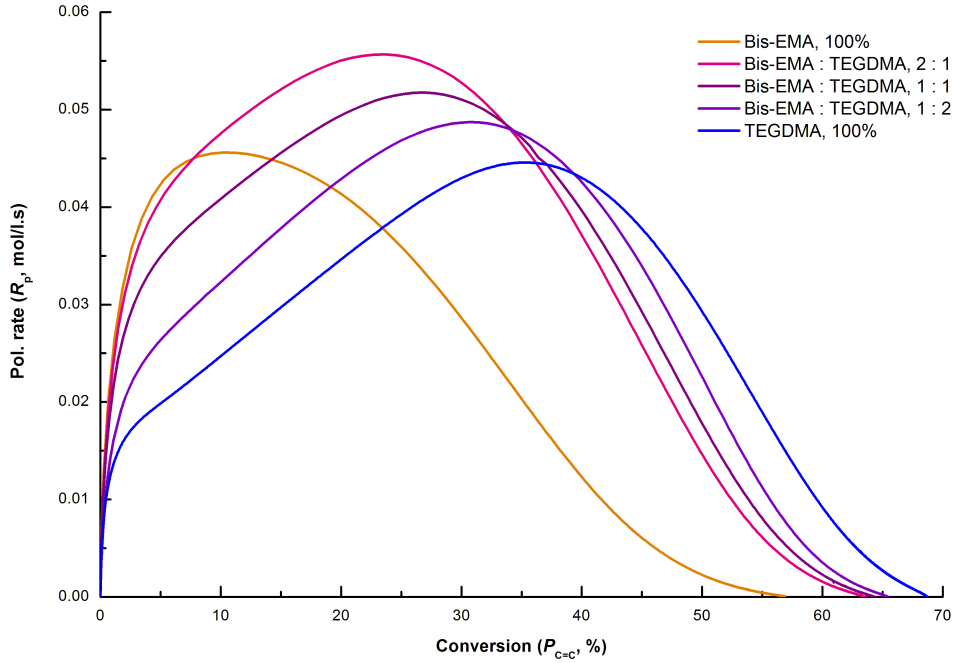

Figure 22: Photo-polymerization kinetic data, reaction rate (R_p) normalized by the initial double bond concentration; Bis-EMA based systems.

Table 8 summarizes the threshold parameters of thermal degradation process of copolymers based on different molar ratio of base and diluent monomers.

Table 8: Mean and standard deviation values of temperature where thermal degradation start (T_0), and the first (T_1) and second (T_2) maximum of thermal decomposition and residual mass at 600 ºC; Bis-GMA/TEGDMA and Bis-EMA/TEGDMA copolymers.

Designation	T_0 [ºC]	T_1 [ºC]	T_2 [ºC]	Residual mass at 600 ºC [%]
Bis-GMA	258.26 (0.72)	/	399.71 (1.22)	14.22 (0.52)
Bis-GMA:TEGDMA, 2:1	243.88 (1.03)	/	400.05 (0.71)	11.06 (0.10)
Bis-GMA:TEGDMA, 1:1	239.30 (2.01)	333.63 (1.30)	401.07 (1.14)	8.73 (0.17)
Bis-GMA:TEGDMA, 1:2	234.35 (1.88)	315.58 (0.91)	399.27 (1.25)	6.75 (0.14)
Bis-EMA	238.97 (1.23)	/	418.71 (0.34)	0.94 (0.13)
Bis-EMA:TEGDMA, 2:1	238.11 (2.20)	341.93 (0.89)	421.30 (1.41)	0.60 (0.29)
Bis-EMA:TEGDMA, 1:1	234.97 (1.73)	339.64 (1.68)	422.10 (1.35)	0.55 (0.12)
Bis-EMA:TEGDMA, 1:2	232.34 (1.54)	330.82 (2.18)	421.37 (1.52)	0.75 (0.13)
TEGDMA	212.37 (2.89)	300.68 (0.46)	379.12 (0.99)	0.46 (0.45)

In case of both Bis-GMA and Bis-EMA based copolymers, with higher content of TEGDMA in the network structure of the copolymer, the temperature of the onset of weight loss (T_0) decreases (Figures 23, 25). This suggests that the degree of effective crosslinking in the network structure decreases along with decreasing concentration of the base monomers which are not prone to the primary cyclization reactions. Temperature of the highest degradation rate (T_1) of the first phase fluctuates in TEGDMA containing mixtures. The height of dTGA curve decreases and T_1 increases along with increasing content of base monomers (Figures 24, 26). This may be the evidence that the origination of structural inhomogeneities is partially suppressed thanks to the incorporation of base monomers with rigid monomer backbone into the network structure. Based on that assumption, the key parameter affecting the thermal stability of the networks at temperatures above 250 º C is the degree of effective crosslinking, not the limiting vinyl conversion. The temperature (T_2) giving the highest degradation rate in the final phase was constant regardless of the molar concentration of the base and diluent monomers and limiting conversion. Since the height of the dTGA curve implies the quantitative portion of the network with certain structural parameters, it can be concluded that with the growing proportion of rigid base monomer in the comonomer formulation, also the density of effective crosslinks increases and resulting structure appears to be homogeneous. On the other hand, if the proportion of flexible diluent monomer increases, the heterogeneous character of the network becomes more pronounced. The origin of structural heterogeneity was discussed above and interpreted by varying pendant functional groups reactivity and formation of domains with varying extent of effective crosslinking. The kinetics of thermal decomposition of copolymerized networks was also studied by Achilias *et al*. [120] and Rigoli *et al*. [121], reaching the similar conclusions in terms of complexity of thermal decomposition process. The process was characterized by performing isoconversional kinetic analysis. Variations in activation energy attributed to distinct degradation steps were interpreted in the similar way, i.e. by the differences in the structure and the existence of inhomogeneities associated with the kinetic behavior of individual monomer species during copolymerization.

The final point to be discussed are the differences arising from the specific structural features of Bis-GMA and Bis-EMA base monomers. Copolymer Bis-GMA 2:1 follows a behavior of pure Bis-GMA, whereas in the case of the same composition of Bis-EMA based copolymer, a shoulder on dTGA curve appears clearly. This may be the evidence that the primary cyclization reactions are suppressed due to the intermolecular pre-association with Bis-GMA monomer, which is in molar excess. In agreement with Lee *et al*. [124], the presence of hydroxyl groups can lead to formation of multimeric aggregated species thanks to the possible hydrogen bonding interactions between hydroxyl groups, carbonyl and ether functionalities. As the concentration of TEGDMA increases, greater tendency towards origination of inhomogeneities is observed due to greater likelihood of cyclization. The substitution of glycerolate-based side chain for 3 ethoxylated units leads to greater likelihood of primary cyclization reactions, even when the base monomer is in molar excess. This is due to the absence of the hydrogen bond donor functionalities and greater flexibility of Bis-EMA side chains. On the other hand, the temperature giving the highest rate of thermal decomposition in the second step (T_2) is higher in the case of Bis-EMA including copolymers. As it was already

mentioned above, this is due to a higher degree of covalent crosslinking, which is allowed thanks to the lower initial viscosity of the resin mixture and the fact, that non-covalent interactions associated with the hydrogen bonds are disrupted by increase of the temperature.

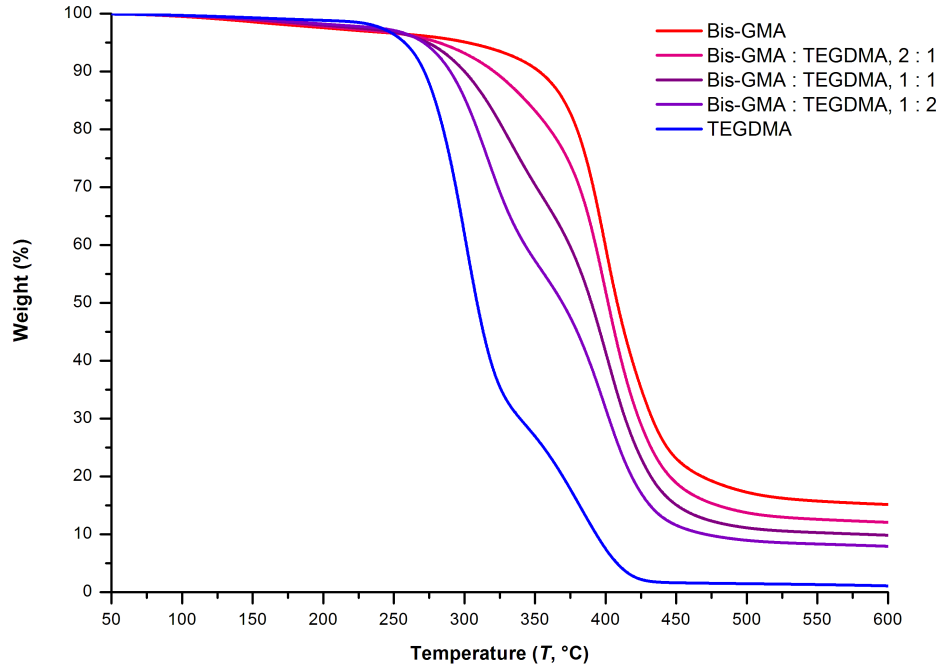

Figure 23: TGA scans, mass loss vs. temperature; Bis-GMA based systems.

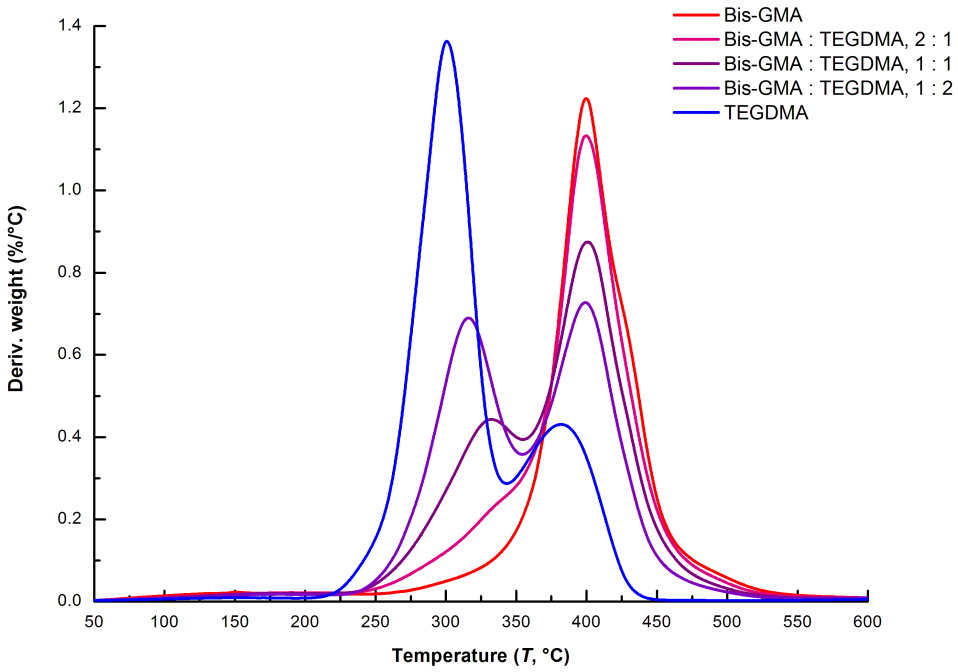

Figure 24: Derivative curves, mass loss vs. temperature; Bis-GMA based systems.

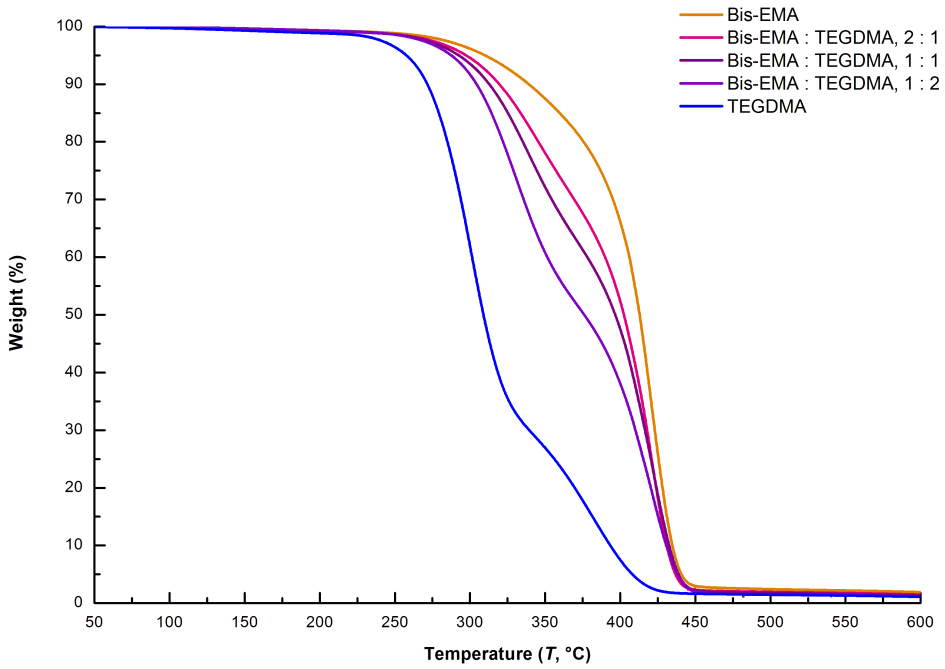

Figure 25: TGA scans, mass loss vs. temperature; Bis-EMA based systems.

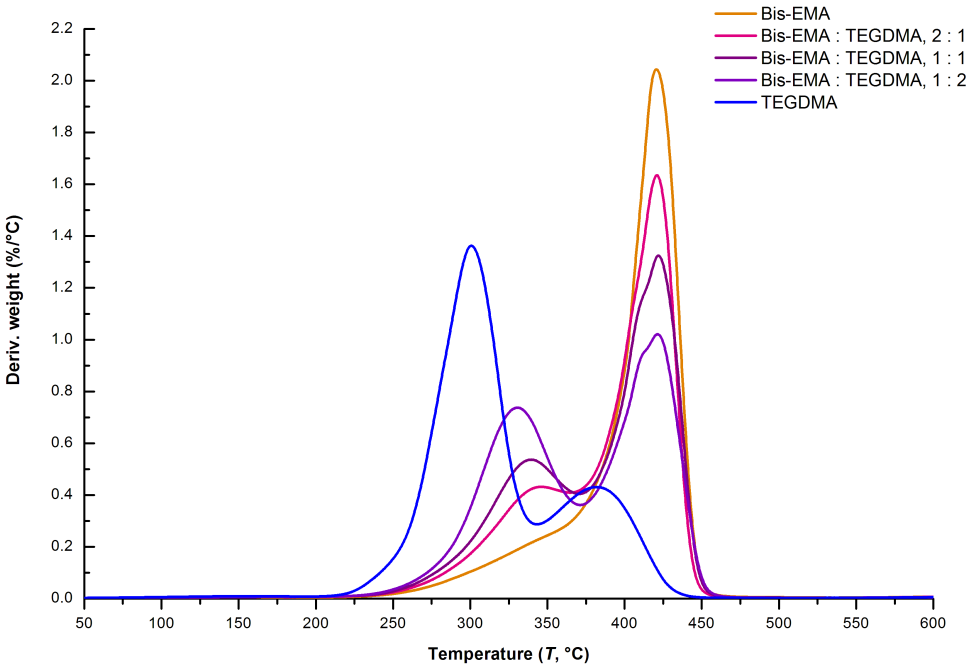

Figure 26: Derivative curves, mass loss vs. temperature; Bis-EMA based systems.

5.1.3 Effects of monomer backbone length

The analysis was performed on the series of poly-ethylene glycol dimethacrylate monomers to understand, how the number of ethylene glycol units affects the curing behavior. The kinetic characteristics accompanying polymerization of low-viscous monomers with flexible backbone were discussed in detail above. The general shape of the kinetic curves of PEGDMA homopolymerizations, associated with a changing of proportionality of the rates of propagation and termination, is the same for all monomers and is not further discussed in this chapter. The content of this chapter is limited to a description of specific effects related to the ethylene glycol chain length. Kinetic profiles obtained at the constant temperature, molar concentration of photo-initiation system and light intensity of the curing unit are shown in Figures 27 and 28. Table 9 summarizes the key kinetic parameters of PEGDMA homopolymerizations.

Table 9: Mean and standard deviation values of maximum rate of polymerization ($R_{p,\,max}$), degree of conversion ($P_{C=C}$) at $R_{p,\,max}$ and limiting degree of conversion ($P_{C=C}$) as determined by DPC and FTIR, different molecular weight (number of ethylene glycol units).

Designation	$R_{p,\,max}$ [mol/l·s]	$P_{C=C}$ at $R_{p,\,max}$ [%]	$P_{C=C}$ [%], DPC	$P_{C=C}$ [%], FTIR
PEGDMA 2	0.0357 (0.0012)	27.42 (0.79)	58.18 (0.81)	54.91 (2.17)
PEGDMA 3 (TEGDMA)	0.0448 (0.0015)	35.15 (1.27)	68.68 (1.17)	63.17 (1.32)
PEGDMA 4	0.0307 (0.0008)	41.61 (1.68)	75.35 (1.09)	71.93 (2.12)

Both, position of the $R_{p,\,max}$ on the conversion scale and limiting degree of double bond conversion, are shifted to higher values with increasing molecular weight of the monomers. This is attributed to the enhanced mobility of the system introduced by the increasing number of ethylene glycol units in the monomer. The mobility restrictions in the polymerizing system are partially suppressed due to the decreased concentration of double bonds and limited crosslink density and hence, reaction-diffusion-controlled propagation (i.e. onset of auto-deceleration) is shifted towards higher conversion. However, based on the kinetic gelation model estimations, higher degree of effective crosslinking and earlier onset of gelation are expected in the systems based on the monomers with greater molecular weight, because the probability of primary cyclization reactions is lower [76,116]. In agreement with Anseth *et al.* [35,76], the reactivity of each system is a result of few opposing effects. In general, the decrease in the maximum rate of polymerization is given by the concentration of double bonds in the monomer system. Furthermore, as the mobility in the reacting system increases with increasing molecular weight (from PEGDMA 2 to PEGDMA 4), the onset of auto-acceleration is delayed. This effect is related to the increase of active radical population which increases the rate of polymerization accordingly. The magnitude of these effects is the highest in case of PEGDMA 2. On the other side, the faster evolution of the networks leads to the earlier onset of strong mobility restrictions. This effect limits the maximal attainable rate of

polymerization. With respect to the aforementioned effects on $R_{p,\,max}$, PEGDMA 3 (TEGDMA) seems to stand somewhat between the other monomer species under the given conditions and hence, reaches the highest $R_{p,\,max}$.

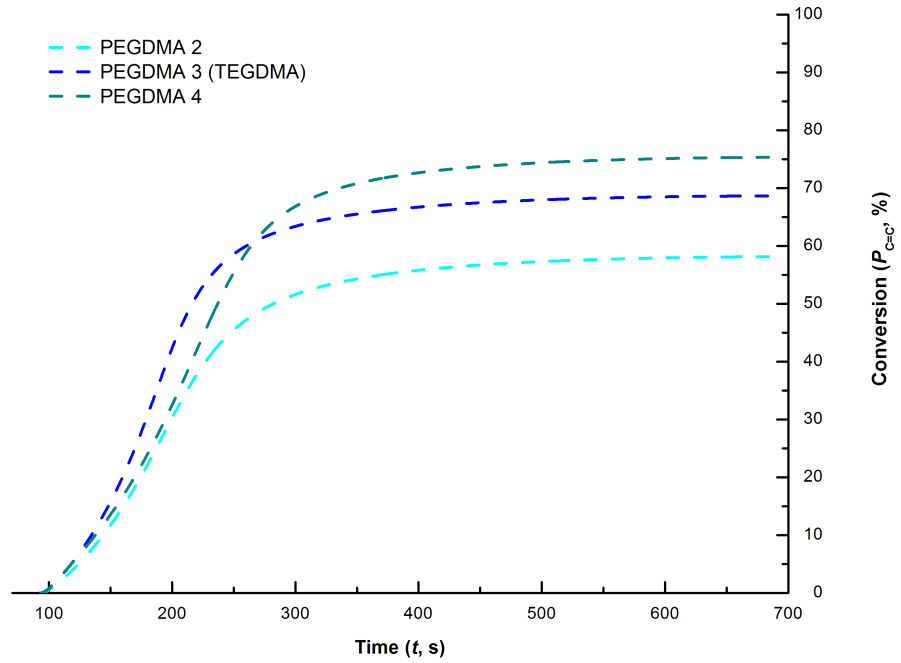

Figure 27: Photo-polymerization kinetic data, degree of double bond conversion as a function of time; PEGDMA, different molecular weight (number of ethylene glycol units).

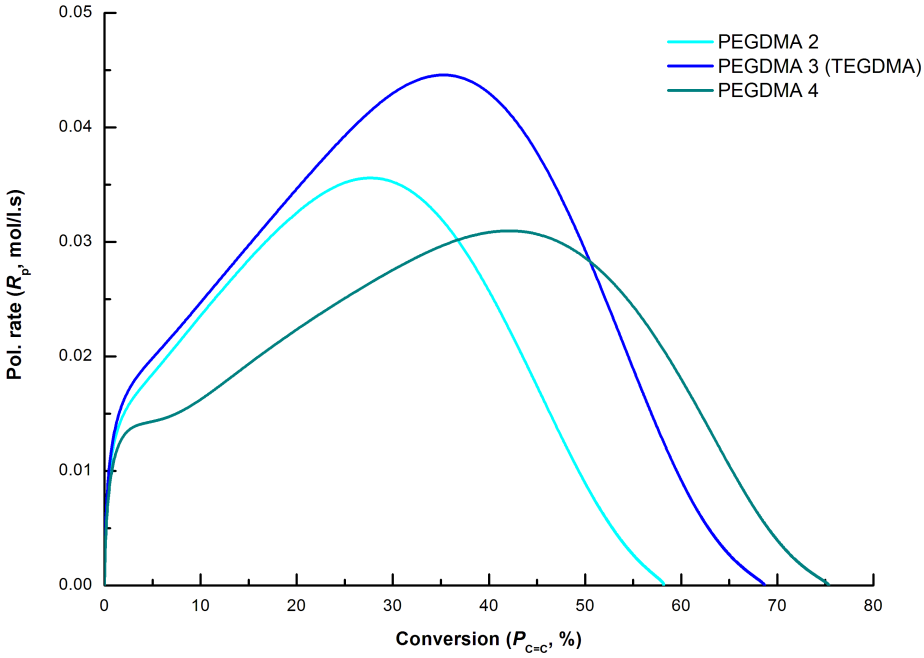

Figure 28: Photo-polymerization kinetic data, reaction rate (R_p) normalized by the initial double bond concentration; PEGDMA, different molecular weight (number of ethylene glycol units).

Table 10 summarizes the threshold parameters of thermal degradation process of the series of poly-ethylene glycol dimethacrylate homopolymers with different molecular weight.

Table 10: Mean and standard deviation values of temperature where thermal degradation start (T_0), and the first (T_1) and second (T_2) maximum of thermal decomposition and residual mass at 600 ºC; PEGDMA, different molecular weight (number of ethylene glycol units).

Designation	T_0 [ºC]	T_1 [ºC]	T_2 [ºC]	Residual mass at 600 ºC [%]
PEGDMA 2	217.98 (1.67)	308.30 (1.38)	395.02 (0.98)	0.34 (0.33)
PEGDMA 3	212.37 (2.89)	300.68 (0.46)	379.12 (0.99)	0.46 (0.45)
PEGDMA 4	202.13 (2.16)	307.34 (0.28)	383.81 (0.72)	0.11 (0.07)

Thermal decomposition behavior of poly-ethylene glycol dimethacrylate monomers is given by two interrelated features associated with molecular weight of the monomer species. These are the concentration of functional groups and different tendency towards primary cyclization reactions.

The onset of weight loss (T_0) fluctuates within the temperature range of 15 ºC (Figure 29), which may be attributed to the degree of crosslinking in loosely crosslinked regions given by the initial concentration of double bonds. As it was already discussed above, the first degradation step (T_1) reflects the degradation that originates in the loosely crosslinked regions of the network, whereas the second step (T_2) is associated with the decomposition of the densely, internally crosslinked domains [105,121]. Thermal stability is primarily related to the density of covalent crosslinks located on the outer shell of the microgel domains (i.e. the first degradation step) and in the internal structure of the domains (i.e. the second degradation step). Thermal stability of the networks slightly decreases with increasing molecular weight of the monomers. Due to the higher concentration of double bonds in the initial monomer system, more densely crosslinked domains are formed during the initial phase of the polymerization, followed by their interconnections in the later phase. Thus PEGDMA 2 homopolymer shows the highest temperatures of distinct steps of the degradation process.

On the other hand, since the height of the dTGA curve is related to the quantitative portion of the network with certain structural parameters, the change in the extent of thermal degradation in first and second step implies higher tendency towards primary cyclization in case of monomers with lower molecular weight (Figure 30). The already mentioned kinetic model enabling the estimation of cyclization probability based *inter alia* on the molecular weight was developed by Elliot *et al*. [16,125]. The model was validated by the comparative study of PEGDMA 2 (DEGDMA) and PEG(600)DMA copolymerization reactions with monofunctional methacrylate monomer. It was found that the higher degree of effective crosslinking was reached when PEG(600)DMA was used. Because the end-to-end distance is larger and the pendant double bond is removed from the immediate location of propagating radical, the probability of primary cyclization decreases. Thus, the higher extent of the

effective crosslinking may be the reason of slightly higher thermal stability PEGDMA 4 homopolymer when compared with PEGDMA 3 (TEGDMA).

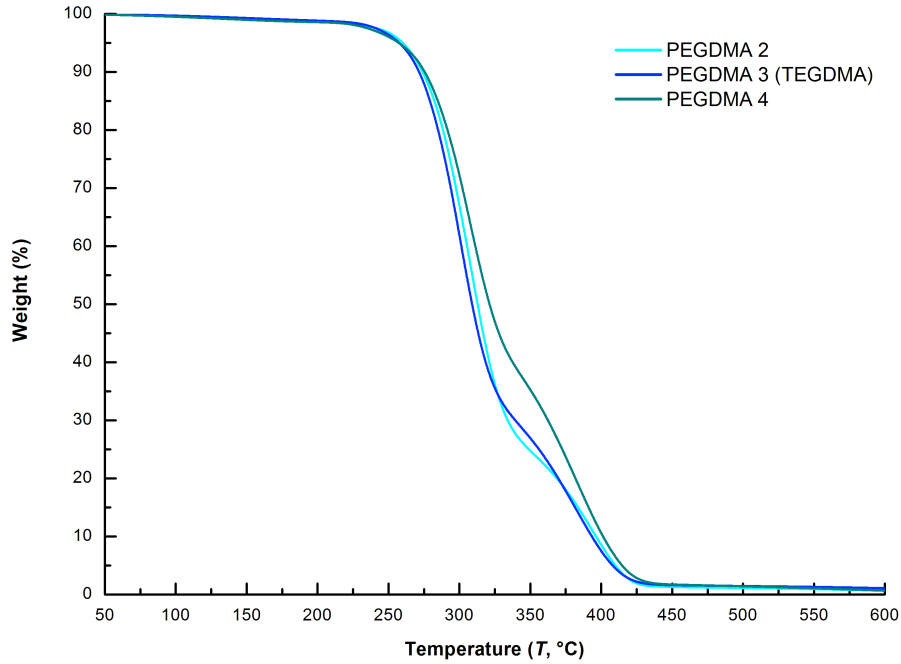

Figure 29: TGA scans, mass loss vs. temperature; PEGDMA, different molecular weight (number of ethylene glycol units).

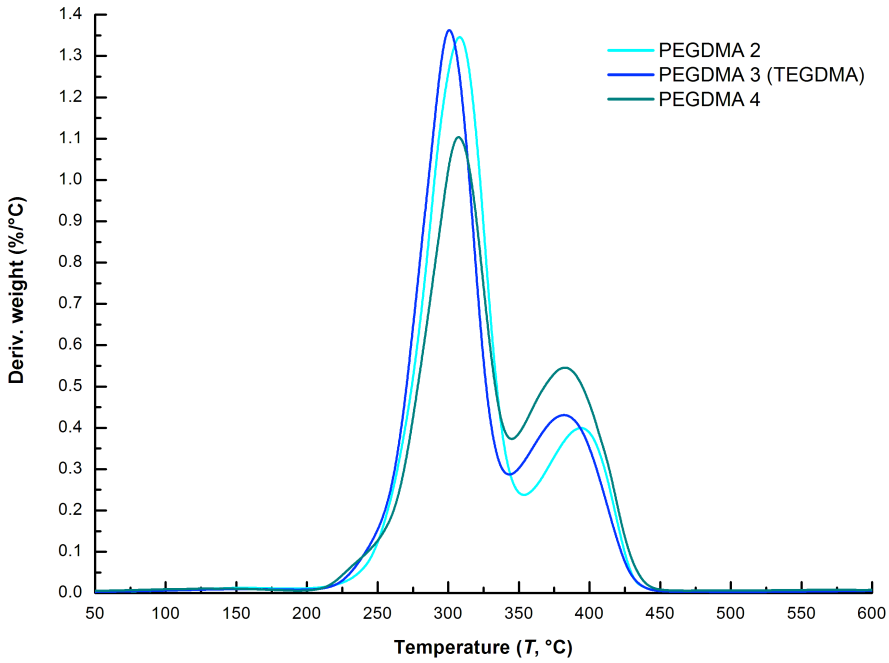

Figure 30: Derivative curves, mass loss vs. temperature; PEGDMA, different molecular weight (number of ethylene glycol units).

5.1.4 Effects of initiator concentration

The effect of concentration of photo-initiation system on photo-polymerization kinetics was studied on two monomer systems, chosen specifically to distinguish between two molecular species differing in their specific structural features and the polymerization kinetic parameters. Important kinetic parameters including $R_{p,\,max}$ and its position on the conversion scale, onset of auto-deceleration and limiting degree of double bond conversion are largely affected by the concentration of photo-initiation system. Kinetic profiles, obtained at the constant temperature and light intensity of the curing unit, are shown in Figures 31–34. Table 11 summarizes the key kinetic parameters of Bis-EMA and TEGDMA homopolymerizations with different molar concentrations of photo-initiation system.

Table 11: Mean and standard deviation values of maximum rate of polymerization ($R_{p,\,max}$), degree of conversion ($P_{C=C}$) at $R_{p,\,max}$ and limiting degree of conversion ($P_{C=C}$) as determined by DPC and FTIR; Bis-EMA and TEGDMA with different molar concentration of photo-initiation system.

Designation	$R_{p,\,max}$ [mol/l·s]	$P_{C=C}$ at $R_{p,\,max}$ [%]	$P_{C=C}$ [%], DPC	$P_{C=C}$ [%], FTIR
Bis-EMA 0.2	0.0182 (0.0009)	6.65 (0.71)	43.51 (1.82)	40.97 (1.12)
Bis-EMA 0.6	0.0357 (0.0019)	9.27 (0.89)	51.70 (2.46)	50.03 (1.66)
Bis-EMA 1.0	0.0427 (0.0010)	9.64 (0.17)	54.06 (1.14)	51.40 (1.70)
Bis-EMA 1.4	0.0452 (0.0014)	10.19 (0.60)	56.90 (1.45)	52.18 (1.29)
Bis-EMA 1.8	0.0478 (0.0014)	15.29 (0.32)	59.19 (1.21)	55.97 (2.03)
TEGDMA 0.2	0.0235 (0.0005)	31.45 (0.64)	62.09 (0.56)	58.80 (1.63)
TEGDMA 0.6	0.0354 (0.0010)	32.23 (0.65)	63.59 (1.17)	59.31 (1.23)
TEGDMA 1.0	0.0418 (0.0025)	32.73 (1.02)	64.48 (1.53)	61.30 (2.11)
TEGDMA 1.4	0.0448 (0.0015)	35.15 (1.27)	68.68 (1.17)	63.17 (1.32)
TEGDMA 1.8	0.0495 (0.0010)	37.68 (1.07)	72.82 (1.57)	68.12 (2.34)

The concentration of photo-initiation system controls the rate of polymerization through the active radical concentration and hence, dramatic increase in reactivity was observed with the increasing concentration of initiating compounds in both Bis-EMA and TEGDMA based systems. In agreement with kinetic gelation models [76,116], the concentration of radicals in the system affects the kinetic length of propagating chains at the point of termination. Based on the model developed by Achilias *et al*. [94], shorter propagating chains exhibit higher rates of termination, because their mobility in the reacting system is enhanced due to a diffusion rate. As it was stated by Stansbury [4], higher initiation rates and propagating radical concentration lead to shorter chain lengths. Because shorter chains with fewer pendant functional groups do not cause severe mobility restrictions in the reacting system, when

compared with longer chains, the position of $R_{p,\,max}$ and the onset of auto-deceleration are delayed on the conversion scale (Figures 32, 34). As a result, also the degree of limiting double bond conversion reaches higher values (Figures 31, 33). Conversely, a photo-polymerizations with a low initial active radical concentration leads to the earlier onset of gelation, because the propagating chains are longer at the point of termination. A transition from initial chain-length dependent termination to diffusion-controlled termination appears earlier on the conversion scale. Due to the rapid increase in viscosity of the reacting system, also the segmental diffusion of the monomers in the polymerizing system becomes restricted in earlier stages of the reaction, resulting in the earlier onset of reaction-diffusion-controlled propagation (i.e. auto-deceleration) and lower degree of limiting double bond conversion. Similar conclusions, related to the increased light intensity which influences the rate of polymerization by the same way as the concentration of photo-initiation system, were reported in literature [47,65,90].

Described phenomenon is obvious in both, Bis-EMA and TEGDMA based systems. The differences in kinetic polymerization profiles, given by the specific structural features of the monomers, were discussed above in detail. Higher viscosity and stiffness of Bis-EMA monomer backbone are related to the steady progress of the reaction rate during auto-acceleration period (Figure 32). Reaction-diffusion-controlled termination (i.e. gelation), allowing for effective auto-acceleration, dominates essentially from the beginning of the polymerization in all Bis-EMA formulations regardless the molar concentration of photo-initiation system. On the other hand, flexibility, lower molecular volume and lower monomeric viscosity of TEGDMA monomer are related to the bimodality of the reaction rate profile (Figure 34). As it was already discussed, this behavior is primary related to the delayed onset of diffusion-controlled termination, since low initial resin viscosity and extensive reactivity through primary cyclization contribute to the increased mobility of macroradicals in the polymerizing system and the termination by translation. The break, indicating the change in the termination mode, is also clearly influenced by the concentration of the photo-initiation system (Figure 34). Since higher propagating radical concentration leads to the presence of shorter chain lengths with fewer pendant functional groups in the polymerizing system, the onset of reaction-diffusion-controlled termination is even more delayed and the break indicating the change of the termination mode is slightly shifted on the conversion scale. Faster rates of polymerization also contribute to the increased number of microgel domains, causing a difference in the resulting structure of the networks, as it is expected on the basis of kinetic gelation models [76,116].

Due to the stronger mobility restrictions associated with Bis-EMA monomer structure, the position of $R_{p,\,max}$ is ranging between 7–15 %, whereas in the case of less viscous and more flexible TEGDMA, $R_{p,\,max}$ is ranging from 31 to 38 % on the conversion scale. Similar trend is obvious for limiting degree of double bond conversion, ranging from 44 to 59 % in Bis-EMA based systems and from 62 to 73 % in TEGDMA based systems.

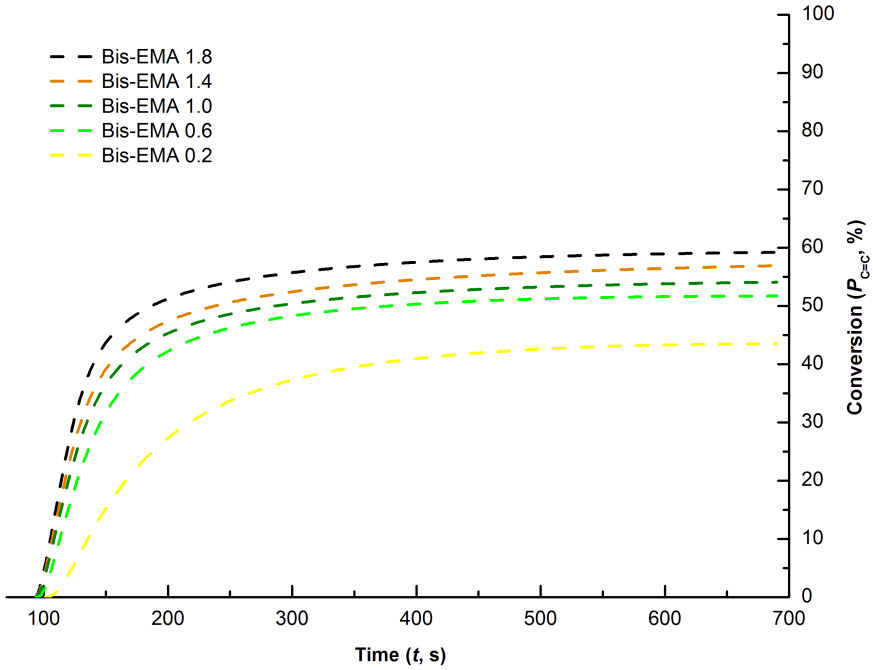

Figure 31: Photo-polymerization kinetic data, degree of double bond conversion as a function of time; Bis-EMA, different molar concentration of photo-initiation system.

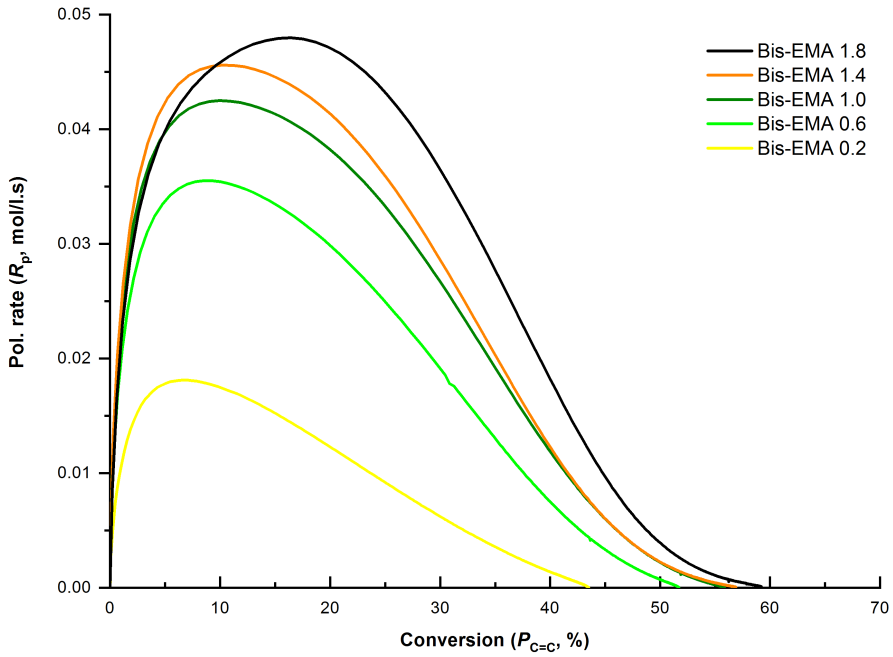

Figure 32: Photo-polymerization kinetic data, reaction rate (R_p) normalized by the initial double bond concentration; Bis-EMA, different molar concentration of photo-initiation system.

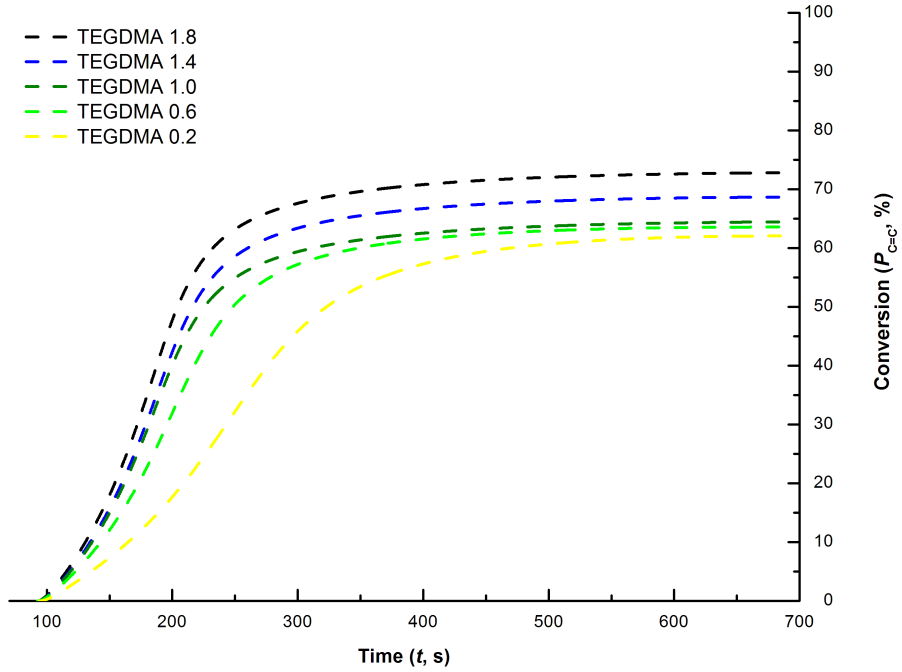

Figure 33: Photo-polymerization kinetic data, degree of double bond conversion as a function of time; TEGDMA, different molar concentration of photo-initiation system.

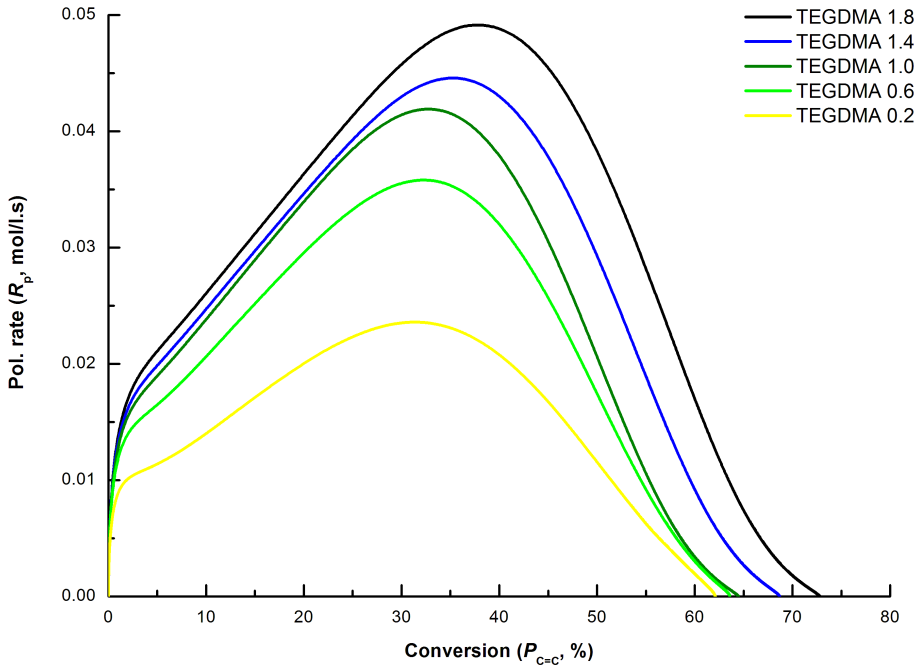

Figure 34: Photo-polymerization kinetic data, reaction rate (R_p) normalized by the initial double bond concentration; TEGDMA different molar concentration of photo-initiation system.

Table 12 summarizes the threshold parameters of thermal degradation process of the Bis-EMA and TEGDMA homopolymers with different initial molar concentration of photo-initiation system. The interpretation of the results is difficult due to the fact that the nature of

structural differences of the homopolymers, given by the differing active radical concentration, was partially disrupted by thermally-induced post-polymerization during measurement (i.e. re-activation of trapped radicals). However, the course of the TGA curves Figures 35–38) is still indicative to the differences in polymerization kinetics, affected by the concentration of photo-initiation system.

Table 12: Mean and standard deviation values of temperature where thermal degradation start (T_0), and the first (T_1) and second (T_2) maximum of thermal decomposition and residual mass at 600 ºC; Bis-EMA and TEGDMA with different molar concentration of photo-initiation system.

Designation	T_0 [ºC]	T_1 [ºC]	T_2 [ºC]	Residual mass at 600 ºC [%]
Bis-EMA 0.2	225.62 (1.85)	/	414.92 (0.83)	0.82 (0.23)
Bis-EMA 0.6	227.20 (1.34)	/	416.28 (0.70)	0.79 (0.18)
Bis-EMA 1.0	232.84 (1.45)	/	419.24 (0.81)	0.95 (0.20)
Bis-EMA 1.4	238.97 (1.23)	/	418.71 (0.34)	0.94 (0.13)
Bis-EMA 1.8	239.11 (1.13)	/	422.60 (0.72)	0.83 (0.22)
TEGDMA 0.2	196.13 (3.22)	276.22 (0.79)	369.48 (0.50)	0.47 (0.37)
TEGDMA 0.6	196.88 (2.79)	292.54 (0.37)	368.98 (0.89)	0.53 (0.42)
TEGDMA 1.0	200.19 (3.62)	297.37 (0.43)	373.13 (0.72)	0.51 (0.38)
TEGDMA 1.4	212.37 (2.89)	300.68 (0.46)	379.12 (0.99)	0.46 (0.45)
TEGDMA 1.8	216.60 (3.27)	306.00 (0.71)	379.81 (0.87)	0.39 (0.35)

Despite the aforementioned effect of thermally-induced post-curing, the onset of weight loss (T_0) fluctuates within the region of 14 ºC in Bis-EMA based system and 20 ºC in TEGDMA based systems. The start of the thermal degradation shifts to higher temperatures along with increasing initial concentration of photo-initiation system. This is primarily related to the level of crosslink density and thus also to the limiting degree of double bond conversion. Based on the conclusions of Teshima *et al*. [104] and Rigoli *et al*. [121], the initial products of pyrolysis are methacrylic acid and 2-hydroxyethyl methacrylate, generated from the pendant functional groups. Higher concentration of pendant functional groups and residual free monomers is expected in the systems with lower initial concentration of active radicals. This is due to the kinetic aspects described at the beginning of this chapter. In brief, higher initiation rates and propagating radical concentration lead to shorter chains with fewer pendant functional groups and consequently, to a higher crosslinking density and limiting degree of double bond conversion, since shorter chains do not restrict the mobility in the system to such extent, as longer chains. Higher crosslink density is also attributed to slightly higher thermal stability of the networks in the later stages of degradation (T_1, T_2).

The differences in decomposition kinetics between Bis-EMA and TEGDMA homopolymers with different concentration of photo-initiation system are again related to the degree of structural heterogeneity. In the case of Bis-EMA homopolymers, a higher extent of post-curing is expected due to the lower initial degree of double bond conversion and more homogeneous character of the network, allow for steady development when heated up above the glass transition temperature. Thus, beyond the slight differences related to the onset of thermal degradation (T_0), there are no substantial differences in the course of thermal degradation. Appearance of the shoulder on the dTGA curve of Bis-EMA homopolymers (Figure 36) is more prominent in the case of the systems with lower concentration of photo-initiation system, which may be attributed to higher proportion of unreacted functional groups in the network structure. On the other hand, higher initial degree of double bonds conversion, and substantial heterogeneity of the network structure in the case of TEGDMA homopolymers, do not allow high extent of post-curing. The radicals entrapped in the densely internally crosslinked microgel domains are not able to further propagate since there is limited concentration of accessible double bonds in the vicinity and thus, further development of the network is limited to the loosely crosslinked regions in the network structure [81]. Thus, the differences given by the initial concentration of photo-initiation system are more pronounced from the perspective of thermal degradation kinetics. The onset of weight loss occurs in wider temperature range than in the case of Bis-EMA homopolymers. Also, significant shift towards higher temperatures is obvious in the first degradation step (T_1) of TEGDMA homopolymers with higher concentration of photo-initiation system, suggesting a higher degree of effective crosslinking in the interconnecting regions between densely crosslinked microgel domains (Figure 38).

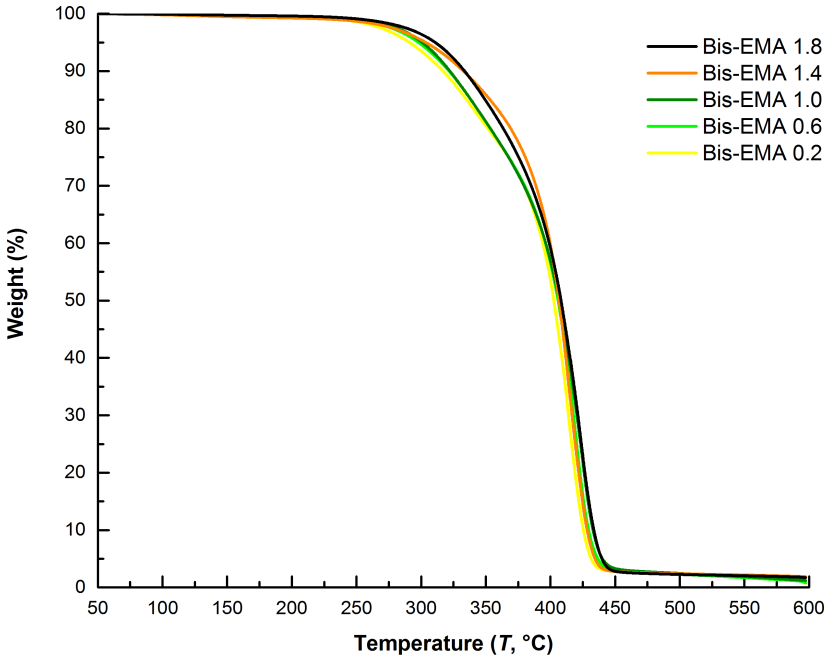

Figure 35: TGA scans, mass loss vs. temperature; Bis-EMA, different molar concentration of photo-initiation system.

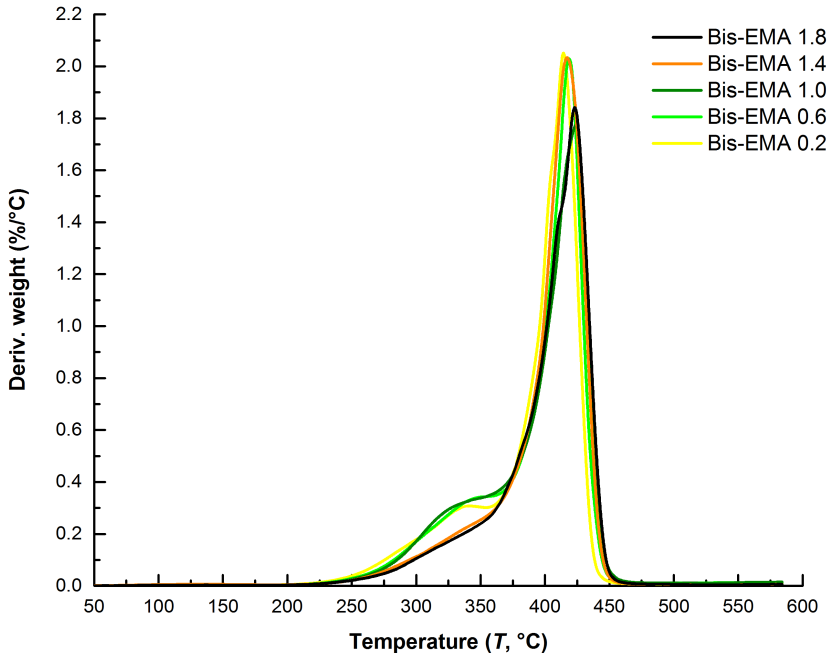

Figure 36: Derivative curves, mass loss vs. temperature; Bis-EMA, different molar concentration of photo-initiation system.

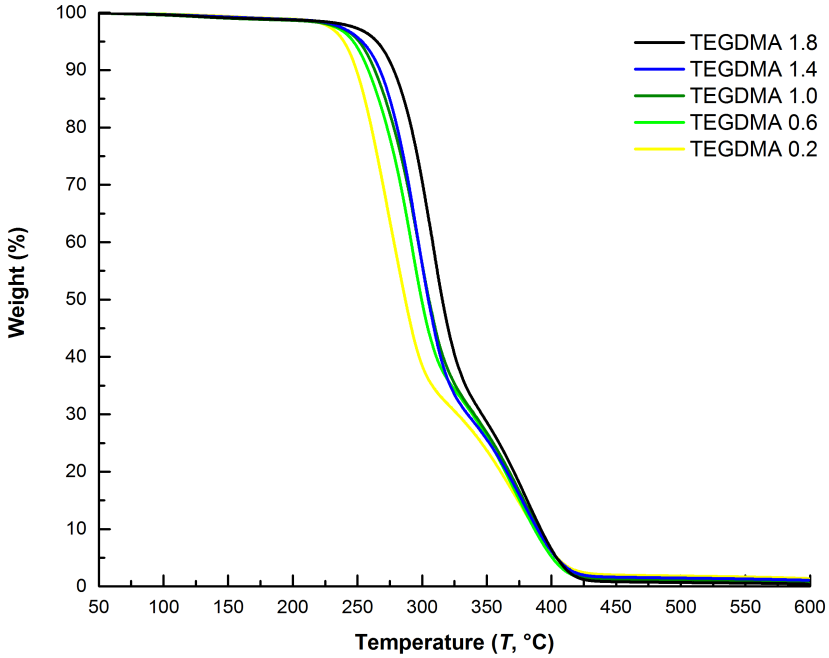

Figure 37: TGA scans, mass loss vs. temperature; TEGDMA, different molar concentration of photo-initiation system.

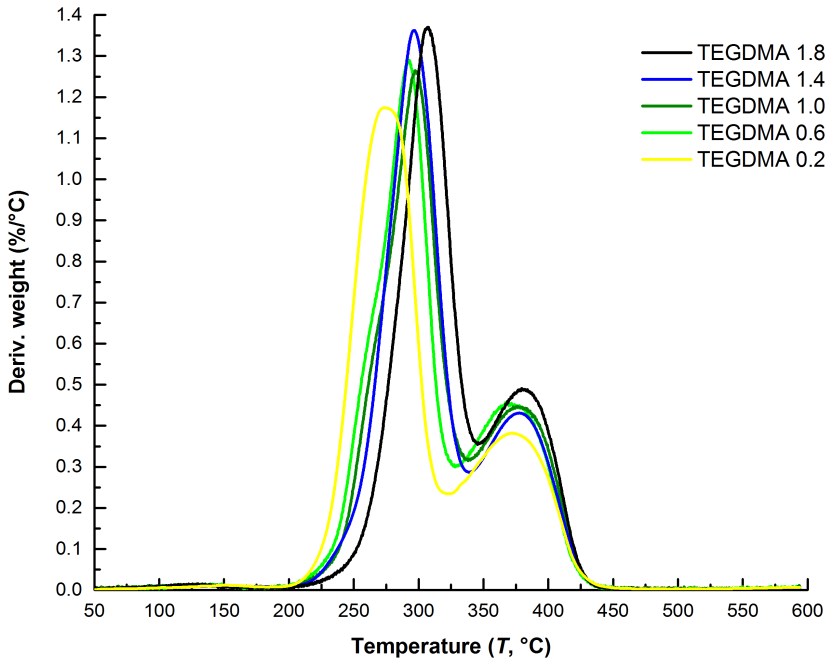

Figure 38: Derivative curves, mass loss vs. temperature; TEGDMA, different molar concentration of photo-initiation system.

5.2 Viscoelastic behavior of dimethacrylate networks

Dynamic-mechanical thermal analysis was used for further structural characterization of homo- and copolymerized dimethacrylate networks. For the purpose of the analysis, conventional photo-initiation system was replaced by organic peroxide, which undergoes homolytic cleavage when exposed to elevated temperatures. Conventional photo-initiator causes complications in the interpretation of the viscoelastic behavior because network structure continues to develop when the temperature is increased above the T_g. When heated above T_g, remaining functional groups, residual monomers and unreacted pendant groups with excess free volume regain enough mobility to react further [126]. The temperature range of the curing protocol was chosen to exceed the expected T_g of dimethacrylate networks during the post-curing period. Experimental observations and theoretical predictions support the hypothesis of close correlation between the cure kinetics of thermally-cured and photo-cured dimethacrylate networks [127]. The increased curing temperature resulted in much higher limiting degree of double bond conversion when compared with photo-cured resin systems, as determined by FTIR analysis (Tables 13 and 14).

To study the complex relation between viscoelastic response and structural parameters of dimethacrylate (co)polymerized networks, complex modulus and damping behavior were recorded under bending load applied at 1 Hz frequency within the temperature range 40–250 ºC, i.e. up to and beyond glass transition temperature. The upper temperature is limited by the onset of thermal degradation process.

The course of the storage modulus (E') and loss tangent in the given temperature range are indicative of specific structural features of dimethacrylate networks including effective crosslink density, diverse distribution of micro-environments related to structural heterogeneity, degree of double bonds conversion etc. The storage modulus undergoes a change from the stiff glassy state (~ 2.0–4.0 GPa) to a rubbery state (~ 0.5–0.7 GPa). This change is obvious for all characterized dimethacrylate systems, although from the damping behavior (i.e. the width of the loss tangent curve, Figures 39–44) it is clear that the change from the glassy to the rubbery state spreads over a wide range of temperatures. A wide distribution of relaxation times implies a high degree of structural heterogeneity of the networks, consisting of primary chains, effective crosslinks and primary cycles, pendant side chains bearing unreacted functional groups, regions with varying crosslink density etc. Therefore, the glass transition temperature (Tables 13, 14) should not be considered as the specific point at which the whole polymer undergoes glass transition. However, on the comparative basis, the peak of the tangent delta is taken as the glass transition temperature (T_g) of the networks. Another important feature that enables to distinguish between the degree of effective crosslinking is the value of the storage modulus in the rubbery region, associated with the concentration of elastically active strands. However, as it was already discussed in the chapter 4.2.4, due to the non-Gaussian distribution of chains in highly crosslinked networks and the structural differences between monomer species, the theory of rubber elasticity allowing for calculation of crosslinking density cannot be used [91,128]. The theory, assuming the Gaussian distribution of chains, is limited to the calculations of covalent crosslink density of the networks, where the concentration of crosslinking agent is low, and

where there are at least 25 repeating units between two crosslinks. Due to the aforementioned context, the value of the storage modulus in the rubbery region is used as the measure of crosslink density on the qualitative bases.

5.2.1 Homopolymers

The evolution of storage modulus and loss tangent obtained by performing the temperature scans on various homopolymers based on the structurally distinct monomer species (Figures 39, 40), shows considerable differences related to their viscoelastic behavior. As it was extensively discussed in chapter 5.1, the specific structural features of monomers determine the complexity of network-formation kinetics and the resulting supramolecular structure, which is reflected in the viscoelastic response of the networks. Table 13 summarizes the key viscoelastic parameters and limiting degree of conversion of the studied homopolymers.

Table 13: Mean and standard deviation values of the storage modulus at 40 ºC (E') and at the point of glass transition ($E'_{rubbery}$), glass transition temperature (T_g) and limiting degree of double bonds conversion ($P_{C=C}$) as determined by FTIR; neat monomers.

Designation	*E'* [GPa], 40 ºC	$E'_{rubbery}$ [GPa]	T_g [ºC]	$P_{C=C}$ [%], FTIR
Bis-GMA	3.85 (0.38)	0.70 (0.08)	178.27 (0.03)	64.32 (2.14)
Bis-EMA	3.51 (0.30)	0.54 (0.06)	154.13 (0.07)	76.43 (1.87)
UDMA	3.25 (0.47)	0.38 (0.04)	151.94 (0.04)	78.92 (3.11)
TEGDMA	1.98 (0.25)	0.54 (0.07)	114.62 (0.02)	89.32 (3.50)

At 40º C, the networks are in the glassy state and the value of the storage modulus is related to the network stiffness, which is highest in the case of Bis-GMA homopolymer regardless the lowest limiting degree of double bonds conversion. This is due to the rigid aromatic character of the Bis-GMA monomer and the presence of two pendant hydroxyl groups providing the additional reinforcement by the strong hydrogen bonding interactions. A slightly lower value of storage modulus of Bis-EMA is given by the lacking hydrogen bonding functionalities, which is partially compensated by a higher achievable limiting degree of conversion when compared with Bis-GMA. UDMA and TEGDMA contain aliphatic spacer group, however, UDMA reaches higher values of storage modulus due to the urethane groups, forming hydrogen bonds [25,124]. Also, higher degree of effective crosslinking is expected in the UDMA based networks. This is related to the larger end-to-end distance, lowering the probability of primary cyclization [76,125], and to the labile hydrogen abstractions from –NH– groups, favoring chain transfer reactions. Thus, the network is more rigid, considering that there are more crosslinking sites than those based on pendant double bonds [30]. In the case of TEGDMA homopolymer, high degree of primary cyclization does not contribute to the overall mechanical stability of the network.

As the temperature and mobility of the polymer chain increases, steeper decrease of storage modulus occurs in the case of homopolymer systems based on flexible monomers (i.e. UDMA and TEGDMA) and in the system with lacking hydrogen bonding functionalities. Presence of hydrogen bonds delays the point, where the major portion of the network undergoes the transition to the rubbery state by tightening the network structure. Thermal stability of hydrogen bonding interactions was studied by Kammer *et al*. [129] and later by Morita [130] on Bis-GMA and HEMA polymers, using temperature dependent FTIR and FT-Raman spectroscopy. Even if Bis-GMA polymer is thermally cured up to the degree of conversion of nearly 70 %, only the vibrations of hydroxyl groups, associated with either hydrogen bonding between two hydroxyl groups or between hydroxyl and carbonyl groups are observable [129]. In the case of HEMA homopolymer, it was found that with increasing temperature, the nature of hydrogen bonding interactions slightly changes. The dissociation of hydrogen bonding between hydroxyl groups occurs on one side, whereas in contrast, the association between hydroxyl groups and carbonyl groups occurs on the other [130]. However, this shift is primarily associated with the glass transition temperature of the linear polymer, when the dynamic movements of the whole chain become possible. The hydrogen bond distribution therefore reflects the dynamic nature of the whole system, not only the local dynamics of proton transfer, as it was stated by Li and Brisson [131], who studied the thermal stability of hydrogen bonds in methacrylate copolymers above and below the glass transition temperature within the temperature range of 20–200 ºC. As it reported, due to the increased mobility of chains, the number of hydrogen bonding carbonyls decreases above glass transition. When compared with room temperature, it was quantified that about 0.5–3.5 % hydrogen bonds are broken at T_g + 30 ºC, depending on the methacrylate comonomer composition.

In the case of Bis-GMA, the expected decrease of hydrogen bonding interactions should be below the decrease quantified in the case of linear methacrylate copolymers. This is due to the presence of covalent crosslinking, affecting the dynamics of chains (mobility becomes increasingly restricted). Thus, as described by van't Hoff relationship, it can be expected, that a small number of hydrogen bonds can be broken or the nature can be slightly changed above T_g. However, since the T_g and the value of storage modulus in the rubbery plateau are highest in the case of Bis-GMA homopolymer, despite the lowest limiting degree of conversion (Table 13, Figures 39, 40), it is clear that the physical crosslinks based on hydrogen bonding interactions serves as an effective reinforcement of the network structure in both glassy and rubbery state. As expected, due to the non-Gaussian distribution of chains, the course of the storage modulus in rubbery plateau do not correspond to the concentration of functional groups in the resin mixture (Table 1). Lower values of T_g and the course of the storage modulus in rubbery plateau are given either by lacking hydrogen bonding functionalities (Bis-EMA), or by aliphatic character of the monomer backbone and the potential for primary cyclization (UDMA and TEGDMA). The different degree of effective crosslinking between UDMA and TEGDMA is given by the different concentration of functional groups and the fact, that the hydrogen bonding interactions associated with the urethane functionalities are weak [25]. A severe disruption of the hydrogen bonding potential is expected to occur above T_g due to the flexible character of the network.

Besides the measuring of storage modulus and T_g, the valuable insight into the morphology of the networks is related to the height and breadth of the tangent delta peak (Figure 40), providing a measure of the range of mobilities existing in the network structure. The height of the transition peak is related to the number of kinetic units contributing to the transition, whereas the breadth depends on the distribution of environments where these units are located [91,100,110,111]. In other words, these characteristics are directly related to the degree of structural heterogeneity given by the width of the distribution of relaxation times. The heterogeneous character of the networks is attributed to the complexity of parameters that affects polymerization kinetics, including diffusion limitations, physical interactions, and the behavior of pendant functional groups in the vicinity of radical site.

In case of Bis-GMA, the broadness of transition region is related to the low limiting degree of double bonds conversion (i.e. higher concentration of chain ends, pendant side chains or unreacted monomers), and physical crosslinking that may be broken or its character may be slightly changed within the temperature range. Relatively narrower transition regions of Bis-EMA and UDMA are given mainly by the higher degree of double bonds conversion (Table 13). In the case of UDMA, lower extent of primary cyclization is expected to occur when compared with TEGDMA due to the greater molecular weight [16,76,116,125]. Moreover, the effective crosslinking is promoted due to the chain transfer reactions [13,30]. Very wide distribution of relaxation times is apparent from the course of loss tangent in the case of TEGDMA homopolymer, despite the highest degree of conversion. This confirms the idea of spatial heterogeneity associated with the primary cyclization, and coexistence of structurally distinct domains in the network structure. Highly crosslinked microgel regions require more energy to undergo the transition to the rubbery state, whereas the loosely crosslinked regions and pendant side chains are more mobile. Thus, some portions of the network may remain in the rubbery state, deteriorating mechanical properties of the polymer.

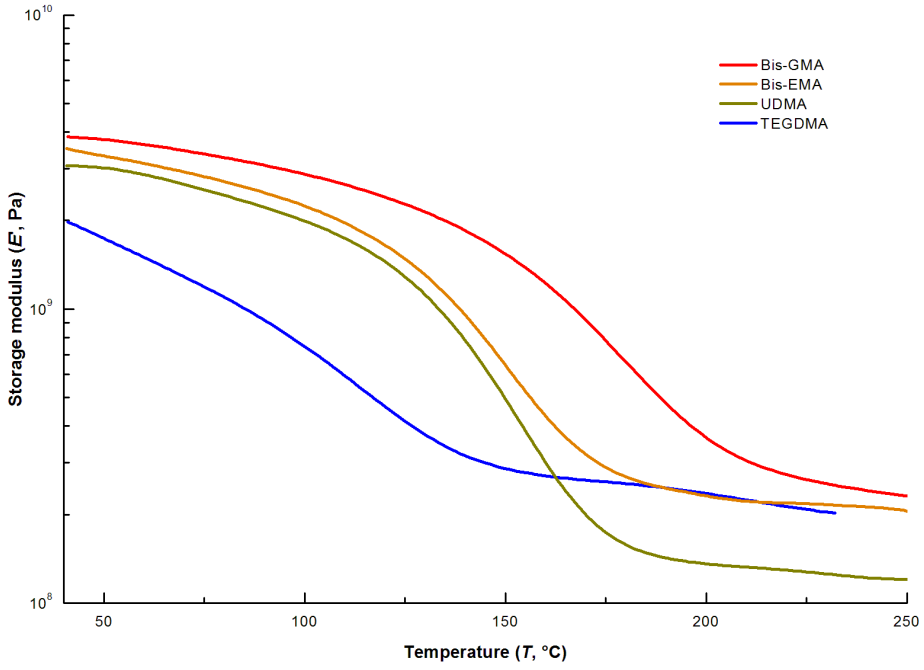

Figure 39: Evolution of the storage modulus as a function of temperature; neat monomers.

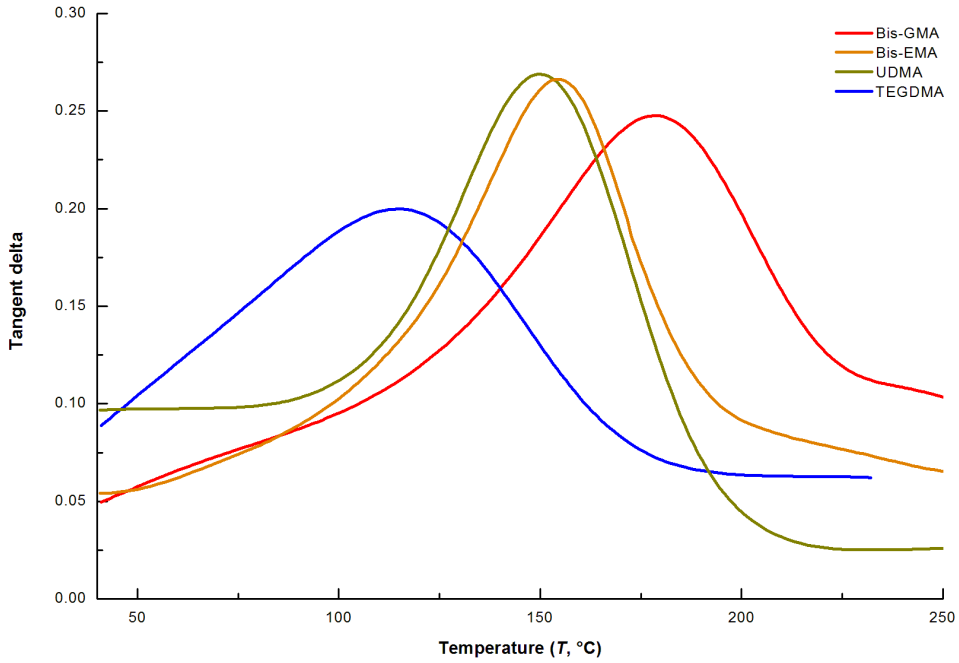

Figure 40: Tangent delta curves as a function of temperature; neat monomers.

5.2.2 Copolymers

Evolution of the storage modulus and loss tangent captured over the range of temperature of the systems based on Bis-GMA or Bis-EMA base monomers copolymerized with TEGDMA diluent monomer in different molar ratios are shown on Figures 41–44. Table 14 summarizes the key viscoelastic parameters and limiting degree of double bonds conversion of the studied copolymers. In general, with increasing content of diluent monomer, the storage modulus in the glassy region and the glass transition temperature decrease. Also, single glass transition temperature of the copolymerized systems shows that the polymerization process is random in nature, however, the progress of curing reaction is inhomogeneous due to its kinetic complexity.

The decrease of the storage modulus is given by the increasing proportion of the flexible monomer, which leads to the decrease of network stiffness despite the fact, that the limiting degree of double bonds conversion considerably increase along with increasing proportion of diluent monomer. Thus, it is clear that the decrease in storage modulus and T_g is not the effect of residual unsaturations, but it is rather associated with the flexibility of the network and effectivity of crosslinking, which may be deteriorated by the occurrence of primary cycles in the network structure. Also, increased range of mobilities coexisting within the network is manifested by broadening of the relaxation times spectra with increasing concentration of diluent monomer (Figures 42, 44). When compared with homopolymers, this is attributed primarily to the varying mobility of the pendant side chains, flexibility of chains between crosslinks, occurrence and the extent of primary cyclization reactions in the Bis-GMA based copolymers and also the variations in the character of physical interactions. The potential

range of hydrogen bonding interactions in the copolymerized Bis-GMA/TEGDMA networks is increased due to the incorporation of electronegative ether donor functionalities in the backbone of TEGDMA [25].

Table 14: Mean and standard deviation values of the storage modulus at 40 ºC (E') and at the point of glass transition ($E'_{rubbery}$), glass transition temperature (T_g) and limiting degree of double bonds conversion ($P_{C=C}$) as determined by FTIR; Bis-GMA/TEGDMA and Bis-EMA/TEGDMA copolymers.

Designation	*E'* [GPa], 40 ºC	*E'* [GPa], rubbery	T_g [ºC]	$P_{C=C}$ [%], FTIR
Bis-GMA	3.85 (0.38)	0.70 (0.08)	178.27 (0.03)	64.32 (2.14)
Bis-GMA:TEGDMA, 2:1	3.47 (0.19)	0.69 (0.06)	172.77 (0.02)	75.02 (2.65)
Bis-GMA:TEGDMA, 1:1	2.93 (0.18)	0.67 (0.08)	166.15 (0.02)	78.23 (1.86)
Bis-GMA:TEGDMA, 1:2	2.84 (0.21)	0.75 (0.05)	167.28 (0.03)	80.42 (1.70)
Bis-EMA	3.51 (0.30)	0.54 (0.06)	154.13 (0.07)	76.43 (1.87)
Bis-EMA:TEGDMA, 2:1	3.33 (0.27)	0.53 (0.08)	150.83 (0.05)	81.72 (1.35)
Bis-EMA:TEGDMA, 1:1	3.07 (0.22)	0.53 (0.08)	146.49 (0.04)	83.27 (1.69)
Bis-EMA:TEGDMA, 1:2	2.90 (0.19)	0.51 (0.05)	138.80 (0.05)	85.13 (1.80)
TEGDMA	1.98 (0.25)	0.54 (0.07)	114.62 (0.02)	89.32 (3.50)

As it was already suggested, the key difference related to the viscoelastic behavior between Bis-GMA and Bis-EMA copolymers is the presence or absence of hydrogen bond donor functionalities. Thus, Bis-GMA based copolymers reach considerably higher T_g (Table 14), since the hydrogen bonding interactions tightens the network structure. This is also reflected in the course of the storage modulus in the rubbery plateau, indicating the contribution of physical interactions to the overall level of crosslink density. The decrease of extent of primary cyclization reactions of TEGDMA in the copolymerized systems with rigid base monomers is expected in relation to reduced accessibility of the pendant functional groups to the radical site. This is due to the steric hinderance effects in the network structure which is developing with considerable proportion of effective crosslinking. Thus, even if the diluent monomer is in molar excess, there is a significant increase in the storage modulus and T_g. This increase is more pronounced in the Bis-GMA based systems due to the pre-association between Bis-GMA and TEGDMA monomer species and pendant side chains via intermolecular hydrogen bonding [25]. On the contrary, in the backbone of Bis-EMA monomer, glycerolate-based side chains between methacrylate groups and aromatic core are substituted for flexible ethoxylated units, lacking hydrogen bond donor functionalities. This leads to higher flexibility of the network and greater likelihood of the primary cyclization reactions, resulting in the lower values of the storage modulus in the glassy state as well as in the rubbery plateau, when compared with Bis-GMA based systems.

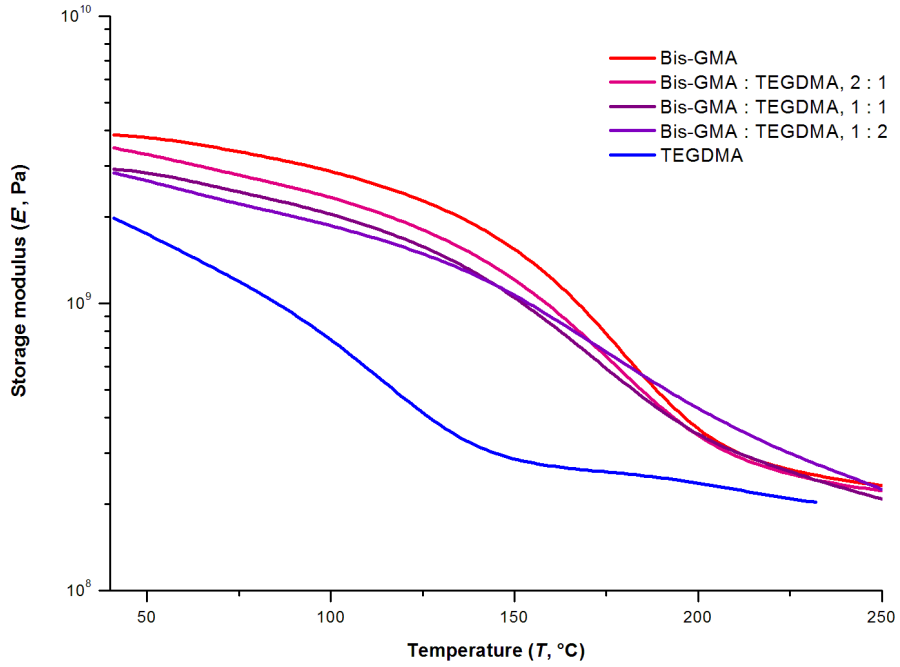

Figure 41: Evolution of the storage modulus as a function of temperature; Bis-GMA based systems.

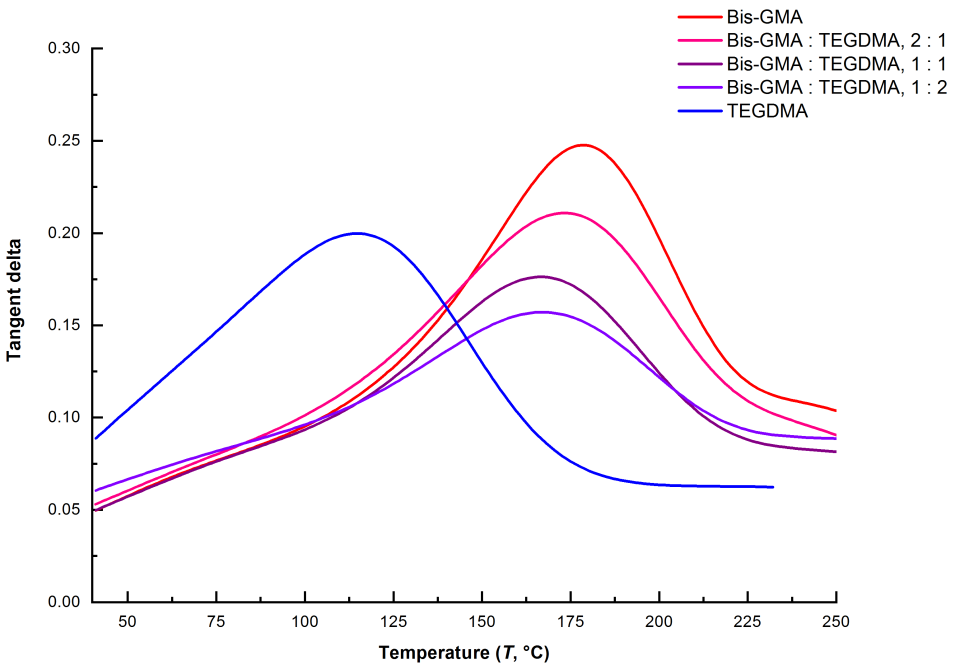

Figure 42: Tangent delta curves as a function of temperature; Bis-GMA based systems.

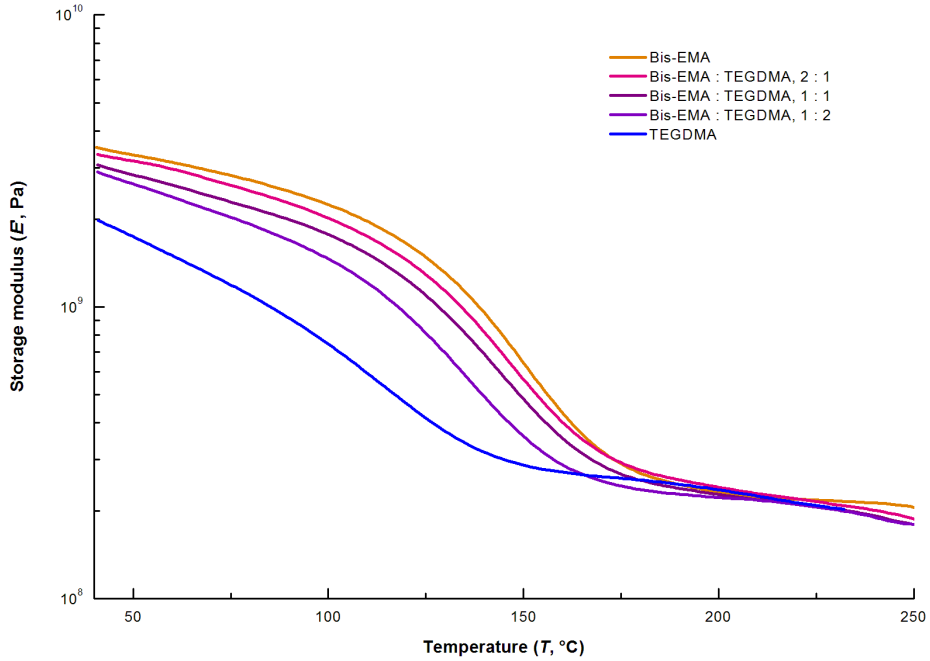

Figure 43: Evolution of the storage modulus as a function of temperature; Bis-EMA based systems.

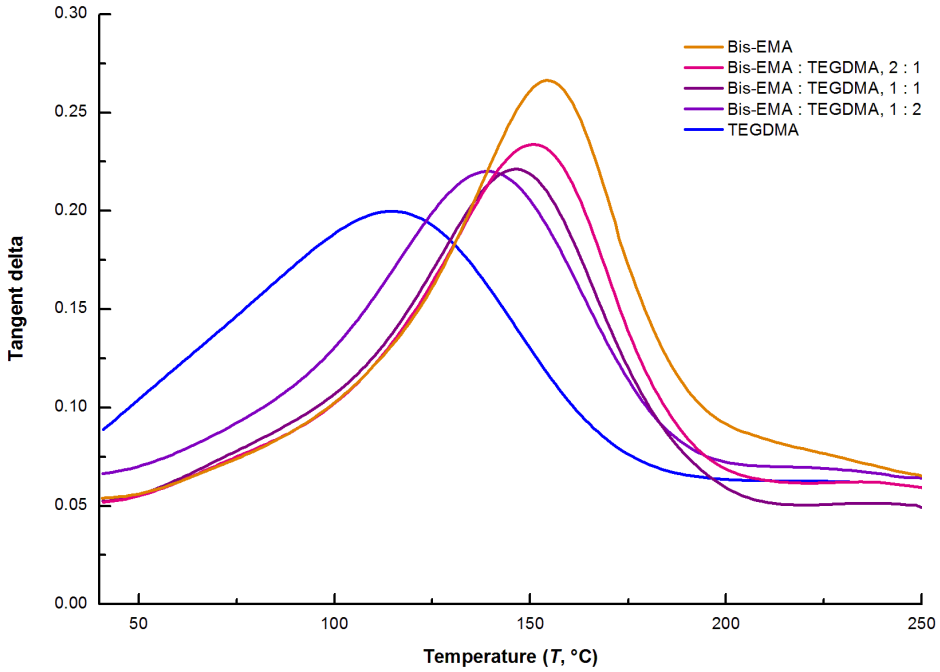

Figure 44: Tangent delta curves as a function of temperature; Bis-EMA based systems.

6 CONCLUSION

In this work, the inter-relationship between the structural parameters of dimethacrylate monomers, evolution mechanisms of the network structures and resulting morphology were investigated. Furthermore, viscoelastic parameters of thermally cured networks were determined. Within the scope of this thesis, the resin systems consisting of following monomer species were studied: Bis-GMA, its non-hydroxylated alternative, Bis-EMA, UDMA and PEGDMA with varying molecular weight. In the comonomer resin formulations consisting of base and diluent monomers, TEGDMA was used as the diluent monomer.

The study of kinetics, including the evolution of functional groups conversion and polymerization rate profile, provided insight into the mechanisms of network morphogenesis. In general, due to the crosslinking nature, dimethacrylate systems exhibit complex reaction kinetics including strong mobility restrictions of kinetic units during the network development. This includes auto-acceleration, auto-deceleration, and varying pendant functional groups reactivity throughout the polymerization process. Incomplete curing reaction and entrapment of radicals are the inevitable result of diffusion-controlled reaction.

Based on the homopolymerization kinetics of the aforementioned monomers, it was found that the rate of polymerization and the degree of conversion are severely limited by the stiff aromatic character of monomer backbone in case of Bis-GMA, Bis-EMA, and high initial viscosity of the resin systems given by the contribution of strong hydrogen bonding interactions (Bis-GMA). On the other hand, rigidity of these monomers decreases the probability of primary cyclization reactions due to the steric hinderance effects, which leads to higher effectivity of crosslinking. Higher reactivity is related primarily to a lower molecular volume, and higher flexibility of aliphatic monomer backbone (UDMA, PEGDMA). However, flexibility of the monomer and proximity of the pendant functional group to the radical site, given by the decreasing molecular weight of monomers, lead to a greater probability of the propagation via primary cyclization, and inhomogeneous course of the network formation. Heterogeneous polymerization is reflected in the morphogenesis characterized by microgel domains formation preceded by extensive cyclization, followed by formation of interconnections among the domains. These results are in good agreement with the numerical models that simulate the kinetics of free radical network polymerization (i.e. kinetic gelation models) and the kinetics of primary cyclization reactions.

A copolymerization kinetics of base (Bis-GMA, Bis-EMA) and diluent monomers (TEGDMA) show intermediate behavior between those of the corresponding pure monomers. The dilution leads to an increased mobility in the polymerizing systems. Hence, the optimal reactivity can be reached by optimizing a molar ratio of the base and diluent monomers under the given conditions. However, despite the higher limiting degree of conversion reached in relation to the dilution effect, the effectivity of crosslinking decreases as the potential for inhomogeneous progress of curing reaction increases along with increasing concentration of TEGDMA. Because the gelation occurs very early on the conversion scale, the phase separation is suppressed despite any thermodynamic instability of the marginally compatible mixture of monomers during copolymerization, and the process is random. The possible

compositional drift is given only by the differences in mobility of the monomer species in the polymerizing systems. Thus, the inhomogeneous curing character is given predominantly by the anomalous behavior of the various kinetic units during the polymerization.

The rate of polymerization given by the concentration of active radicals controls the kinetic chain length at the point of termination. Shorter chains with fewer functional groups do not restrict the mobility in the reacting system as much as longer chains do, allowing for higher rate of segmental diffusion. Hence, the mobility of macroradicals and monomers becomes severely restricted by diffusion slightly later on the conversion scale and the systems reach higher limiting degree of conversion.

Differences in the morphology of cured resins influence the degradation behavior. Bis-GMA and Bis-EMA monomers form a more rigid networks due to their rigid aromatic backbone and higher degree of effective crosslinking, decomposing at higher temperatures when compared with the series of PEGDMA and UDMA. The presence of structural inhomogeneities in the structure of the networks based on the monomers that undergo cyclization reactions to a greater extent is manifested by the appearance of two degradation steps. This is associated with the different thermal stability of the coexisting regions with varying crosslink density.

The progress of the storage modulus vs. temperature, recorded under the bending load applied at given frequency across the glass transition, reflects the network stiffness, effectivity of crosslinking, degree of conversion and the reinforcement of the network structure by physical interactions. In case of copolymers, the occurrence of the single transition temperature confirms that the copolymerization process is random in nature. The stiffness of the monomer backbone, as well as tightening of the structure by the hydrogen bonding interactions, leads to higher values of the storage modulus in a glassy state and higher temperatures of the transition into a rubbery state. Thus, both aforementioned values are the highest for the Bis-GMA homopolymer despite the lowest limiting degree of conversion. The qualitative estimation of the effective crosslink density, given by the progress of the storage modulus in the rubbery plateau, confirms the assumption that the effectivity of crosslinking is not directly related to the initial concentration of double bonds and the degree of conversion, but rather to the reactivity of pendant functional groups. The degree of structural heterogeneity is manifested by the broadness of the relaxation times spectra, providing a measure of the range of mobilities in the network structure.

The results of this work provide the basis for a rational design of crosslinking systems including matrices of dental resin composites. However, further characteristics beyond the scope of this work related to particular application must be taken into the consideration to develop the systems with optimized outcome. Although Bis-GMA monomer was introduced nearly 60 years ago, the results of this work identifies Bis-GMA as an essential component of the resin formulations, because its stiffness as well as the potential for strong intermolecular hydrogen bonding contribute to the formation of durable and more homogeneous polymer networks.

7 REFERENCES

[1] BOWEN, R. L. Dental filling material comprising vinyl-silane treated fused silica and a binder consisting of the reaction product of bisphenol and glycidyl methacrylate [patent]. *US patent*. 3,006,112. 1962.

[2] BOWEN, R. L. Silica-resin direct filling material and method of preparation [patent]. *US patent.* 3,194,783. 1965.

[3] PEUTZFELD, A. Resin composites in dentistry: the monomer systems. *European Journal of Oral Sciences*. 1997, 105(2), 97–116.

[4] STANSBURY, J. W. Dimethacrylate network formation and polymer property evolution as determined by the selection of monomers and curing conditions. *Dental Materials*. 2012, 28(1), 13–22.

[5] TANTBIJORN, D., C. S. PFEIFER, R. R. BRAGA and A. VERSLUIS. Do low-shrink composites reduce polymerization shrinkage effects? *Journal of Dental Research*. 2011, 90(5), 596–601.

[6] LEPRINCE, J. G., W. M. PALIN, M. A. HADIS, J. DEVAUX and G. LELOUP. Progress in dimethacrylate-based dental composite technology and curing efficiency. *Dental Materials*. 2013, 29(2), 139–156.

[7] GONÇALVES, F., Y. KAWANO, C. PFEIFER, J. W. STANSBURY and R. R. BRAGA. Influence of Bis-GMA, TEGDMA and Bis-EMA contents on viscosity, conversion and flexural strength of experimental resins and composites. *European Journal of Oral Sciences*. 2009, 117(4), 442–446.

[8] PFEIFER, C. S., L. R. SILVA, Y. KAWANO and R. R. BRAGA. Bis-GMA co-polymerizations: Influence on conversion, flexural properties, fracture toughness and susceptibility to ethanol degradation of experimental composites. *Dental Materials*. 2009, 25(9), 1146–1141.

[9] JANCAR, J., W. WANG and A. T. DIBENEDETTO. On the heterogeneous structure of thermally cured bis-GMA/TEGDMA resins. *Journal of Materials Science: Materials in Medicine*. 2000, 11(11), 675–682.

[10] SHAH, P. K. and J. W. STANSBURY. Conversion dependent evolution of shrinkage, modulus and stress: Filler effects. *Dental Materials* [online]. 2009, 25(5), e29.

[11] ANDRZEJEWSKA, E. Photo-polymerization kinetics of multifunctional monomers. *Progress in Polymer Science*. 2001, 26(4), 605–665.

[12] ANDRZEJEWSKA, E., E. SOCHA and M. ANDRZEJEWSKI. Crosslinking photo-copolymerization of dodecyl methacrylate with oxyethyleneglycol dimethacrylates: Kinetics and reactivity ratios. *Polymer*. 2006, 47(19), 6513–6523.

[13] SIDERIDOU, I. D., D. S. ACHILIAS and N. C. KOSTIDOU. Copolymerization kinetics of dental dimethacrylate resins initiated by a benzoyl peroxide/amine redox system. *Journal of Applied Polymer Science*. 2008, 109(1), 515–524.

[14] DICKENS, S. H., J. W. STANSBURY, K. M. CHOI and C. J. E. FLOYD. Photopolymerization kinetics of methacrylate dental resins. *Macromolecules*. 2003, 36(16), 6043–6053.

[15] PODGÓRSKI, M. Structure-property relationship in new photo-cured dimethacrylate-based dental resins. *Dental Materials*. 2012, 28(4), 398–409.

[16] ELLIOTT, J. E., L. G. LOVELL and C. N. BOWMAN. Primary cyclization in the polymerization of bis-GMA and TEGDMA: a modeling approach to understanding the cure of dental resins. *Dental Materials*. 2001, 17 (3), 221–229.

[17] STANSBURY, J. W. and S. H. DICKENS. Network formation and compositional drift during photo-initiated copolymerization of dimethacrylate monomers. *Polymer*. 2001, 42(15), 6 363–6 369.

[18] ANTONUCCI, J. M. and J. W. STANSBURY. Molecularly designed dental polymers. ARSHADY, R. *Desk Reference of Functional Polymers: Syntheses and Applications.* American Chemical Society, 1997, 719-737. ISBN 0-8412-3469-8.

[19] FERRACANE, J. L. Resin composites – State of the art. *Dental Materials*. 2011, 27(1), 29-38.

[20] JANDT, K. D. and B. W. SIGUSH. Future perspectives of resin-based dental materials. *Dental Materials*. 2009, 25(8), 1001–1006.

[21] NGUYEN, T. P., B. KIM, Y. J. KIM, S. H. LEE, S. SHIN and J. K. CHO. Synthesis of the bio-based alternative to Bis-GMA and its application to photo-polymerizable adhesives. *International Journal of Adhesion and Adhesives*. 2018, 80(1), 60–65.

[22] MARTIM, G. C., C. S. PFEIFER and E. M. GIROTTO. Novel urethane-based polymer for dental applications with decreased monomer leaching. *Materials Science and Engineering: C*. 2017, 72(1), 192–201.

[23] LOVELL, L. G., J. W. STANSBURY, D. C. SYRPES and C. N. BOWMAN Effects of composition and reactivity on the reaction kinetics of dimethacrylate/dimethacrylate co-polymerizations. *Macromolecules*. 1999, 32(12), 3913–3921.

[24] ELLAKWA, A., N. CHON and I. B. LEE. The effect of resin matrix composition on the polymerization shrinkage and rheological properties of experimental dental composites. *Dental Materials*. 2007, 23(10), 1229–1235.

[25] LEMON, M. T., M. S. JONES and J. W. STANSBURY. Hydrogen bonding interactions in methacrylate monomers and polymers. *Journal of Biomedical Materials Research A*. 2007, 83(3), 734–746.

[26] KHATRI, C. A., J. W. STANSBURY, C. R. SCHULTHEISZ and J. M. ANTONUCCI. Synthesis, characterization and evaluation of urethane derivatives of Bis-GMA. *Dental Materials*. 2003, 19(7), 584–588.

[27] ANSETH, K. S., M. D. GOODNER, M. A. REIL, A. R. KANNURPATTI, S. M. NEWMAN and C. N. BOWMAN. The influence of co-monomer composition on dimethacrylate resin properties for dental composites. *Journal of Dental Research*. 1996, 75(8), 607–1612.

[28] FONSECA, A. S. Q. S., A. D. L. MOREIRA, P. P. A. C. DE ALBUQUERQUE, L. R. DE MENEZES, C. S. PFEIFER and L. F. J. SCHNEIDER. Effect of monomer type on the C=C degree of conversion, water sorption and solubility, and color stability of model dental composites. *Dental Materials*. 2017, 33(4), 394–401.

[29] MOSZNER, N. and U. SALZ. New developments of polymeric dental composites. *Progress in Polymer Science*. 2001, 26(4), 535–576.

[30] SIDERIDOU, I., V. TSERKI and G. PAPANASTASIOU. Effect of chemical structure on degree of conversion in light-cured dimethacrylate-based dental resins. *Biomaterials*. 2002, 23(8), 1819–1829.

[31] WATTS, D. and N. SILIKAS. *Dental hard tissues and bonding: interfacial phenomena and related properties*. 1st. ed. New York, NY: Springer, 2005, 123–154. ISBN 978-3-540-23408-1.

[32] ANSETH, K. S., C. M. WANG, and C. N. BOWMAN. Reaction behavior and kinetic constants for photo-polymerizations of multi (meth)acrylate monomers. *Polymer*. 1994, 35(15), 3243–3250.

[33] ANSETH, K. S., L. M. KLINE, T. A. WALKER, K. J. ANDERSON and C. N. BOWMAN. Reaction kinetics and volume relaxation during polymerizations of multi-ethylene glycol dimethacrylates. *Macromolecules*. 1995, 28(7), 2491–2499.

[34] LEPRINCE, J. G., G. LAMBLIN, J. DEVAUX, M. DEWAELE, M. MESTDAGH, W. M. PALIN, B. GALLEZ and G. LELOUP. Irradiation mode's impact on radical entrapment in photoactive resins. *Journal of Dental Research*. 2010, 89(12), 1494–1498.

[35] ANSETH, K. S., C. M. WANG and C. N. BOWMAN. Kinetic evidence of reaction diffusion during the polymerization of multi(meth)acrylate monomers. *Macromolecules*. 1994, 27(3), 650–655.

[36] FINK, J. K. *Reactive polymers fundamentals and applications: a concise guide to industrial polymers*. Norwich, NY: William Andrew Pub., 2005, 349–372. ISBN 0-8155-1515-4

[37] KARMAKER, A. C., A. T. DIBENEDETTO and A. J. GOLDBERG. Extent of conversion and its effect on the mechanical performance of Bis-GMA/PEGDMA based resins and their composites with continuous glass fibers. *Journal of Materials Science: Materials in Medicine*. 1997, 8(6), 369–374.

[38] LOVELL, L. G., S. M. NEWMAN, M. M. DONALDSON and C. N. BOWMAN. The effect of light intensity on double bond conversion and flexural strength of a model, unfilled dental resin. *Dental Materials*. 2003, 19(6), p. 458–465.

[39] SAKAGUCHI, R. L. and J. L. FERRACANE. Effect of light power density on development of elastic modulus of a model light-activated composite during polymerization. *Journal of Esthetic Restorative Dentistry*. 2001, 13(2), 121–130.

[40] EMAMI, N., K. J. SÖDERHOLM and L. A. BERGLUND. Effect of light power density variations on bulk curing properties of dental composites. *Journal of Dentistry*. 2003, 31(3), 189–196.

[41] FENG, L., R. CARVALHO and B. I. SUH. Insufficient cure under the condition of high irradiance and short irradiation time. *Dental Materials*. 2009, 25(3), 283–289.

[42] LIM, B. S., J. L. FERRACANE, R. L. SAKAGUCHI and J. R. CONDON. Reduction of polymerization contraction stress for dental composites by two-step light-activation. *Dental Materials*. 2002, 18(6), 436–444.

[43] VISVANATHAN, A., N. ILIE, R. HICKEL and K. H. KUNZELMANN. The influence of curing times and light curing methods on the polymerization shrinkage stress of a shrinkage-optimized composite with hybrid-type prepolymer fillers. *Dental Materials*. 2007, 23(7), 777–784.

[44] VILLAT, C., N. P. PLASSE, B. PICARD and P. COLON. Characterization method of photo-polymerization kinetics of two dental composite resins using two types of light sources. *Materials Science and Engineering*. 2008, 28(5–6), 971–976.

[45] DANESH, G., H. DAVIDS, K. J. REINHARDT, K OTT and E SCHÄFER. Polymerization characteristics of resin composites polymerized with different curing units. *Journal of Dentistry*. 2004, 32(6), 479–488.

[46] FARIA-E-SILVA, A. L. and C. S. PFEIFER. Delayed photo-activation and addition of thio-urethane: Impact on polymerization kinetics and stress of dual-cured resin cements. *Journal of Dentistry*. 2017, 65, 101–109.

[47] SILIKAS, N., G. ELIADES and D. C. WATTS. Light intensity effects on resin-composite degree of conversion and shrinkage strain. *Dental Materials*. 2000, 16(4), 292–296.

[48] HOFMANN, N., B. HUGO, K. SCHUBERT and B. KLAIBER. Comparison between a plasma arc light source and conventional halogen curing units regarding flexural strength, modulus, and hardness of photo-activated resin composites. *Clinical Oral Investigations*. 2000, 4(3), 140–147.

[49] PEUTZFELDT, A., A. SAHAFI and E. ASMUSSEN. Characterization of resin composites polymerized with plasma arc curing units. *Dental Materials*. 2000, 16(5), 330–336.

[50] JANDT, K. D. and R. W. MILLS. A brief history of LED photo-polymerization. *Dental Materials*. 2013, 29(6), 605–617.

[51] NAKAMURA, S., T. MUKAI and M. SENOH. Candela-class high brightness InGaN/AlGaN double hetero-structure blue-light-emitting diodes. *Applied Physics Letters*. 1994, 64(13), 1687–1689.

[52] IKEMURA, K. and T. ENDO. A review of the development of radical photo-polymerization initiators used for designing light-curing dental adhesives and resin composites. *Dental Materials Journal*. 2010, 29(5), 481–501.

[53] STANSBURY, J. W. Curing dental resins and composites by photo-polymerization. *Journal of Esthetic Dentistry*. 2000, 12(6), 300–308.

[54] JAKUBIAK, J., X. ALLONAS, J. P. FOUASSIER and J. RABEK. Camphorquinone-amines photo-initiating systems for the initiation of free radical polymerization. *Polymer*. 2003, 44(18), 5219–5226.

[55] ANDRZEJEWSKA, E., L-A. LINDÉN and J. F. RABEK. The role of oxygen in camphorquinone-initiated photo-polymerization. *Macromolecular Chemistry and Physics*. 1998, 199(3), 441–449.

[56] SUN, G. J. and K. H. CHAE. Properties of 2,3-butanedione and 1-phenyl-1,2-propanedione as new photosensitizers for visible light cured dental resin composites. *Polymer*. 2000, 41(16), 6205–6212.

[57] ASMUSSEN, S. and C. VALLO. Light absorbing products during polymerization of methacrylate monomers photo-initiated with phenyl-1,2-propanedione/amine. *Journal of Photochemistry and Photobiology A: Chemistry*. 2009, 202(2–3), 228–234.

[58] SCHNEIDER, L. F., C. S. PFEIFER, S. CONSANI, S. A. PRAHL and J. L. FERRACANE. Influence of photo-initiator type on the rate of polymerization, degree of conversion, hardness and yellowing of dental resin composites. *Dental Materials*. 2008, 24(9), 1169–1177.

[59] SCHNEIDER, L. F. J., S. CONSANI, R. L. SAKAGUCHI and J. L. FERRACANE. Alternative photo-initiator system reduces the rate of stress development without compromising the final properties of the dental composite. *Dental Materials*. 2009, 25(5), 566–572.

[60] EMAMI, N. and K. J. M. SÖDERHOLM. Influence of light-curing procedures and photo-initiator/co-initiator composition on the degree of conversion of light-curing resins. *Journal of Materials Science: Materials in Medicine*. 2005, 16(1), 47–52.

[61] SCHROEDER, W., W. D: COOK and C. VALLO. Photo-polymerization of N,N-dimethylaminobenzyl alcohol as amine co-initiator for light-cured dental resins. *Dental Materials*. 2008, 24(5), 686–693.

[62] LIZYMOL, P. P. and V. K. KRISHNAN. A comparison of efficiency of two photo-initiators for polymerization of light-cure dental composite resins. *Journal of Applied Polymer Science*. 2008, 107(5), 3337–3342.

[63] SCHROEDER, W., G. ARENAS and C. VALLO. Monomer conversion in a light-cured dental resin containing 1-phenyl-1,2-propanedione photosensitizer. *Polymer International*. 2007, 56(9), 1099–1105.

[64] BRANDT, W. C., O. L. TOMASELLI, L. CORRER-SOBRINHO and M. A. SINHORETI. Can phenyl-propanedione influence Knoop hardness, rate of polymerization and bond strength of resin composite restorations? *Journal of Dentistry*. 2011, 39(6), 438–447.

[65] KURDIKAR, D. L. and N. A. PEPPAS. A kinetic model for diffusion-controlled bulk crosslinking photo-polymerizations. *Macromolecules*. 1994, 27(15), 4084–4092.

[66] COOK, W. D. Photo-polymerization kinetics of dimethacrylates using the camphorquinone/amine initiator system. *Polymer*. 1992, 33(3), 600–609.

[67] WATTS, D. C. Reaction kinetics and mechanics in photo-polymerized networks. *Dental Materials*. 2005, 21(1), 27–35.

[68] DECKER, C. and K. MOUSSA. Radical trapping in photo-polymerized acrylic networks. *Journal of Polymer Science*. 1987, 25(2), 739–742.

[69] BERCHTOLD, K. A., L. G. LOVELL, J. NIE, B. HACIOĞLU and C. N. BOWMAN. The significance of chain length dependent termination in crosslinking polymerizations. *Polymer*. 2001, 42(11), 4925–4929.

[70] PFEIFER, C. S., N. D. WILSON, Z. R. SHELTON and J. W. STANSBURY. Delayed gelation through chain-transfer reactions: Mechanism for stress reduction in methacrylate networks. *Polymer*. 2011, 52(15), 3295–3303.

[71] BOULDEN, J. E., N. B. CRAMER, K. M. SCHRECK, C. L. COUCH, C. BRACHO-TROCONIS, J. W. STANSBURY and C. N. BOWMAN. Thiol–ene–methacrylate composites as dental restorative materials. *Dental Materials*. 2011, 27(3), 267–272.

[72] CRAMER, N. B., C. L. COUCH, K. M. SCHRECK, J. E. BOULDEN, R. WYDRA, J. W. STANSBURY and C. N. BOWMAN. Properties of methacrylate–thiol–ene formulations as dental restorative materials. *Dental Materials*. 2010, 26(8), 799–806.

[73] SZCZEPANSKI, C. R. and J. W. STANSBURY. Modification of linear pre-polymers to tailor heterogeneous network formation through photo-initiated polymerization-induced phase separation. *Polymer*. 2015, 70, 8–18.

[74] DUŠEK, K. Special features of network formation by chain crosslinking copolymerization. *Collection of Czechoslovak Chemical Communications*. 1993, 58(10), 2245–2265.

[75] BARSZCZEWSKA-RYBAREK, I. M. and M. KRASOWSKA. Fractal analysis of heterogeneous polymer networks formed by photo-polymerization of dental dimethacrylates. *Dental Materials*. 2012, 28(6), 695–702.

[76] ANSETH, K. S., and C. N. BOWMAN. Kinetic gelation model predictions of cross-linked polymer network microstructure. *Chemical Engineering Science*. 1994, 49(14), 2207–2217.

[77] ELLIOTT, J. E. and C. N. BOWMAN. Kinetics of primary cyclization reactions in crosslinked polymers: an analytical and numerical approach to heterogeneity in network formation. *Macromolecules*. 1999, 32(25), 8621–8628.

[78] SIDERIDOU, I. a M. M. KARABELA. Sorption of water, ethanol or ethanol/water solutions by light-cured dental dimethacrylate resins. *Dental Materials*. 2011, 27(10), 1003–1010.

[79] NAGHASH, H. J., O. OKAY and Y. YAĜCI. Gel formation by chain-crosslinking photopolymerization of methyl methacrylate and ethylene glycol dimethacrylate. *Polymer*. 1997, 38(5), 1187–1196.

[80] FUNKE, W. E., O. OKAY a B. JOOS-MÜLLER. Microgels, Intramolecularly Crosslinked Macromolecules with a Globular Structure. *Advances in Polymer Science*. 1998, 136, 139–234.

[81] KRZEMINSKI, M., M. MOLINARI, M. TROYON a X. COQUERET. Calorimetric Characterization of the Heterogeneities Produced by the Radiation-Induced Cross-Linking Polymerization of Aromatic Diacrylates. *Macromolecules*. 2010, **43**(8), 3757–3763.

[82] LIPATOV, Y. S. Interfacial regions in the phase-separated, inter-penetrating networks. *Polymer Bulletin*. 2007, 58(1), 105–118.

[83] PFEIFER, C. S., Z. R. SHELTON, C. R. SZCZPANSKI, M. D. BARROS, N. D. WILSON and J. W. STANSBURY. Tailoring Heterogeneous Polymer Networks through Polymerization-Induced Phase Separation: Influence of Composition and Processing Conditions on Reaction Kinetics and Optical Properties. *Journal of Polymer Science, Part A: Polymer Chemistry*. 2014, 52(13), 1796–1806.

[84] CHEN, F. and W. D. COOK. Curing kinetics and morphology of IPNs from a flexible dimethacrylate and a rigid epoxy via sequential photo and thermal polymerization. *European Polymer Journal*. 2008, 44(6), 1796–1813.

[85] SZCZEPANSKI, C. R., C. S. PFEIFER and J. W. STANSBURY. A new approach to network heterogeneity: Polymerization induced phase separation in photo-initiated, free-radical methacrylic systems. *Polymer*. 2012, 53(21), 4694–4701.

[86] SZCZEPANSKI, C. R. and J. W. STANSBURY. Acessing photo-based morphological control in phase-separated, cross-linked networks through delayed gelation. *European Polymer Journal*. 2015, 67, 314–325.

[87] OKAY, O., Y. YILMAZ, D. KAYA, M. KESKINEL and Ö. PESKAN. Heterogeneities during the formation of poly(sodium acrylate) hydrogels. *Polymer Bulletin*. 1999, 43(4–5), 425–431.

[88] JIAN, Y., Y. HE, L. ZHAO, W. YANG and J. NIE. Dynamic-mechanical analysis of elastic modulus development of dental composites. *Polymer Composites*. 2013, 34(4), 580–586.

[89] BOTELLA, A., J. DUPUY, A. A. ROCHE and V. VERNEY. Photo-rheometry/NIR spectrometry: An *in-situ* technique for monitoring conversion and viscoelastic properties during photo-polymerization. *Macromolecular Rapid Communications*. 2004, 25(12), 1155–1158.

[90] ABU-ELANAIN, D. A., S. H. LEWIS and J. W. STANSBURY. Property evolution during vitrification of dimethacrylate photopolymer networks. *Dental Materials*. 2013, 29(11), 1173–1181.

[91] YU, Q., M. ZHOU, Y. DING, B. JIANG and S. ZHU. Development of networks in atom transfer radical polymerization of dimethacrylates. *Polymer*. 2007, 48(24), 7058–7064.

[92] YU, Q., S. XU, H. ZHANG, Y. DING a S. ZHU. Comparison of reaction kinetics and gelation behaviors in atom transfer, reversible addition–fragmentation chain transfer and conventional free radical copolymerization of oligo(ethylene glycol) methyl ether methacrylate and oligo(ethylene glycol) dimethacrylate. *Polymer*. 2009, 50(15), 3488–3494.

[93] LEUNG, D. a C. N. BOWMAN. Reducing Shrinkage Stress of Dimethacrylate Networks by Reversible Addition– Fragmentation Chain Transfer. *Macromolecular Chemisty and Physics*. 2012, 213(2), 198–204.

[94] ACHILIAS, D. S. and G. D. VERROS. Modeling of diffusion-controlled reactions in free radical solution and bulk polymerization: Model validation by DSC experiments. *Journal of Applied Polymer Science*. 2010, 116(3), 1842–1856.

[95] BOWMAN, C. N. and C. J. KLOXIN. Toward an enhanced understanding and implementation of photo-polymerization reactions. *AIChE Journal*. 2008, 54(11), 2775–2795.

[96] YE, S., N. B. CRAMER and C. N. BOWMAN. Relationship between glass transition temperature and polymerization temperature for cross-linked photopolymers. *Macromolecules*. 2011, 44(3), 490–494.

[97] YOUNG, J. S. a C. N. BOWMAN. Effect of Polymerization Temperature and Cross-Linker Concentration on Reaction Diffusion Controlled Termination. *Macromolecules*. 1999, 32(19), 6073–6081.

[98] HOWARD, B., N. D. WILSON, S. M. NEWMAN, C. S. PFEIFER and J. W. STANSBURY. Relationships between conversion, temperature and optical properties during composite photo-polymerization. *Acta Biomaterialia*. 2010, 6(6), 2053–2059.

[99] LOVELL, L. G., H. LU, J. E. ELLIOTT, J. W. STANSBURY and C. N. BOWMAN. The effect of cure rate on the mechanical properties of dental resins. *Dental Materials*. 2001, 17(6), 504–511.

[100] LOVELL, L. G., K. A. BERCHTOLD, J. E. ELLIOTT and C. N. BOWMAN. Understanding the kinetics and network formation of dimethacrylate dental resins. *Polymers for Advanced Technologies*. 2001, 12(6), 335–345.

[101] KRZEMINSKI, M., M. MOLINARI, M. TROYON and X. COQUERET. Characterization by atomic force microscopy of the nano-heterogeneities produced by the radiation-induced crosslinking polymerization of aromatic diacrylates. *Macromolecules*. 2010, 43(19), 8121–8127.

[102] ROSENTRITT, M., A. C. SHORTALL and W. M. PALIN. Dynamic monitoring of curing photoactive resins: A methods comparison. *Dental Materials*. 2010, 26(5), 565–570.

[103] BRESCHI, L., M. CADENARO, F. ANTONIOLLI, S. SAURO, M. BIASOTTO, C. PRATI, F. R. TAY and R. DI LENARDA. Polymerization kinetics of dental adhesives cured with LED: correlation between extent of conversion and permeability. *Dental Materials*. 2007, 23(9), 1066–1072.

[104] TESHIMA, W., Y. NOMURA, A. IKEDA, T. KAWAHARA, M. OKAZAKI and Y. NAHARA. Thermal degradation of photo-polymerized Bis-GMA/TEGDMA based dental resins. *Polymer Degradation and Stability*. 2004, 84(1), p. 167–172.

[105] ACHILIAS, D. S., M. M. KARABELA and I. D. SIDERIDOU. Thermal degradation of light-cured dimethacrylate resins: Part I. Isoconversional kinetic analysis. *Thermochimica Acta*. 2008, 472(1–2), 74–83.

[106] VOUVOUDI, E. C., D. S. ACHILIAS and I. D. SIDERIDOU. Dental light-cured nano-composites based on a dimethacrylate matrix: Thermal degradation and isoconversional kinetic analysis in N_2 atmosphere. *Thermochimica Acta*. 2015, 599, 63–72.

[107] STANSBURY, J. W. and S. H. DICKENS. Determination of double bond conversion in dental resins by near infrared spectroscopy. *Dental Materials*. 2001, 17(1), 71–79.

[108] GUERRA, R. M., I. DURÁN and P. ORTIZ. FTIR monomer conversion analysis of UDMA based dental resins. *Journal of Oral Rehabilitation*. 1996, 23(9), 632–637.

[109] GAUTHIER, M. A., STANGEL, T. H. ELLIS and X. X. ZHU. A new method for quantifying the intensity of the C=C band of dimethacrylate dental monomers in their FTIR and Raman spectra. *Biomaterials*. 2005, 26(33), 6440–6448.

[110] KALAKKUNNATH, S., D. S. KALIKA, H. LIN and B. D. FREEMAN. Viscoelastic characteristics of UV polymerized poly(ethylene glycol) diacrylate networks with varying extents of crosslinking. *Journal of Polymer science: Part B: Polymer Physics*. 2006, 44(15), 2058–2070.

[111] COOK, W. D., J. S. FORSYTH, N. IRAWATI, T. F. SCOTT and W. Z. XIA. Cure kinetics and thermo-mechanical properties of thermally stable photo-polymerized dimethacrylates. *Journal of Applied Polymer Science*. 2003, 90, 3753–3766.

[112] MESQUITA, R. V. and J. G. GERSTORFER. Influence of temperature on the viscoelastic properties of direct and indirect dental composite resins. *Dental Materials*. 2008, 24(5), 623–632.

[113] MESQUITA, R. V., D. AXMANN and J. G. GERSTORFER. Dynamic visco-elastic properties of dental composite resins. *Dental Materials*. 2006, 22(3), 258–267.

[114] JIAN, Y., L. ZHAO, W. YANG and J. NIE. Dynamic Mechanical Analysis of Elastic Modulus Development of Dental Composites. *Polymer Composites*. 2013, 34(4), 580–586.

[115] BARSZCZEWSKA-RYBAREK, I. M. Characterization of urethane-dimethacrylate derivatives as alternative monomers for the restorative composite matrix. *Dental Materials*. 2014, 30(12), 1336–1344.

[116] WEN, M., L. E. SCRIVEN and A. V. MCCORMICK. Kinetic Gelation Modeling: Kinetics of Cross-Linking Polymerization. *Polymer*. 2003, 36(11), 4151–4159.

[117] PIELICHOWSKI, K. and J. NJUGUNA. *Thermal Degradation of Polymeric Materials*. Shawbury, Shropshire, SY4 4NR, United Kingdom: Smithers Rapra Technology, 2005. ISBN 1-85957-498-X.

[118] REY, L., J. DUCHET, J. GALY, H. SAUTERAU, D. VOUAGNER and L. CARRION. Structural heterogeneities and mechanical properties of vinyl/dimethacrylate networks synthesized by thermal free radical polymerization. *Polymer*. 2002, 43(16), 4375–4384.

[119] BARSZCZEWSKA-RYBAREK, I. M. Structure–property relationships in dimethacrylate networks based on Bis-GMA, UDMA and TEGDMA. *Dental Materials*. 2009, 25(9), 1082–1089.

[120] ACHILIAS, D. S. and I. SIDERIDOU. Thermal degradation and isoconversional kinetic analysis of light-cured dimethacrylate copolymers. *Journal of Thermal Analysis and Calorimetry*. 2010, 99(3), 917–923.

[121] RIGOLI, I. C., C. C. S. CAVALHEIRO, M. G. NEUMANN and E. T. G. CAVALHEIRO. Thermal Decomposition of Copolymers Used in Dental Resins Formulations Photocured by Ultra Blue IS. *Journal of Applied Polymer Science*. 2007, 105(6), 3295–3330.

[122] FLOYD, C. J. E. and S. H. DICKENS. Network structure of Bis-GMA-, and UDMA-based resin systems. *Dental Materials*. 2006, 22(12), 1143–1149.

[123] PFEIFER, C. S., Z. R. SHELTON, R. R. BRAGA, D. WINDMOLLER, J. C. MACHADO and J. W. STANSBURY. Characterization of dimethacrylate polymeric networks: a study of the crosslinked structure formed by monomers used in dental composites. *European Polymer Journal*. 2011, 47(2), 162–170.

[124] LEE, T. Y., T. M. ROPER, E. S. JÖNSSON, C. A. GUYMON and C. E. HOYLE. Influence of Hydrogen Bonding on Photopolymerization Rate of Hydroxyalkyl Acrylates. *Macromolecules*. 2004, 37(10), 3659–3665.

[125] ELLIOT, J. E., J. W. ANSETH and C. N. BOWMAN. Kinetic modeling of the effect of solvent concentration on primary cyclization during polymerization of multifunctional monomers. *Chemical Engineering Science*. 2001, 56(10), 3173–3184.

[126] LEE, J. K., J. CHOI, B. LIM, Y. LEE and R. L. SAKAGUCHI. Change of Properties during Storage of a UDMA/TEGDMA Dental Resin. *Journal of Biomedical Materials Research, Part B, Applied Biomaterials*. 2004, 68(2), 216–221.

[127] C. E. HOYLE and P. S. PAPPAS. Radiation curing: science and technology. 1st ed. New York: Springer Science Business Media, 1992, s. 57-133. Topics in applied chemistry. ISBN 978-1-4899-0714-1.

[128] DUŠEK, K. and W. J. M. PRINS. Structure and Elasticity of Non-Crystalline Polymer Networks. *Advances in Polymer Science*. 1969, 6(16), 1–102.

[129] KAMMER, S., K. ALBINSKY, B. SANDNER and S. WARTEWIG. Polymerization of hydroxyalkyl methacrylates characterized by combination of FT-Raman and step-scan FT-i.r. photoacoustic spectroscopy. *Polymer*. 1999, 40(5), 1131–1137.

[130] MORITA, S. Hydrogen-Bonds Structure in Poly(2-Hydroxyethyl Methacrylate) Studied by Temperature-Dependent Infrared Spectroscopy. *Frontiers in Chemistry*. 2014, 2(10), 1–5.

[131] LI, D. and J. BRISSON. Hydrogen bonds in poly(methyl methacrylate)- poly(4-vinyl phenol) blends: Quantification near the glass transition temperature. *Polymer*. 1998, 39(4), 801–810.

LIST OF FIGURES

LIST OF TABLES

Table 13: Mean and standard deviation values of the storage modulus at 40 ºC (E') and at the point of glass transition ($E'_{rubbery}$), glass transition temperature (T_g) and limiting degree of double bonds conversion ($P_{C=C}$) as determined by FTIR; neat monomers.

Table 14: Mean and standard deviation values of the storage modulus at 40 ºC (E') and at the point of glass transition ($E'_{rubbery}$), glass transition temperature (T_g) and limiting degree of double bonds conversion ($P_{C=C}$) as determined by FTIR; Bis-GMA/TEGDMA and Bis-EMA/TEGDMA copolymers.

LIST OF ABBREVIATIONS

Chemicals

BD	2,3-butanedione
Bis-EMA	Bisphenol A ethoxylate dimethacrylate
Bis-GMA	Bisphenol A glycidyl methacrylate
CQ	Camphorquinone; 2,3-bornanedione
CQ (S)	CQ excited singlet state
CQ (T)	CQ excited triplet state
DEGDMA	Diethylene glycol dimethacrylate
DMAEMA	(2-dimethylaminoethyl) methacrylate
EDMAB	Ethyl-4-dimethylamino benzoate
PEGDMA	Polyethylene glycol dimethacrylate
PMMA	Poly (methyl methacrylate)
PPD	1-phenyl-1,2-propanedione
UDMA	Urethane dimethacrylate
TEGDMA	Triethylene glycol dimethacrylate

Experimental methods, others

AFM	Atomic Force Microscopy
ATR	Attenuated Total Reflection (mode of FTIR)
DC	Degree of double bond conversion
DEA	Dielectric Analysis
DMA	Dynamic Mechanical Analysis
DSC	Differential Scanning Calorimetry
DPC	Differential Photo Calorimetry
EPR	Electron Paramagnetic Resonance spectroscopy
FTIR	Fourier Transform Infra-Red Spectroscopy
LCU	Light Curing Unit
LED	Light Emitting Diode
NMR	Nuclear Magnetic Resonance spectroscopy
PAC	Plasma Arc
PALS	Positron Annihilation Lifetime Spectroscopy
QTH	Quartz Tungsten Halogen
SEM	Scanning Electron Microscopy
TGA	Thermo-Gravimetric Analysis

Equations

A	Pre-exponential factor
$[A]$	Concentration of amine photo-reductant
β	Fraction of excited state complex forming free radicals
$[C_s]$	Concentration of photo-initiator
$[CQ_T^*]$	Concentration of CQ triplet state
E'	Storage modulus
E''	Loss modulus
E^*	Complex modulus
E_a	Activation energy
ε	Molar absorptivity of the photo-initiator
h	Heat flow
ΔH	Enthalpy of reaction
I_a	Absorbed light intensity
I_0	Incident light intensity per unit area
$[M]$	Concentration of double bonds or monomer concentration
$[M^*]$	Concentration of all chain radicals
N	Number of measurements
k	Rate constant of the reaction
k_a	Rate constant for the exciplex formation
k_p	Propagation reaction kinetic constant
k_t	Termination reaction kinetic constant
$P_{C=C}$	Double bond conversion
R	Reaction-diffusion proportionality constant
R	Universal gas constant
R_i	Rate of initiation
R_p	Rate of propagation
$R_{p,\,max}$	Maximal polymerization rate on the time/conversion scale
R_r	Rate of production of primary free radicals from photosensitizer
R_t	Rate of termination
ρ	Density of the resin system
T	Absolute temperature
T_g	Glass transition temperature
ϕ	Quantum yield for photo-initiation